ENERGY AND INTENSITY OF THE GAMMA RADIATION FROM $F^{19} + H^1$ AND $Be^9 + D^2$

Thesis by

Volney Kinne Rasmussen, Jr.

In Partial Fulfillment of the Requirements

For the Degree of

Doctor of Philosophy

California Institute of Technology

Pasadena, California

1950

ACKNOWLEDGMENTS

It is a pleasure to acknowledge the active participation of Professor T. Lauritsen in most of the work described in this thesis. I am also greatly indebted to Professors C. C. Lauritsen, R. F. Christy, and W. A. Fowler for much advice and assistance.

As is usual in present day work in nuclear physics, the construction and successful operation of the beta-ray spectrometer resulted from the joint efforts of several people. In addition to the faculty members mentioned, Dr. C. Y. Chao of the Institute of Physics, Academia Sinica, Nanking, China, Mr. C. B. Dougherty, Dr. W. F. Hornyak, and Mr. R. G. Thomas have, at various times, given valuable assistance in construction of the spectrometer and in interpretation of the results obtained. Mr. L. J. Gililland, Mr. G. Fastle, and Mr. J. F. Hill of the Kellogg Laboratory machine shop, Mr. W. D. Gibbs of the electronics shop, and Mr. V. F. Ehrgott, Mr. G. L. Dorr, and Miss J. Antz of the drafting department have all, at various times, been of considerable assistance.

This work was supported by the joint program of the Office of Naval Research and the Atomic Energy Commission. Entirely aside from the merit or lack of merit of the present thesis, I would like to take this opportunity to commend these two government agencies for their far-sighted support of basic scientific research.

Finally, I am indebted above all to my wife, Janette, without whose help this thesis would neither have been written nor typed.

ABSTRACT

A magnetic lens β-ray spectrometer with a large (~4.5% of a sphere) solid angle and with good shielding against the neutron and γ-ray backgrounds encountered in the investigation of the prompt γ-radiation from nuclear reactions is described. Methods for determining the intensities of γ-radiation by observation of photoelectron and Compton electron secondaries with the spectrometer are discussed. It is concluded that where their use is feasible, Compton secondaries will give the more accurate values for the intensity and energy of γ-radiation.

The nuclear pairs and γ-radiation from excited states of O^{16} have been investigated. The pair spectrum agrees well with that calculated theoretically, and the end point indicates that the first excited state of O^{16} is at 6.04 ± 0.03 Mev. The γ-radiation observed corresponds to levels at 7.09 ± 0.06, 6.9, and 6.14 ± 0.04 Mev. Estimates of the relative and absolute intensities of the γ-radiation are given.

The rather complicated γ-ray spectrum resulting from the bombardment of beryllium with deuterons has been investigated. The assignment of these γ-rays to the possible residual nuclei is discussed, and it is determined that most of them can be attributed to excited states of B^{10}, as formed in the $Be^{9}(d,n)B^{10*}$ reaction. By comparing the γ-ray intensities with the neutron intensities observed by other experimenters, a level scheme for B^{10} is constructed.

TABLE OF CONTENTS

I. Introduction

Recently developed magnetic spectrometers for measuring the energies of heavy particles[1,2] and gamma rays[3,4] produced in nuclear reactions have made it possible to determine many more of the pertinent facts about the excited levels of light nuclei. Many such levels have been identified, even with earlier and less precise techniques, by observing resonances in the yield as the incident particle energy is varied, by observing various particle groups of different energy that represent end products of the possible nuclear reactions, or by measuring the energy of γ-radiation that may be emitted from nuclei left in an excited state by the reaction. The heavy particle groups, or resonances in the simple capture reactions, indicate those levels in a certain nucleus that are excited by the reaction. If γ-radiation of a single energy is emitted, we immediately know the location of the level in the nucleus. In some cases, levels initially excited by a heavy particle reaction decay by cascade γ-radiation. We must then compare the energy available in the reaction, as given by the differences in mass of the original and final sets of particles, with the energy observed as γ-radiation and heavy particle kinetic energies, in trying to decide where the levels are located in the nucleus. It is clear that the increased resolution and accuracy of the most recent methods will make this task much easier, and much success has been attained in locating energy levels by these methods, as reviewed by Hornyak and Lauritsen,[5] and Lauritsen.[6] However, we still encounter certain ambiguous situations where the determination of particle and γ-ray energies is not sufficient to establish a unique level scheme, where we can only say that there are several possible locations for an unknown number of levels. Further

experimental evidence is then required. One possible approach is to investigate particle-γ and γ-γ coincidences. Very little work of this potentially fruitful kind has been done with nuclear reactions. It is anticipated, however, that one would have to use methods that give a large solid angle, and consequently a low energy resolution, to get reasonable counting rates. Especially in the more complicated cases, a useful alternate approach to this problem is by means of intensity measurements, where one determines the initial population of a particular level by measuring the yield of the corresponding heavy particle group and then measures the yield of the various γ-ray lines that may come from this level. If reasonably accurate intensity measurements are available, then the construction of a unique level scheme will usually be possible.

The present thesis is concerned basically with such intensity measurements--in particular with the measurement of γ-ray intensities by means of a β-ray spectrometer. No great success can be claimed, in good part because equally reliable values for the corresponding heavy particle intensities are not available. It is shown, however, that this approach is both practicable and potentially fruitful, and the techniques required for the measurement of γ-ray intensities are investigated in some detail.

II. Spectrometer

A. Magnetic lens type spectrometers

Several β-ray spectrometers of the magnetic lens type have been recently described in the literature (e.g.--Refs. 4, 7-9). They are all characterized by a magnetic field with cylindrical symmetry, the simplest case being that of the uniform field, $\vec{B} = B_z \vec{e}_z$. It is well known that the uniform field has focussing properties; an electron originating on the z-axis will return to it at a Δz that depends on the electron momentum and its initial angle with the z-axis. By introducing appropriate limiting apertures and a detector one can measure the momentum of the electrons, i.e., one has a β-ray spectrometer. One can show that other field forms also have focusing properties, indeed, for electrons whose initial angle with the axis is small it is only necessary, as shown by Busch,[10] that the field have cylindrical symmetry. Each of the three general types of field form has its particular merits. The "thin lens" type of Deutsch, Elliott and Evans,[7] for example, will focus the maximum momentum electrons for a given expenditure of power in the magnet coils. The equations of motion for the electrons have particularly simple solutions for the uniform field, so that trajectories may be calculated, and an absolute calibration, based on a simple current measurement is possible. The other extreme in field form, the U-shaped field, strongest at the source and image, has been discussed by Siegbahn.[9] Using the usual "point" focus, Siegbahn, and Lauritsen and Christy[11] have shown that this field form gives a larger solid angle (fraction of a sphere into which electrons can be emitted and subsequently focused) for a given spherical aberration that do either the thin lens or uniform field spectrometer.

An important recent development is the suggestion of Frankel[12] that it is generally characteristic of a magnetic lens that those electrons making a larger initial angle with the axis reach the axis again at smaller Δz, so that the paths for two given initial angles α_1 and α_2 must cross at some intermediate point (more properly, because of the cylindrical symmetry, a circle). With a finite range of α, this circle becomes a zone or "ring" focus that is appreciably sharper than the focus on the axis. The use of this ring focus for a uniform field spectrometer has been discussed in detail by Persico[13] and DuMond.[14] The ring focus has been used in this laboratory with both thin lens and U-shaped field spectrometers (see Figs. 1 and 2).

B. Discussion of techniques

Some mention of the general techniques of working with a lens type spectrometer is perhaps in order, and will serve to collect in one place definitions of various terms that will be used frequently. The use of iron in such spectrometers is usually avoided, mostly because of its non-linearity. The magnetic field is then directly proportional to the current through the lens coils. This current is determined by measuring with a potentiometer the potential drop across a resistor (shunt) with a low temperature coefficient. The momentum of the electrons focused is directly proportional to the magnetic field, and is classically measured in units of gauss-centimeters (radius of curvature in a uniform field times field strength). Calibration is usually in terms of one or more electron lines of known energy. Such lines are the internal conversion photoelectron lines from the natural radioactive elements. Very thin (essentially monomolecular) sources of certain of these elements can be prepared by electro-

static collection from the emanation (gasses thoron and radon) (Ref. 15, p. 560). These deposits are usually made on thin flat foils which are placed perpendicular to the spectrometer axis. The internal conversion electrons from such sources are very nearly monoenergetic and their energy has been measured quite accurately (see, for example, Ref. 16). If the spectrometer field is set to correspond to one of these lines, it focuses all electrons of this line emitted within a certain angular range of the axis, the acceptance angle, the corresponding solid angle being usually expressed in per cent of a sphere. The electrons focused are recorded by a thin-window Geiger counter (which counts practically all the electrons received, as long as the counting rate does not get too high). If the field is changed slightly, the number of electrons counted is reduced, but does not go to zero, even though no electrons of this different momentum are being emitted by the source, as a simple result of the finite resolving power of the instrument, which is expressed most completely in terms of the "window" curve, or the plot of counting rate vs. magnetic field in the neighborhood of a monoenergetic line. This window curve may be made symmetric by adjustment of the various apertures and is then quite closely approximated by a Gaussian function. The "resolution" is defined as $\Delta p/p$,* the full width at half maximum of the window curve (usually expressed in millivolts potentiometer reading) divided by the peak value in the same units. This turns out to be a constant, independent of p. If one is examining a continuous electron spectrum, then the curve observed is distorted by the instrument window. Ideally, one would like to remove this distortion

---

* The reciprocal of this quantity is frequently called the resolution.

completely and approximate methods for doing this exist (mathematically, "unfolding") but are laborious. If changes in the continuous spectrum within the instrument resolution are small, however, one may remove the important part of the distortion by dividing the counts at a given momentum (millivolt reading) by this momentum, thus taking account of the fact that $\Delta p/p$ is a constant.

It may be noted that except for the direction of rotation of the spiral path, electrons and positrons are treated alike in the lens type spectrometer. They may be separated by means of suitable helical baffles.

C. Description of spectrometer

The magnetic lens type spectrometer used in these investigations has been previously described in detail.(17) The magnetic field required is furnished by four coils, each of 5.6 inch inner radius, 15 inch outer radius, and 4.2 inch length (exclusive of the spools on which they are wound) and consisting of 850 turns of #6AWG double cotton covered magnet wire. The vacuum chamber is a thin-wall brass tube of 5.0 inch inside radius and 48 inch length. Since the four field coils are entirely separate, one may get field forms ranging from the thin lens to the U-shaped field. The thin lens arrangement (with Frankel's ring focus--see Fig. 1) which was used in some of the experiments to be discussed is described in Ref. (17). In some cases, it was clear that a considerable increase in solid angle was desirable. The lens coils were therefore rearranged (Fig. 2) to give approximately the U-shaped field of Siegbahn. It was found that, using the ring focus again, this arrangement gave three times the solid angle with no loss of resolution, but that the maximum momentum electrons that could be focused with the ampere-turns available was reduced by a factor of two.

D. Electron trajectories

In principle, one must calculate various electron paths to determine the location of the ring focus, such calculations being long and complicated for the case of the U-shaped field.* However, it may be noted that the ring focus is only a poorly-defined intersection of rays with a small divergence, so that it would seem possible to trace various rays experimentally with sufficient precision. This was indeed found to be the case, experimental details being given in App. I.

The complete trajectories for this field form are of interest in that they account for some of its important properties. The r-components (or envelope of the family of trajectories making the same initial angle with the z-axis) of two trajectories are shown in Fig. 2. These were obtained by a method, suggested by Dr. C. Y. Chao, depending on the apparently not well-known fact that the equilibrium position in a magnetic field of a taut, current-carrying wire is the same as the path of a free electron of momentum $p = -eT/I$ (in the same field) provided only that the mass and stiffness of the wire are negligible. This condition was satisfied in our case with an .003 inch diameter soft copper wire carrying ~1 1/2 amperes and with 50 amperes through the field coils. The wire was run from the source to the desired image position, and its distance from the axis at various points was measured (no attempt was made to measure the rather small tension in the wire). It was noted in particular that the plotted trajectories are almost parallel (neglecting rotation) to the axis for a considerable part of their length. This is of importance in that it results in a larger range of acceptance angle (larger solid angle), as if the source to

---

* The approximate equations for paraxial rays, as usually used in such calculations, would probably not be suitable here.

image distance were much smaller, without actually reducing this distance and consequently the amount of shielding that can be used between the source and counter.

Dr. Chao, in some unpublished work, has also developed a semi-empirical expression that enables one to estimate the effect on the resolution of the finite size of the electron source. The various distances and angles are defined in Fig. 3 (where rotation is neglected). With a very small source of electrons one must measure experimentally $\Delta\theta/\Delta z$ and $\Delta I/\Delta R$ for small arbitrary changes in the current ΔI (strictly, $\Delta\theta/\Delta z$ should be measured by moving both the source and image point, leaving the current constant). Then Δ_s, the contribution of the source to the full width of the window curve (full width at the base of the equivalent triangle) is given by

$$\Delta_s = \left(\frac{\Delta p}{p}\right)_s = \left(\frac{\Delta I}{I \Delta R}\right)_1 s \left(1 + \frac{R}{\sin\theta} \frac{\Delta\theta}{\Delta z}\right)$$

Since we are here using the width at the base of the window curve, Δ_s may be added to the instrument width as obtained with a point source to give the total expected width. One may also estimate the width expected with a point source from

$$\Delta_L = \left(\frac{\Delta I}{I \Delta R}\right)_1^L$$

if an estimate of the width L of the ring focus can be made, as is usually possible after the ray tracing described in App. I has been done. These expressions will be applied to specific cases later in this section.

E. Two separated coil configuration

With the separation of the coils fixed at the spacing shown in Fig. 2 one may still vary the field form by using only part of the available turns. The first experiments with the U-shaped field were made using only the outer pair of coils. Although this configuration proved to be not too useful, mostly because of the limit on the maximum energy electrons that could be focused (~ 4 Mev) and because it was too sensitive to source size and location, some of its properties are interesting. In particular, there was evidence that the outer part of the transmission zone corresponded to a surprisingly large solid angle. Fig. 4a, for example, was obtained using a small source and counter opening (0.078 inch) and a transmission zone from 2.5 inch to 5.0 inch radius (in the plane midway between source and counter). When the source and counter opening are axially symmetric with respect to the magnetic field coils, a prominent peak appears at the low current side of the rectangular distribution (this shape is found because spherical aberration makes the image much larger than the counter opening). The disappearance of this peak when asymmetry between the source and counter is introduced is not surprising if one notes the behavior of the trajectories as shown by the current-carrying wire. If the wire is fixed on the axis at symmetric points, then it is symmetric over its whole length. If one (or both) of the axial points are moved along the axis (to the right, say) then the point of maximum excursion from the axis moves much further in the same direction, and the trajectory becomes markedly asymmetric. No detailed measurements were made, but it was estimated that a 1/16 inch displacement of the axial points resulted in a 1 to 2 inch displacement of the point of maximum excursion. Some measure of the asymmetry was also obtained in the course of ray tracing (as in App. I) to set up the ring focus, when it was

found that in the neighborhood of the counter, and for a ray of maximum excursion from the axis of 3 7/8 inches, $\Delta\theta/\Delta z$ = .077 rad./inch (change in angle with the axis with change in point of intersection). For the extreme rays (5 inch maximum excursion) $\Delta\theta/\Delta z$ is several times as large. The focusing properties thus change rapidly if one moves the source away from the symmetric location and the large solid angle associated with the outer rays disappears.

Results of a further investigation of the large solid angle associated with the outer zone are shown in Fig. 5.

Using a transmission zone from 4 to 5 inch radius, the location of the ring focus was determined approximately by the crossed slit method of App. I. With a "standard" Co^{60} source (see section F below) a resolution of 2% and a solid angle of $\approx 5.8\%$ of a sphere were obtained. It also seemed probable that the width of the transmission zone could be reduced by 30% without appreciable loss in solid angle, although the experiments involved were not conclusive. An example of the effect of source size is given in Fig. 4b.

Slätis and Siegbahn[18] have recently published details of an extended study of a spectrometer with an even more extreme field form than ours, for which they claim a solid angle of 8% with a resolution of 4%. Their results corroborate ours, in general. However, they found the ring focus, if it can still be thus named, in the median plane, in contrast to our case where there was clearly a ring focus at 1/9 the source to counter distance from the counter. They also traced electron trajectories, using a photographic technique, and found the type of asymmetries described above, but regard them as representing the focusing properties of the field with a point source, rather than as the effect of source size. Since they used a 2 mm diameter spherical source, which can hardly be regarded as a point source

(as they themselves proved by showing that the intensity dropped to half value if the source was moved 2 1/2 mm axially), some large part of their observed asymmetry must be attributed to the finite source size. This is of importance principally because it would appear that their solid angle was determined by measuring the initial angle with the axis for the extreme trajectories. If this is so, their solid angle estimate must be reduced appreciably.

F. Four separated coil configuration

With all four coils of Fig. 2 carrying current, electrons up to 10 Mev could be focused, thus covering the range of interest in almost all cases. There was no large loss of solid angle from that obtained with only two coils, and this arrangement was less sensitive to source size and position.

The location of the ring focus for a 2 1/2 to 5 inch radius transmission zone was determined by ray tracing (details described in App. I). The two extreme complete trajectories shown in Fig. 2 were determined with a current-carrying wire. It was noted in particular that the asymmetry introduced by small changes in the source position was much less than when only the two outer coils were used.

To measure absolute intensities of γ-radiation, the solid angle from which the spectrometer collects secondary electrons must be measured. As discussed in Sec. III, there are two possible definitions of the solid angle. The more natural, and perhaps more significant in considering the merits of a particular spectrometer design is as the total solid angle between the minimum and maximum initial angles an electron can make with the spectrometer axis and still be counted at some value of the spectrometer field (for a given momentum electron, the field corresponding to the

maximum angle may not be the same as that corresponding to the minimum angle). This solid angle will be designated by Ω. The second definition is of the solid angle Θ (which must be used in intensity calculations) as the ratio of the number of counts at the peak of an internal conversion line to the number of electrons per steradian emitted by the source.

Ω is measured easily and directly according to its definition. Care must be taken to use a small enough source and to measure the angles sufficiently close to the source.

Θ, on the other hand, is somewhat more difficult to measure to the accuracy that is desirable, because of the difficulty involved in obtaining an internal conversion line source for which the number of electrons emitted is accurately known. Although suitable sources of known total activity (or disintegration rate) are available, the number of internal conversion electrons per disintegration is difficult to measure experimentally and is generally not known to closer than 10 to 20%. For sources of known β-activity (continuous spectrum) or γ-activity, the methods of Sec. III may be used to measure Θ. One may also obtain a fairly accurate value of Θ by determining the maximum and minimum initial angles with the axis of electrons corresponding to the peak of an internal conversion line, calculating the corresponding solid angle and subtracting the effect of obstructions such as the helical baffles and supports for the central stops.

Because of the lack of suitable sources, this last method was used to measure both Ω and Θ for our spectrometer. An annular aperture, shown in Fig. 6, was used. It was arranged so that it could be moved accurately measured distances along the spectrometer axis and would remain well centered. An 0.02-inch diameter ThB F line source was used, the curves obtained for various source to slit distances being shown in Fig. 7.

Taking account of the change in solid angle subtended by the annulus with changes in distance from the source, one can calculate from these curves and the known geometry the angles with the axis corresponding to both Ω and Θ as $\alpha_{min} = 15^{\circ}$, $\alpha'_{max} = 27^{\circ}10'$ and $\alpha_{max} = 28^{\circ}45'$. Here α_{min} corresponds to a source to slit distance of 0.95 inch, which gives a factor of two reduction in peak height. Since this peak occurs at the same magnetic field (28.6 mV) as that for the whole transmission zone, α_{min} is the minimum angle appropriate to both Ω and Θ. α'_{max} corresponds to a source to slit distance of 0.50 inch, where the intensity at 28.6 mV is down by one half, and thus is the maximum angle to use in calculating Θ. α_{max}, on the other hand, corresponds to the source to slit distance of 0.475 inch at which the peak height is down by one half. Since the peak has shifted (i.e., is now at 28.4 mV) α_{max} is the maximum angle to use in calculating Ω.

Certain relative positions of the source and slit are shown in Fig. 8a. It may be noted in particular that a source to slit distance of 1.00 inch should also have been tried, to ascertain positively that the peak height was falling off more rapidly than would be expected just from the decrease of the solid angle of the annulus with distance. From purely geometric considerations, it is certain that α_{min} is not less than $\approx 13^{\circ}$, and the error in Ω and Θ from this cause is less than 10%.

The correction to Θ for obstructions in the transmission zone is estimated as $20 \pm 5\%$. This gives $\Omega = 4.45 \pm .2\%$ of 4π steradians and $\Theta = 0.80 \times 3.81 \pm .2\% = 3.05 \pm .2\%$ of 4π steradians. It may be noted that the source used was so small that effects due to its size were negligible, that the slits were close enough to the source that the (projected) electron paths could be considered as straight lines, and that, as illus-

trated in Fig. 8b, effects of malalignment (estimated as < 0.015 inch) are negligible.

The same source was also run with the slits moved completely out of the transmission zone, as could be done without moving the source. The ratio of peak heights without the slits and with the slits in roughly the center of the whole acceptance cone, then gives Θ, in terms of the solid angle subtended by the slits, as 0.80 x 3.65% = 2.92% of 4π. There is some question as to the validity of this method, and small errors in determining the solid angle subtended by the slits become important, so that it is regarded mostly as a rough check of the other results.

The curve for the whole transmission zone shows an asymmetry and a flat top, both attributed to slight malalignment, which is verified by other runs of the window curve with the same source size and aperture locations that gave resolutions of 1.90 to 1.95%. The results of these measurements were used to determine the solid angle of other spectrometer configurations through the intermediary of a "standard" Co^{60} source (half-life = 5.3 years). This source* consisted of a few mg/cm^2 of $CoCl_2$ (natural Co + radioactive Co^{60}) precipitated in an 0.12 by 0.15 inch rectangle on 0.001 inch copper, held in place by shellac and covered with a 3/8 inch diameter thorium foil of superficial density 16 mg/cm^2. Photoelectrons from the two γ-rays of Co^{60} (1172 and 1331 kev)[4] are ejected from the thorium foil over an area whose effective diameter is estimated as $\approx$0.15 inch. In some cases the ThB X-line was used instead of the Co^{60}, the activity of the source being measured by a monitor Geiger counter in a standard position. The difficulty

---

* Kindly prepared by Dr. J. H. Sullivan of the Chemistry Department of the California Institute from Co^{60} supplied by the Atomic Energy Commission.

of reproducing this geometry made the method not too satisfactory. In using these sources, it was assumed that both Ω and Θ were proportional to the peak height, the factor being given by the measurements of Θ and Ω described above.

To determine the effect of source size and alignment on the resolution for the four separated coil configuration, a small F-line source was moved radially off center by measured amounts. The results are given in Fig. 9 and in Table I. The width (as determined by the extrapolated edges) at the base of the window curve with an off-center source should be roughly the same as that for a full source whose radius is equal to the distance of the extreme source point from the axis. Chao's formulas (Sec. II D) may then be used to calculate this width.

Table I

L (inch)	Δ_L * (%)	S_{eff} (inch)	Δ_S * (%)	$\Delta_L + \Delta_S$ (%)	$\Delta_{obs.}$ † (%)
.23	1.60	.06	0.47	2.1	3.5
.23	1.60	.18	1.4	3.0	5.1
.23	1.60	.30	2.4	4.0	6.4
.23	1.60	.42	3.3	4.9	8.1

* Calculated. Note that S is the source diameter.

† It may be noted that experimentally the width at the base is generally found to be somewhat less than twice the full width at half maximum.

C. Comparison of various field forms

A tabulation of the resolution and solid angle experimentally obtained, as given in Table II, may be of interest. The widths at the base of the window as calculated from Chao's expressions are also given. In most cases, the experimental resolution must be regarded as an upper limit--it cannot be guaranteed that the alignment of the source and stops with respect to the magnetic field was perfect or that the ring focus stops were located at the optimum position, although in no case would more improvement in the resolution than about 30% be expected under optimum conditions. Chao's expressions thus give consistently low values as would be expected from the several simplifying assumptions involved in their derivation. They are still of much practical use in estimating the change in resolution for a given change in source size, however. For our work, the main advantage of the U-shaped field over the thin lens is not, as would seem at first glance, the larger solid angle, for the solid angle of the thin lens may also be increased by decreasing the source to counter distance,* but the large source to counter distance at which that solid angle is obtained. This is of some importance in cutting down background from scattered electrons and γ-rays and is of special importance when weak γ-rays from nuclear reactions with a large neutron background are to be studied, for our attempts to reduce this background (see Sec. V D) have shown that the most useful type of "shielding" is the $1/r^2$ decrease of neutron flux from a point source.

---

* Assuming that the diameter of the vacuum chamber is fixed. The principal difficulty encountered in setting up such a configuration would be expected to be that of finding a large enough thin-window Geiger counter to count all the rays through the ring focus zone at a given field setting. Also, the background rate of such a counter would increase with size.

Table II

L (inch)	Δ_L (%)	S (inch)	Δ_S (%)	$\Delta_L + \Delta_S$ (%)	$\Delta_{obs.}$ [b] (%)	$\Delta p/p$ (%)	$\Omega_{geom.}$ [d] (% of 4π)
A. Thin lens							
"Point"	focus [a]	.12	—	—	~13		~ 1.6
.345	2.0	.12	0.7	2.7	3.4	1.9 [c]	≈ 1.05
.47	2.8	.12	0.7	3.5	4.0	2.3	≈ 1.5
.25	1.5	.12	0.7	2.2	2.5	1.45	≈ 1.05
B. Two separated coils							
"Point"	focus [a]	≈ .05	—	—	~10%		~ 6%
.24	1.5	≈ .15	1.8	3.3	3.8	2.2	≈ 5.8
.15	0.96	≈ .04	0.48	1.44	2.1	1.2	— [e]
.15	.96	≈ .12	1.44	2.40	3.5	2.1	— [e]
C. Four separated coils							
"Point"	focus [a]	≈ .05			~15		≈ 4.5
.083	0.59	.12	.95	1.54	2.05	1.1	2.1
.23	1.60	.12	.95	2.55	4.2	2.3	4.4
.23	1.60	≈ .15	1.18	2.78	4.1	2.3	4.4
.23	1.60	.02	.16	1.76	3.4	1.90	4.4

A. $\left(\frac{\Delta I}{I \Delta R}\right)_1 = .059 \text{ inch}^{-1}$; $\left(\frac{\Delta \theta}{\Delta z}\right)_1 = 0$; $\bar{\theta} = 12.5°$; R = 1 3/16 inch.

B. $\left(\frac{\Delta I}{I \Delta R}\right)_1 = .064 \text{ inch}^{-1}$; $\left(\frac{\Delta \theta}{\Delta z}\right)_1 = .077 \text{ inch}^{-1}$ [f]; $\bar{\theta} \approx 31°$; R = 2.83 inch.

C. $\left(\frac{\Delta I}{I \Delta R}\right)_1 = .070 \text{ inch}^{-1}$; $\left(\frac{\Delta \theta}{\Delta z}\right)_1 = .012 \text{ inch}^{-1}$; $\bar{\theta} = 23°40'$; R = 1 1/8 inch.

a. Estimated.
b. From linear extrapolation of front and back edges.
c. Mechanical alignment was apparently quite bad.
d. No allowance for ≈20% loss in baffles and supports.
e. See Fig. 4b. Transmission zone 4 inch to 5 inch radius.
f. For rays with maximum excursion from axis = 3 7/8 inch.

H. Use of spectrometer with electrostatic accelerator

In the investigations described in this thesis, the β-ray spectrometer was used to investigate the γ-radiation produced in nuclear reactions resulting from the proton or deuteron bombardment of light elements. The proton or deuteron beam was obtained from the 1.6 Mev Kellogg Radiation Laboratory electrostatic accelerator.(19) The beam is analyzed into its atomic and molecular ion components by a magnetic deflection of a few degrees, and the selected component is deflected through 90° by a second magnet. This magnet served to determine the energy of the protons or deuterons to about ± 0.2%. By means of insulated slits plus suitable corona controls the variations with energy of the deflection of the beam were used to control the accelerator voltage.(20) The analyzer magnet was not calibrated. Rough voltage measurements were made by referring to the generating voltmeter(19) and fairly accurate measurements could be made by holding the voltage as measured by the generating voltmeter constant and switching the beam from the magnetic analyzer to the electrostatic analyzer described by Fowler, et al.(20)* Excitation functions (variation of yield with voltage) could be measured by changing the voltage by equal steps either with reference to the generating voltmeter or the current through the field coils of the analyzer magnet, the latter method being more satisfactory so long as hysteresis effects in the iron of the magnet were avoided.

Because of the large stray field of the analyzer magnet, the spectrometer had to be placed about four feet from it, the beam travelling this distance in a 1-inch copper pipe open to both the spectrometer and accelerator vacuum systems. The beam was defined in direction, position, and size

---

* As described in (20), a portion of the lower electrostatic analyzer deflecting plates could be moved to allow the beam to come straight through. The beam would then enter the magnetic analyzer.

by a system of adjustable slits at distances of 6 to 21 inches from the outside face of the spectrometer end plate. Since it was found that the thin-window Geiger counter in the spectrometer was sensitive to the soft x-rays resulting when protons were scattered off the edge of these slits, an orifice only slightly larger than the beam was placed at the spectrometer end plate and was found to eliminate such counts almost completely. Targets to be bombarded were placed at the source position of the spectrometer (see Fig. 2), any converters desired being fastened directly to them, and this whole assembly was supported by a fine copper wire to avoid extraneous conversion and scattering effects.

This wire was insulated so that the beam current to the target could be measured and was kept at +100 to 300 volts with respect to the spectrometer to collect low energy secondary electrons ejected from the target by the beam. When a thin target without any backing or converter was used, so that the beam penetrated completely through the target, the beam current was measured by an insulated plate 5 inches directly behind the target. Currents measurements made in this manner were not reliable, probably because of secondary electrons from residual gas in the vacuum chamber. Spectrometer counts were taken either for a given integrated beam current to the target or for a given total γ-ray yield from the reaction, as measured by a shielded γ-ray counter an appropriate distance from the target.

Most of the beam at the target position was within a rectangle $\sim 1/8$ by 3/16 inch. This was usually trimmed, by setting the slits, to ~ 0.1 by 0.1 inch without any large loss of current. Targets and converters, except where specifically noted, were 0.3 to 0.4 inch in diameter.

The axis of the spectrometer was horizontal and along the magnetic meridian. The vertical component of the earth's field and the stray field of the analyzer magnet were approximately cancelled out by two pairs of large rectangular coils, the criterion for satisfactory cancellation being that resolution be the same for a 150 kev electron line and a 2.50 Mev line (internal conversion "F" and "X" lines from a ThB deposit). As discussed by Hornyak (Ref. 17, p. 79) a correction was made for the component of the earth's field along the axis.

III. Measurement of Gamma-ray Intensities

A. Introduction

With a β-ray spectrometer one observes γ-radiation by observing the secondary electrons produced by the radiation in traversing matter. The various processes in which these electrons are formed are well understood, and the probabilities for their occurrence have been calculated, insofar as such calculation is feasible. The basic relations between the energy of the γ-quantum and that of the secondaries are simple. The accurate determination from a secondary electron spectrum of the energy of the primary γ-quantum is, on the other hand not simple because of the energy losses of the electrons in escaping from the converter, as discussed in detail in Ref. (17). This difficulty arises basically from the fact that the conversion probabilities are low, so that one must usually use converters of appreciable thickness to get statistically significant numbers of electrons. Calculation of these energy losses is possible but, even with many simplifying assumptions, complicated, and has been the subject of many published papers, of which the most recent and most general is by Niels Bohr.[21] There is also very little experimental verification of calculations that have been made, not so much because the experiments are difficult as because they represent a case where the basic physical principles seem to be well understood and where detailed application would seem to be not too fruitful.

For a detailed discussion of this problem, reference is made to the paper of Bohr mentioned above. Mention of the salient features may be made here, however. A fast (velocity ~ velocity of light) electron traversing matter loses energy principally by collision with free electrons and by exciting and ionising the atoms of the matter (radiation is also possible,

as Bremsstrahlung, but not important in our case). Since it is interacting with other electrons, energy losses up to half its original energy are possible (for greater losses, the struck electron with more than half the energy replaces the original electron) and losses of several times the average ionization energy of the atom are probable, although not as probable as smaller losses. For a given path length, ℓ, both the number of collisions and the amount of energy lost in each are subject to statistical fluctuations, or straggling. The total energy lost by the electron in the distance ℓ can be represented by a Gaussian probability distribution on which is superposed a long tail representing the relatively improbable large energy losses. The peak of the Gaussian is the "most probable" energy loss and is a function of ℓ as well as of the stopping material. One may also take into account the tail and calculate the "average" energy loss, which is the quantity more commonly given. The path ℓ will not correspond in length to a straight line in the original direction of the electron, for the electron also interacts with Coulomb field of the atomic nucleus, with a probability roughly proportional to Z^2 (Z = nuclear charge). Since the electron is much lighter than the nucleus, it does not lose energy but does change direction. This scattering is also subject to statistical fluctuations which appear as variations in the increase in path length and contribute further to the straggling in energy loss.

When the electron in question is one that has been ejected by a γ-quantum and counted by the spectrometer, we know only that it has been ejected somewhere within the converter and emerged from it with its direction and momentum within certain appropriate ranges. It is clear that it is not a simple matter to determine the energy of the primary γ-radiation easily and accurately from a collection of such data. A reasonably accurate

solution of this problem has been obtained by Hornyak.[17] It is also clear that there will be some difficulty in determining the intensity of the primary γ-radiation, since this requires essentially that we account for all the secondary electrons.

B. Photoelectrons

The most generally useful secondary electrons for detecting γ-radiation from a few kev to ~4 Mev with a β-ray spectrometer are photoelectrons, because they are initially practically monoenergetic* and their intensity compares favorably with that of other secondaries in this energy range. Sauter[22] has found the differential photoelectric cross section to be given by

$$d\sigma = f(h\nu)\, Z^5 \frac{\sin^2\omega\, d\Omega}{(1-\beta\cos\omega)^3}\left[\frac{\sqrt{1-\beta^2}}{(1-\beta\cos\omega)} + \frac{3(1-\sqrt{1-\beta^2})-2\beta^2}{2(1-\beta^2)}\right] \quad (1)$$

where $h\nu$ is the quantum energy, Z is the nuclear charge, β = the velocity of the ejected electron in units of the velocity of light, and ω = the angle between the quantum and the ejected electron. This expression is relativistically correct, but has been derived by the Born approximation, and thus holds only for $(2\pi Z/137\beta) << 1$. The Z^5 dependence indicates that it will be desirable to use the largest possible Z (e.g. thorium, Z = 90), where Sauter's result is not valid. However, the differential cross section has not been calculated to any better approximation, so that we are forced to use his important result that for high energy quanta the photoelectrons are ejected mostly in the direction of the quantum, half of the electrons

---

* It may be noted that photoelectrons ejected from the K-shell are of the order of five times as intense as those from the other shells, providing, of course, that the quantum energy is greater than the K binding energy.

being within a cone of half angle ω_o, where ω_o is given by

$$\cos \omega_o = \beta. \tag{2}$$

Exact numerical calculations of the total cross section for certain large values of Z and for two energies (0.69 and 2.2 $m_o c^2$) have been made by Hulme, et al.[23] They verify the values calculated from a formula due to Hall[24] and use Hall's expression to interpolate between their calculated points, although they point out that Hall's derivation is open to criticism. The calculations of Hulme, et al, have been experimentally checked, according to Heitler (Ref. 25, p. 124) at two points.

To determine the number of photoelectrons per γ-quantum that are ejected into the spectrometer acceptance angle we must know the effective thickness of the converter. The converter geometry is shown in Fig. 10a. The γ-radiation is considered to be isotropic and monoenergetic. The coordinates needed to describe photoelectric conversion are shown in Fig. 10b, where

ϵ = the angle between the γ-quantum and the spectrometer axis.

θ = the angle between the photoelectron and the spectrometer axis.

ω = the angle between the photoelectron and the γ-quantum.

ψ = the azimuthal angle of the photoelectron about the direction of the γ-quantum.

n,t = number of atoms per cm^3 and thickness of the converter.

We shall first neglect scattering. The effective converter thickness is

$$t' = \frac{t}{\overline{\cos \epsilon}} \tag{3}$$

where $\overline{\cos \epsilon}$ is the mean cosine of the angle between the spectrometer axis and the γ-ray, and may be estimated as follows.

If $\phi_K(\omega)$ is the probability per K electron that one quantum per unit solid angle in the range ϵ to $\epsilon + d\epsilon$ will eject a photoelectron per unit solid angle into the range ω to $\omega + d\omega$ and ψ to $\psi + d\psi$, then the number of such electrons is given by

$$dN = \frac{2nt}{\cos\epsilon} 2\pi\, d(\cos\epsilon)\, \phi_K(\omega)\, d(\cos\omega)\, d\psi. \tag{4}$$

The angles are related by the trigonometric relation

$$\cos\theta = \cos\omega\cos\epsilon + \sin\omega\sin\epsilon\cos\psi. \tag{5}$$

Differentiating, putting $d\epsilon = d\omega = 0$ and eliminating $\sin\psi$ one obtains, after some simplification

$$d\psi = \frac{d(\cos\theta)}{\sqrt{[\cos(\theta-\omega) - \cos\epsilon][\cos\epsilon - \cos(\theta+\omega)]}} \tag{6}$$

When this is substituted in (4) we get

$$\begin{aligned} dN &= \frac{4\pi nt}{\cos\epsilon} \frac{d(\cos\epsilon)\, \phi_K(\omega)\, d(\cos\omega)\, d(\cos\theta)}{\sqrt{[\cos(\theta-\omega) - \cos\epsilon][\cos\epsilon - \cos(\theta+\omega)]}} \\ &= N'(\theta, \epsilon, \omega)\, d\epsilon\, d\theta\, d\omega \end{aligned} \tag{7}$$

Then, with appropriate ranges of integration,

$$\overline{\cos\epsilon} = \frac{\int d\epsilon \int d\theta \int d\omega \cos\epsilon\, N'(\theta, \epsilon, \omega)}{\int d\epsilon \int d\theta \int d\omega\, N'(\theta, \epsilon, \omega)} \tag{8}$$

Since the range of θ corresponding to the acceptance angle of the spectrometer is small, we may replace $2\pi \sin\theta\, d\theta$ by Θ, the solid angle of the spectrometer and neglect this integration, putting in the mean value θ_o. Since the only expression we have for the angular distribution of the photoelectrons is the rather complicated one of Sauter, we make the

assumption that the photoelectrons are all emitted at the angle $\omega_o = \cos^{-1}\beta$ to the quantum direction. If σ_K is the total K-photoelectric cross section, and δ is the Dirac delta function, then the substitution can be written as

$$2\phi_K(\omega) = \sigma_K\, \delta(\omega - \omega_o) \tag{9}$$

Integration over ω then gives

$$\overline{\cos\epsilon} = \frac{\int d(\cos\epsilon) \left\{\left[\cos(\theta_o - \omega_o) - \cos\epsilon\right]\left[\cos\epsilon - \cos(\theta_o + \omega_o)\right]\right\}^{-1/2}}{\int \frac{d(\cos\epsilon)}{\cos\epsilon} \left\{\left[\cos(\theta_o - \omega_o) - \cos\epsilon\right]\left[\cos\epsilon - \cos(\theta_o + \omega_o)\right]\right\}^{-1/2}} \tag{10}$$

The substitution $x = \cos\epsilon$ reduces both of these integrals to forms found in integral tables. The limits of integration are $\epsilon_{min} = \theta_o - \omega$ and $\epsilon_{max} = \theta_o + \omega$.*

The result is

$$\begin{aligned} \overline{\cos\epsilon} &= \sqrt{\cos(\theta_o + \omega)\,\cos(\theta_o - \omega)} \\ &= \sqrt{\cos^2\theta_o - \sin^2\omega} \;=\; \sqrt{\beta^2 - \sin^2\theta_o}\,. \end{aligned} \tag{11}$$

Two possible sources of error in this may be mentioned. The first and most important is that the phenomenon of scattering has been neglected. One important effect of scattering, which has been observed experimentally for several γ-rays between 0.4 and 1.5 Mev, is that the number of photoelectrons that can be associated with the γ-ray (area under the curve--see Sec. D below) does not vary linearly with the converter thickness. This is undoubtedly a scattering phenomenon, and can be visualized roughly as

---

* Except that if $\epsilon_{max} \geq \pi/2$, the appropriate limit is $\pi/2 - \delta$, where δ can be estimated from the attenuation of the γ-radiation in the converter. This is an extreme case requiring, for example, $\theta_o = 60^o$, and photoelectrons of < 160 kev.

follows. For very thin foils, in which scattering is negligible, only those electrons originally ejected in the range $\theta_o \pm \Delta\theta_o$ (acceptance angle of the spectrometer) emerge from the foil in that range, and their energy losses will be small, so that they clearly belong to the photoelectron peak. As the foil thickness is increased, scattering starts to become appreciable. When the root mean square scattering angle, δ, is still small there is no noticeable effect (other than the linear variation with foil thickness), the number of electrons scattered out of the acceptance zone into the ranges $\theta_o + \Delta\theta_o$ to $\theta_o + \Delta\theta_o + \delta$ and $\theta_o - \Delta\theta_o$ to $\theta_o - \Delta\theta_o - \delta$ being roughly compensated by the number scattered into the acceptance zone from these ranges, since the number of electrons originally ejected at an angle θ is proportional to $(\cos^2\theta - \cos^2\omega_o)^{-1/2} \approx \cos\theta^{-1}$. However, in the cases with which we are concerned, where β for the electrons is ~ 1 and θ_o is small (30^o or less), there are a large number of electrons at large $\theta\left[\sim(\pi/2 - \cos^{-1}\beta)\right]$ that were ejected by γ-rays travelling roughly parallel to the converter foil. When δ becomes large enough so that these electrons are scattered into the acceptance zone, a rapid increase in the number of photoelectrons counted is expected (and is observed experimentally).*

On the other hand, for foils thick enough so that scattering is important, we begin to find energy losses sufficient to place the electrons down in the continuous background of Compton electrons or scattered photoelectrons from higher energy γ-rays, so that they can no longer be clearly associated with the photo-peak in question. With further increases in foil thickness, this second effect becomes predominant, and we reach a "saturation" thickness beyond which additional converter produces no effect on the

---

* For examples, see Fig. 27 and Ref. (17), Figs. 34, 35, and 36.

photo-peak (until, eventually, attenuation of the primary radiation becomes noticeable).*

The problem of scattering, with energy loss neglected, can be treated theoretically by considering Bothe's[26] diffusion equation, which may be written for our case

$$(1 - \mu^2) \frac{\partial^2 f}{\partial \mu^2} = 2\mu \frac{\partial f}{\partial \mu} + \mu \frac{\partial f}{\partial x} + \frac{\partial f}{\partial l} \qquad (12)$$

Here $f = f(\mu, x, l)$ is the distribution function (per unit solid angle) for electrons of velocity $\vec{V}$ in an infinite plane sheet of material. The x coordinate axis is taken normal to the plane and μ is the cosine of the angle between $\vec{V}$ and the x-axis. Electrons are presumed to originate at the face $x = 0$ and to have an initial value of $\mu > 0$. l is the actual distance travelled by an electron in going from $x = 0$ to x. x and l are both measured in units of the diffusion length λ, defined by

$$\frac{1}{\lambda} = 2\pi N \int_\alpha \sigma(\alpha, V)(1 - \cos\alpha) \sin\alpha \, d\alpha. \qquad (13)$$

Here N is the number of scattering centers (nuclei) per unit volume and $\sigma(\alpha, V)$ is the cross section for single scattering, α being the scattering angle. The lower limit on α is set by the screening of the nuclear Coulomb field (scattering field) by the atomic electrons. The upper limit, of no great importance since σ becomes small for large angles, is usually taken as $\pi/4$.

Solutions of this equation have been discussed by Bothe[26] and by Bethe, Rose, and Smith.[27] A particularly simple approximate solution, well-adapted to our work, has been developed by R. G. Thomas in unpublished

---

* See footnote, previous page.

work done at this laboratory. He starts by assuming that the second derivative is small, and that for the region of interest $\mu \sim 1$. The first order equation thus obtained is easily solved by standard methods. If $f_o(\mu)$ is the original distribution of electrons before any scattering, then he gets a relation between l and x (the "umweg factor")

$$l = -x_m \ln\left(1 - \frac{x}{\mu x_m}\right) \tag{14}$$

where x_m is a scattering length defined by

$$x_m = \frac{\lambda}{2} , \tag{15}$$

and an electron distribution

$$f = f_o\left(\mu - \frac{x}{x_m}\right) \tag{16}$$

Now according to eq. (11), $f_o(\mu, o)$ is given by

$$f_o(\mu)\ d\mu\, dx = \frac{N \sigma_K d\mu dx}{\cos \epsilon} = \frac{N \sigma_K d\mu\, dx}{\sqrt{\mu^2 - \sin^2 \omega_o}} \tag{17}$$

Those electrons originating at x = 0 then have a distribution

$$f(\mu,x)\ d\mu\, dx = \frac{N \sigma_K d\mu\, dx}{\sqrt{\left(\mu - \frac{x}{x_m}\right)^2 - \sin^2 \omega_o}} . \tag{18}$$

One thing particularly notable about this distribution is that it becomes infinite at $\mu - (x/x_m) = \sin^2 \omega_o$. This we know to be too extreme. Thomas therefore expands $f(\mu,x)$ in a power series in x/x_m and keeps only the first two terms. This gives

$$f(\mu,x)\, d\mu\, dx = \frac{N \sigma_K d\mu dx}{\sqrt{\beta^2 - \sin^2 \theta}} \left[1 + \frac{\cos \theta}{\beta^2 - \sin^2 \theta} \frac{x}{x_m}\right] \tag{19}$$

We can therefore write for the number of electrons formed in the converter and emerging from the face at x = t and at the angle θ_o (acceptance angle of the spectrometer)

$$Id\mu = \frac{N\sigma_K d\mu}{\sqrt{\beta^2 - \sin^2\theta_o}} \int_o^t dx \left[1 + \frac{\cos\theta_o}{\beta^2 - \sin^2\theta_o} \frac{t-x}{x_m}\right]$$

$$= \frac{N\sigma_K d\mu}{\sqrt{\beta^2 - \sin^2\theta_o}} t \left[1 + \frac{1}{2} \frac{t}{x_m} \frac{\cos\theta_o}{\beta^2 - \sin^2\theta_o}\right] \qquad (20)$$

$$= \frac{N\sigma_K t d\mu}{\cos\epsilon}$$

This expression is not too accurate, since the approximations made in the diffusion equation are not valid where it will generally be used. However, it is simple and easy to use, and its general behavior for variations in converter thickness seems quite reasonable. It certainly contributes no more error, and probably much less, than the original assumption we were forced to make in deriving it, that all the electrons corresponding to the known total photoelectric cross section, σ_K, are ejected at the angle $\omega_o = \cos^{-1}\beta$ to the γ-quantum.

The order of magnitude of the error resulting from this approximation, which is the second source of error to be considered, may be estimated roughly. If one calculates from Sauter's expression the ratio of the differential cross section at the median angle $\omega_o = \cos^{-1}\beta$ to that at $\omega = \pi/2$, one gets for 400 kev electrons ($\beta = 0.83$), for example, $d\sigma(\omega_o)/d\sigma(\pi/2) = 36$. With our converter geometry, it is possible for a γ-ray at very close to 90° to the spectrometer axis to have a path through the converter very long compared to the converter thickness (a factor of

100 is possible, and in practice this factor is probably between 25 and 50). This will give an appreciable number of electrons that are not accounted for by eq. 20. It is not clear how this can be corrected, especially since Sauter's formula can be only very approximately correct for the large values of Z of interest. However, a rough correction term may be added to eq. 20. It may be noted that according to the general picture of the effects of scattering, as given above, scattering out for these particular electrons will be compensated by scattering in. Eq. 20 may be then rewritten as

$$Id\mu = Nt\, d\mu \left\{ \frac{\sigma_K}{\cos \epsilon} + b\, \sigma_K \frac{d\sigma(\pi/2)}{d\sigma(\omega_o)} \right\} \qquad (21)$$

Here b is a constant that depends on the converter geometry. For practical cases, it is not too easy to evaluate because of departures from the idealized geometry (e.g.--converters will not be exactly flat), but may be evaluated empirically, as in Sec. V C.

We must conclude, however, that with our general type of source-converter geometry, which is designed to give the maximum conversion efficiency, we cannot expect to get absolute intensities of γ-radiation, or relative intensities for γ-rays differing much in energy, with any great accuracy. Changes in the geometry may be made that would improve this situation. Even then, it would seem that the only completely satisfactory experiment would be one in which the distribution of photoelectrons with respect to the direction of the γ-radiation is actually measured.

C. Compton electrons

The situation as far as the use of Compton secondary electrons is concerned is much better. The differential cross section is given by the well-known Klein-Nishina formula for any energy or converter of interest in the present type of experiment. The number of Compton secondaries ejected depends only on the number of electrons in the converter, so that any element is roughly equally suitable as a converter, and we can thus avoid the heavy elements and the associated large scattering.*

Since the Compton electrons have a continuous energy spectrum, they are not as convenient, in some ways, as photoelectrons. There is some preference, which increases with increasing energy, for electrons to be ejected with the maximum possible energy, but below about 3 Mev, the resulting peak is not as prominent as the photoelectric peak from a heavy converter of equivalent thickness (measured in units of electron energy loss), and the continuous spectrum introduces a troublesome background if more than one γ-ray line is present.

The Klein-Nishina formula has been applied to our spectrometer and converter geometry (as in Fig. 10) by Hornyak.[17,28] His result is given by

$$\frac{dW'}{dp} = \frac{4\pi^2 n_e t r_0^2 \left[(\gamma+1)^2 + a\right]^{1/2}}{\gamma\mu(a+1+2\gamma+2\gamma^2)} \cdot$$

$$\cdot \left[1 + \left(\frac{a-1}{a+1}\right)^2 + \frac{4\gamma^2}{(a+1)(a+1+2\gamma)}\right] \cosh^{-1}\left[\frac{x}{\sqrt{\frac{a}{a+(1+\gamma)^2}}}\right]_{x=\cos\theta_1}^{x=\cos\theta_2} \qquad (22)$$

---

* There is some advantage in using elements in the neighborhood of copper where the energy loss of a fast electron per converter electron is a minimum.

where

$$\frac{p}{p_{max}} = \frac{\left[1 + \frac{a}{(1+\gamma)^2}\right]^{1/2}}{\left[1 + \frac{a}{1+2\gamma}\right]} , \qquad p_{max} = \frac{2\gamma\mu(\gamma+1)}{2\gamma+1} \tag{23}$$

Here dN''/dp is the number of electrons per unit momentum interval ejected into the acceptance angle of the spectrometer (θ_1 to θ_2) by one quantum of isotropic γ-radiation per unit solid angle, a is a convenient parameter, and

p = electron momentum times c, in units of m_0c^2,

n_e = number of electrons/cm^3,

t = converter thickness,

r_0 = classical electron radius,

γ = primary quantum energy in units of m_0c^2,

$\mu = m_0c^2$.

dN''/dp is the primary spectrum, before the effects of the finite resolving power of the spectrometer and of energy loss in the converter have been considered. The effect of finite resolving power will be considered in Section E. Energy loss effects will be considered later, in connection with experimental results.

D. Positron-electron pairs. Internal conversion.

γ-radiation of energy greater than 1.022 Mev can also be detected by positron-electron pairs created as the radiation traverses matter. The positrons and electrons separately exhibit a continuous distribution in energy (the total energy of the two components of one pair must add up to the γ-ray energy, of course), so that a large part of the whole spectrum must be investigated. The cross section for pair production is known

fairly accurately[25,29] but is rather low at energies below 5 to 10 Mev, so that we have not found pairs particularly useful in our work.

An excited nucleus that would normally decay by γ-emission may also decay by ejecting one of its own atomic electrons in a direct interaction between the nucleus and the electron or through the intermediate step of a γ-quantum being emitted and then absorbed. Heitler (Ref. 25, p. 128) points out that the direct interaction is the more probable, and increases rapidly with the multipole order of the radiation, so that these so-called internal conversion electrons cannot be used to measure γ-ray intensity (more exactly, the number of excited states present) but rather if the number of γ-rays can be determined, the number of conversion electrons can be used to determine the multipole order of the γ-radiation from theoretical calculations. These electrons may be very useful in determining γ-ray energies precisely since there is no need for a converter, and thus no problem of energy loss or scattering.* Unfortunately, for the cases we are interested in, nuclear reactions in light elements, the internal conversion electrons are very few, because of the low Z of the nucleus and the high energy of the γ-radiation (indeed, it may happen, because of the recoil velocity of the excited nucleus, that decay by quantum emission may occur before the nucleus has picked up any atomic electrons).

If sufficient energy for pair formation is available, the emission of electron-positron pairs may similarly compete with quantum emission. The probability of such internal pair formation has been discussed most recently by Rose.[30] Such pairs have been detected in this laboratory.[31] Since

---

* The γ-rays from the natural radioactive elements have almost all been identified by the internal conversion lines. See (16), for example.

the probability of forming such pairs does not vary much with the multipole order of the transition, they may be used for rough intensity measurements or, with considerable care, for determining the multipole order of the radiation when the intensity of the γ-radiation is known.

In certain cases, both the excited state and the ground state of the nucleus may have a total spin equal to zero. Transition between these two states by emission of a single quantum is then absolutely forbidden. If there is no intermediate state of different character, then the transition may be by ejection of an internal conversion electron,* by the emission of an electron-positron pair** or by the emission of two quanta with a continuous energy distribution in a double transition through intermediate states of higher energy (possible because of the uncertainty principle).

E. Effect of instrument window

Even if we know the primary energy or momentum spectrum per γ-ray of the secondary electrons as they emerge from a converter into the cone defined by the acceptance angle of the spectrometer, we are still not prepared to say how many electrons will appear at the counter at the other end of the spectrometer at a certain setting of the magnetic field. To do this, we must investigate the effect of the finite resolution of the spectrometer. Analytic functions for calculating this effect have been given by Owen and Primakoff[33] and by Hornyak.[17] The discussion here is from a slightly different point of view, in order to emphasize certain physical features of the result.

---

* If no change in parity is involved. Ellis and Aston[32] report an example of this in the 1.426 Mev level in RaC.

** As in the $F^{19}(p,\alpha)O^{16*}$ reaction discussed in Sec. IV.

The instrument "window" curve may be defined as the plot of counts per electron emitted from a source of monoenergetic and spatially isotropic electrons (e.g., internal conversion electrons from a suitably thin source) versus magnetic field (or current j through the field coils) in the neighborhood of that current j_o corresponding to the momentum p_o of the electrons. The value of j giving the maximum counts is usually taken as j_o (an alternate choice is the straight line extrapolation of the high current edge to zero counts). The resolution is $\sigma = \Delta j/j_o$ where Δj is the full width at half maximum. If we now determine the window curve with an internal conversion line of different momentum, p_o', we find that the peak height (counts per electron from the source) and σ are unchanged, as follows from the focusing properties of the instrument. As was pointed out previously, because σ is constant, and not Δj, we get a clearer picture of a primary spectrum if we divide the number of counts at each current by the current. If this is done for the two internal conversion lines, the area under the curve, rather than the peak height, is constant.

We must decide what the constant of proportionality is between the peak counts and the total number of electrons per steradian emitted by the source. It is related to the solid angle of the spectrometer, of course, and is equal to it to a first approximation. When we attempt to make a better approximation, we encounter certain difficulties which are essentially resolved when we realize that the solid angle is not well defined, even with a very small electron source. This is because the stops that define the transmission zone of the spectrometer are not placed close to the source,*

---

* This is absolutely essential if the spectrometer is to be used in observing secondary electrons from γ-radiation. Any stops in the spectrometer that are irradiated by γ-radiation will be secondary sources of electrons. The number of these electrons counted in the spectrometer will be large if the secondary sources are too close to the true source position.

but more towards the middle of the spectrometer. For example, suppose that with our small internal conversion source, the current is set at j_o, corresponding to the peak. Electrons leaving the source at angles to the axis between a certain θ_{max} and θ_{min} will all be counted where θ_{max} and θ_{min} are determined by the electron paths and the defining stops in the middle of the spectrometer. If we then increase the current by a small amount δj, the curvature of all electron paths will be increased slightly. Since these are concave towards the axis, we now find that an electron leaving the source at a slightly larger angle, $\theta_{max} + \delta\theta$, will be able to get past the first defining stop, and will be counted if $\delta\theta$ is not too large (θ_{min} goes to $\theta_{min} + \delta\theta'$, with $\delta\theta' > \delta\theta$, at the same time, so that there is a net loss in counts to correspond to the observation that we have moved off the peak of the curve). Thus although the natural definition of the solid angle of the spectrometer is as that solid angle corresponding to the maximum and minimum values of θ for any currents in the neighborhood of j_o (this solid angle will be designated by Ω or Ω_{eff} depending on whether or not the effect of obstructions in the transmission zone has been subtracted), for our present purposes we adopt the more restricted definition that it corresponds to θ_{max} and θ_{min} for j_o, the current corresponding to the peak of the window curve obtained with a small internal conversion line source, or that it is by definition equal to the ratio of the number of counts at this peak to the number of electrons per steradian emitted by the source. The solid angle defined this way will be designated by Θ, and is in steradians.

We must next consider the effect of source size. The curves of Fig. 9 show what happens when we move a small source off center by a fairly large

amount. In particular, it is to be noted that the area under the various curves is constant (and will also be constant, because of the small range of currents, if we divide the ordinates by the current). Thus if we increase the diameter of our small source within the limits set by experiments such as the above, keeping the activity constant, the total area under the curve will remain constant. However, we will also observe some flattening of the top of the window curve (see Fig. 4b, where the two sources are not of the same activity, for an example). This flattening may be reduced, if desirable, by increasing the separation of the ring focus stops, which will increase both Ω and Θ to a small extent. We are thus led to two general rules for obtaining values of Θ for various source sizes:*

a. If none of the spectrometer stops are changed, and Θ_0 has been measured with a source giving a half-width σ_0, and if the change in source size is small enough so that the shape of the window curve is not changed greatly, we will have from the equality of the two areas for sources of the same activity

$$\Theta_0 \sigma_0 = \Theta\sigma \tag{24}$$

b. If any stops are adjusted, then Θ must be redetermined, using a source of know activity and of the diameter desired.

---

* Two qualifications may be made at this point. For low energy electrons scattering in the spectrometer, back-scattering in the source, reduction of the counter efficiency (because of the counter window thickness), and stray magnetic fields may all contribute to a distortion of the window curve that must be taken into account. Also, the method for measuring Θ actually used, as described in Sec. II F, is applicable only with "small" sources.

It is generally observed with lens type spectrometers that when the ring focus stops are set to give a window curve of the maximum sharpness the curve is symmetric and quite closely described by a Gaussian function. We therefore take

$$W(j_o,j) = \frac{\Theta}{4\pi} \exp\left[-\frac{(j-j_o)^2}{\Delta^2 j_o^2}\right] \tag{25}$$

where $$\Delta = \frac{\sigma}{2\sqrt{\ln 2}} \ .$$

$W(j_o,j)$ is the probability that an electron of momentum $j_o = p_o$ leaving the source with a random distribution of initial angle will be counted when the spectrometer field current has the value j. Because the Gaussian is only an approximation to the window curve and is probably not valid unless $\Delta << 1$, it will be assumed that the denominator in the exponential can be written as any of the forms $\Delta^2 j_o^2 \cong \Delta^2 p^2 = \Delta^2 j^2 = \Delta^2 jp$. For some purposes it is desirable to use the last form, which makes $W(p,j) \rightarrow 0$ for either $j \rightarrow 0$ or $p \rightarrow 0$.

If we are observing an isotropic primary distribution for which the number of electrons per steradian having momenta between p and p + dp is given by f(p) dp, then the number of counts registered by the spectrometer at a current j will be

$$C(j) = \int_p W(p,j)\ 4\pi\ f(p)\ dp \tag{26}$$

If $\Delta << 1$ and if the primary distribution does not change rapidly within a distance $p\Delta$ (if $\partial f/\partial p \cdot p\Delta \ll f(p)$), then Hornyak[17] has shown that this integral can be evaluated approximately to give

$$C(j) = \Theta\Delta\sqrt{\pi}\ j\ f(j) \tag{27}$$

and for $\Delta << 1$ (with no restriction on the variation of f(p)

$$\int_0^\infty \frac{F(j)\, dj}{j} = \Theta\Delta\sqrt{\pi}\int_0^\infty f(p)\, dp \tag{28}$$

where we note that the integral on the right is the total number of electrons per steradian from the source, and that on the left is the area under the experimental counts per unit momentum interval versus momentum curve.

In practice when it is desired to calculate C(j), and when the conditions for Eq. 27 are not satisfied, it will not always be possible to perform the integration of Eq. 26. The integral must then be evaluated numerically which may be tedious if any large range of j is to be covered, because of the term $\Delta^2 j^2$ in the exponential--i.e., because the width of the window is a function of j. Professor Christy has pointed out that it is quite simple to plot f as a function of $\ln$ p and to fold in a window curve of constant width and height by numerical integration. This is equivalent to folding in a window of constant height and constant percentage width in a plot against p, which is precisely what we want. The process is illustrated in Fig. 11 for two rectangular primary distributions of equal areas (intensity) but different momenta. The results are shown in Fig. 12. The only approximation involved lies in taking the window curve as Gaussian on either plot. Analytically we have

$$\begin{aligned} \frac{C(j)}{j} &= \Theta\int \frac{dp}{j} f(p) \exp\left[-\frac{(j-p)^2}{\Delta^2 j^2}\right] \\ &\approx \Theta\int \frac{dp}{p} f(p) \exp\left[-\frac{(1-p/j)^2}{\Delta^2}\right] \end{aligned} \tag{29}$$

Since $j \approx p$ when the exponential term is $\neq 0$.

Substituting

$$\ln p = \zeta \qquad \text{and} \qquad \ln j = \eta$$

we have

$$1 - \frac{p}{j} = 1 - e^{\zeta - \eta}$$

$$\approx \eta - \zeta .$$

Then

$$\frac{C(j)}{j} \approx \Theta \int d\zeta \, f(e^{\zeta}) \exp\left[- \frac{(\zeta - \eta)^2}{\Delta^2} \right] \tag{30}$$

F. Yields from nuclear reactions

The methods described in the previous section for determining the intensities of γ-radiation are applied in this thesis to γ-radiation arising from certain nuclear reactions. Here we are interested not only in the relative intensities of several γ-rays produced in the same reaction, but also in the absolute yields of the radiation. The general techniques and concepts of experimental nuclear physics have been discussed in many previous papers, of which Bethe's classical articles in the Reviews of Modern Physics[34,35,36] and the recent discussion of γ-ray yields by Fowler, Lauritsen, and Lauritsen[37] may be mentioned in particular. No further discussion will be attempted here, except occasionally in the discussion of particular experiments.

IV. Radiation from the Bombardment of Fluorine with Protons*

A. Reactions

When fluorine is bombarded with protons in the energy range 0 to 2 Mev, γ-radiation, electron-positron pairs not associated with γ-radiation, and α-particles are observed. The several groups of α-particles arise from the reaction

$$F^{19} + H^1 \rightarrow (Ne^{20}) \rightarrow O^{16} + He^4 \qquad (Q = 8.12 \text{ Mev})$$

in which the residual nucleus, O^{16}, may be left in the ground state or in one of a number of excited levels whose subsequent decay to the ground state accounts for the γ-radiation and pairs.** Which of the O^{16} states is formed depends markedly on the proton energy, and the resonances for production of long range α-particles (ground state), pairs, and γ-rays have been intensively studied.(39,40,41)

The pairs arise from the lowest excited state of O^{16}, from which γ-radiation is presumably forbidden by the selection rule excluding $J = 0$ to $J = 0$ transitions. The state thus decays by emission of an electron-positron pair which is created by forces acting only within the nucleus. It is this feature of the forces from which the distinction between "nuclear" and "internal conversion" pairs arises since, in the latter case, the pairs are formed in a distance of the order of the Compton wave length from the emitting nucleus.(42) The maximum energy of the nuclear pairs of O^{16} has been determined by Tomlinson(43) as 4.9 ± 0.2 Mev, giving a level energy of

---

* This section is based on a paper by Rasmussen, Hornyak, Lauritsen, and Lauritsen, Phys. Rev. 77, 617 (1950).

** Capture γ-radiation, from transition to the ground state of Ne^{20} has also been observed.(38)

5.9 ± 0.2 Mev. The spectrum has been investigated by Kojima[41] and shown to be consistent with the hypothesis of their nuclear origin. The angular correlation between electrons and positrons has also been shown by Devons and Lindsay[44] to be consistent with theoretical expectations, and Devons, Hereward, and Lindsay[45] have measured the half-life of the state as 7×10^{-11} sec. A part of the work of this section relates to a more accurate determination of the pair end point and of the momentum distribution.

Walker and McDaniel[3] have shown that the γ-radiation comprises two components, at 6.13 ± 0.06 and 6.98 ± 0.07 Mev, the relative intensities of which depend on bombarding voltage. This result has recently been confirmed by Burcham and Freeman[46] who have observed the corresponding α-particle groups but who find indication of a third α-group at the 939 kev resonance, suggesting that an additional γ-ray of energy about 7.2 Mev should exist. These observations have been extended in this laboratory[47] to show that all three groups exist at this and other resonances, with varying relative intensities. Further measurements of the γ-ray energies and intensities as a function of bombarding voltage are reported in this section.

B. Experimental details

The thin lens arrangement of the spectrometer described in Sec. II was used for most of this work. The stops were set to give a resolution of 2.3%, and electrons leaving the target at angles to the axis of 9° to 16° were accepted. The various resonances were identified by running rough excitation functions for both the γ-radiation as measured by a γ-ray counter shielded by 1 inch of lead and the pairs as measured by the counts recorded by the spectrometer when set to the peak of the pair distribution. The resonance energies quoted are those of Bennett, et al[40] multiplied by

873.5/862 to conform to the presently accepted voltage scale.[48] An example of such an excitation function is given in Fig. 13. This curve was run against the current through the analyzer magnet. The upper voltage scale was obtained by assuming that mid-point of the initial rise on the γ-ray curve corresponded to 873.5 kev (since the target was $\sim$50 kev and the resonance is only 5 kev wide) and that the analyzer current and momentum of the accepted protons were linearly related.*

Particularly in the work on pairs, considerable attention was given to the problem of distortion of the spectrum by scattering. The first experiments were made with a thin ($\sim$50 kev stopping power for 900 kev protons) CaF_2 target evaporated on 0.001 inch copper foil using only the minimum number of baffles required to define the spectrometer acceptance angle and annular focus. The resulting spectra contained a relatively large number of electrons and positrons with energies below 1 Mev. Subsequent work with the spectrometer, using the well known N^{13} positron spectrum for checking, gave indication of excessive scattering in the arrangement used. This scattering was greatly reduced by using additional baffles and by breaking up surfaces that were nearly parallel to the electron paths for long distances. The pair spectrum was redetermined sometime later, using the separated coil configuration, with particular emphasis on the low energy region. As a further precaution against scattering, a target consisting of a 0.3 mg/cm^2 Be foil which had been exposed to HF vapor was used.** Data taken with the new arrangement agreed well with the earlier

---

* The second γ-ray resonance on this curve is not quite well enough defined to allow one to make a correction for the residual magnetism of the magnet, which, however, is probably quite small.

** Blank Be foils showed negligible yield at the proton energies used.

results above 2.0 Mev electron energy, but indicated fewer electrons below this energy, the deviation increasing with decreasing energy to about a factor of 2.5 at 0.5 Mev. All the earlier points below 2.5 Mev have been rejected in plotting the final data.

For γ-ray measurements, Compton electrons ejected from a 250 mg/cm^2 beryllium disc roughly 1 cm in diameter were observed. The same CaF_2 on copper foil target used in the early pair measurements served as the target, and a γ-ray counter, shielded by 1 inch of lead was used as a monitor. Using this same target and a .005-inch thick by 3/8-inch diameter thorium foil as a photoelectric converter, a rough survey of the region corresponding to γ-ray energies from 0.4 to 2.9 Mev was made.

C. Results - Nuclear pairs

Fig. 14a and b presents the momentum distribution of positive and negative components respectively, as observed at the 1236 kev pair resonance. Fig. 15a and b presents the portions near the end points. Field insensitive cosmic ray and local laboratory background of about 3% of the peak height has been subtracted from the data presented. Uncertainties in this background are important only for the first three or four low energy points, where the additional error may amount to as much as the statistical probable error shown.

The solid curves in Figs. 14 and 15 are calculated from the theoretical expressions given by Oppenheimer,[49]* modified slightly by inclusion of the

---

* I am greatly indebted to Dr. E. R. Cohen for these calculations. Oppenheimer's differential distribution for the nuclear pairs is $dN = p_+p_- (E_+E_- - m^2c^4 + p_+p_-c^2 \cos\theta) \sin\theta \, d\theta \, dE_+$. Integrating over all angles and introducing the Coulomb factor gives

$$dN \propto \frac{(E_+E_- - m^2c^4)\, p_+ \, dp_+}{(e^{\zeta_+} - 1)(e^{-\zeta_-} - 1)E_+} \qquad \text{where} \quad \zeta_{\pm} = \frac{2\pi Zmc}{137\, p_{\pm}}$$

Coulomb factor (as in the case of ordinary pair formation) (Ref. 25, p. 197), and including the effect of finite instrument resolution. For comparison, the calculated distribution of internal conversion pairs[50] from electric dipole radiation is shown by the dashed curve in Fig. 14a (higher multipole orders lead to somewhat flatter distributions). It is of interest to observe that the apparent end point of the positron spectrum is some 60 kev higher than that of the electron distribution. The difference results from the effect of the Coulomb factor, which gives a non-zero probability of finding a positron of maximum energy in the primary spectrum but a probability approaching zero of finding an electron of maximum energy. With the resolution used in these experiments, this appears as a difference in the end points for positrons and electrons (compare Figs. 15a and b, where the spectra before folding in the window curve are shown by dashed lines).

The choice of the energy parameter in making the best fit of the theoretical distribution to the experimental points permits the determination of the maximum energy of either the positive or negative component to an accuracy that is limited, in our case, only by the accuracy to which the spectrometer calibration is known. This maximum energy was taken as the same for both positive and negative components, 5.017 ± 0.03 Mev, including the most probable energy loss in the copper backing of 18 kev.* The energy of the O^{16} level involved is obtained by adding the rest mass of the pair to the observed maximum energy, yielding 6.04 ± 0.03 Mev. No Doppler shift

---

* The spectrometer calibration is based on $B\rho$ = 10,000 gauss-cm for the K-line from a ThB deposit. The end point quoted was determined from the data taken with the CaF_2 on copper target. Data taken with the BeF_2 target give 5.022 ± 0.04 Mev. The higher energy points taken with this target have been shifted down by approximately 10 kev to facilitate comparison with the earlier data.

correction has been included in this value, since Devons, et al[45] have shown that the lifetime of this state is 7×10^{-11} sec, while the average stopping time for the excited O^{16} nucleus in the CaF_2 target is about 10^{-13} sec.

The CaF_2 on copper target was also used to observe the upper half of the positron spectrum at the 939 kev γ-resonance. The results are shown in Fig. 16 where the two curves marked "Internal Conversion" represent the distribution of internal conversion pairs from the 6.1 Mev γ-ray if their contribution to the peak of the observed distribution is taken as 10% or 20% respectively. The upper curves are then obtained by adding appropriately normalized nuclear pair distributions (end point = 5.02 Mev) to these.*

The curves for which 10% of the peak height (= 17% of the area) is attributed to internal conversion pairs seem to fit the data reasonably well, although one cannot rule out anything between 5% and 15%. If one takes the yield of 6.1 Mev quanta as 11.5×10^{-8} γ/proton for this target and voltage (see Table IV), one can calculate that this corresponds to a conversion coefficient of 1.9×10^{-3} pairs per quantum. Rose[30] has calculated these coefficients for various multipole orders of γ-radiation. His results for 6.1 Mev γ-radiation are

Table III

Radiation	Electric dipole	Magnetic dipole	Electric quadrupole	Magnetic quadrupole	Magnetic 2^5 pole
pairs per quantum	2.3×10^{-3}	1.6×10^{-3}	1.8×10^{-3}	1.3×10^{-3}	0.97×10^{-3}

* Note that pairs from the conversion of γ-radiation in the copper would be about 1/10 the intensity of the internal conversion pairs. The background sketched in includes roughly the internal conversion pairs from the 7 Mev γ-radiation. The effect of the window curve at the end point has been estimated for the upper curves only.

Our value of the conversion coefficient thus corresponds to electric quadrupole radiation. The uncertainty of $\pm \sim .9 \times 10^{-3}$ however, covers the whole range of radiation for which Rose performed his calculations. It might be pointed out that especially with the larger solid angle (3 times) presently available, the multipole order of the radiation could be determined accurately and with not too much effort. By using a 15 instead of a 50 kev target one would reduce the intensity of the nuclear pairs by a factor of three without affecting the γ-ray yield very much (see excitation curves of Ref. 40), and by running the Compton secondaries from a suitable converter with the same arrangement, the additional errors of an absolute yield determination would be avoided.

The original purpose of this particular experiment was to determine whether or not other pairs would distort the nuclear pair spectrum as taken at a nuclear pair resonance. Since the distortion at the γ-ray resonance is found to be small, that at the pair resonance may be assumed to be completely negligible.

D. Results - Gamma radiation

Curves showing the distribution of recoil Compton electrons observed for proton bombarding energies corresponding to the γ-ray resonances at 873.5, 939 and 1381 kev are presented in Figs. 17 and 18a and b. Sufficient data were also obtained at the 1353 kev resonance to make possible an estimate of the relative intensities of the γ-rays, but not a precise determination of their energies. The energies and relative intensities of the various γ-rays were determined by comparing the observed distributions with those calculated from Eq. 22, Sec. III C.

The instrument window was folded into this by the method of Sec. III E. Assumptions must then be made as to the distribution in energy loss for electrons originating uniformly throughout the thickness of the converter. In view of the high energy of the electrons and the low atomic number of the converter, the distribution was taken as rectangular and of constant width, on a momentum scale, over the range of moments involved. The width of the rectangle was determined experimentally by observing the end point of the nuclear pair distribution through the same 250 mg/cm^2 Be that was used as the Compton converter (see Fig. 15a). The curve was shifted down by 345 ± 15 kev, which is somewhat larger than the most probable energy loss calculated for this thickness of beryllium. To this number must be added the most probable energy loss of 18 kev for .001 inch of copper. The best fits, shown by the curves of Figs. 17 and 18, were finally obtained by using a rectangle 410 kev wide of which perhaps 10 kev may be attributed to the effect of Doppler broadening.* The agreement with the experimental points is considered satisfactory down to and including the peak. The departure below the peak is, at least in great part, the result of using a rectangular distribution in energy loss. Energy loss distributions of the type used in Sec. V, where to a rectangular distribution somewhat less in width than the most probable energy loss, a triangle extending somewhat beyond this value, and a long tail extending beyond the average energy loss are added, would undoubtedly give much better results. The fit on the high energy side is quite insensitive to such modification since both the initial peak of the primary Compton spectrum and the instrument resolution are

---

* The Doppler broadening of the 6.1 Mev γ-ray due to motion of the excited O^{16} nucleus in the center of mass system is about 120 kev. This is small enough compared to the converter thickness that its effect is negligible, as is discussed in Sec. V.

narrower than the assumed rectangle. For this reason, and because the calculated curve makes more effective use of the data than would a simple extrapolation of the high energy edge, the parameters of the best calculated curves were used to obtain the maximum momentum of the Compton electrons from which the γ-ray energies are determined by adding the minimum energy of the recoil quanta. A Doppler correction of 1/4% for the center of mass motion is subtracted from the γ-ray energy to obtain the level energy since the half-life for 6 Mev electric quadrupole radiation, for example, is $\sim 5 \times 10^{-15}$ sec, compared to the stopping time for the O^{16} nucleus of $\sim 10^{-13}$ sec. The results are given in Table IV, where the relative intensities of the two γ-rays appearing at each resonance, as obtained from the calculated fits, are also presented.

The solid angle of the thin lens arrangement used in most of these experiments was extrapolated from the results of the measurements described in Sec. II F, by means of the ThB X-line, a monitor counter being used to check the source activity. The result was $\Theta = 1.15 \pm .2\%$ of 4π. Because of other uncertainties in the current measurement and the target thickness, the yields given in Table IV may be in error by as much as 40%. Table V gives a comparison with yields obtained by other observers. Steps in the calculation of these yields, other than those involving standard resonance yield calculations, are the same as those used in Sec. V C.

The search for low energy γ-radiation, which just overlaps that of Walker and McDaniel,[3] gave essentially negative results, as is seen in Fig. 19 where statistical errors for representative points are given. In particular, at the 939 kev resonance where this data was taken, radiation of 0.95 Mev corresponding to the transition between the 7.09 and the 6.14 Mev states is possible. Since it is expected that the height of the photo-

electron peak from a γ-ray of this energy would be a constant independent of converter thickness (because of large energy loss and straggling effects) at a thickness between .001 and .002 inches, it was assumed that the step in the secondary electron spectrum due to K-photoelectrons from this line would be the same as if the converter were .001 inch thick, all the photoelectrons were emitted in the direction of the γ-ray, and the energy loss in the converter were negligible (i.e., these electrons were monoenergetic). This then gives

$$N = \frac{\text{counts}}{1\ \gamma/4\pi\ \text{ster.}} = \Theta N_a \sigma_K$$

$$= 1.15 \times 10^{-2} \times .725 \times 10^{20} \times .87 \times 10^{-23}$$

$$= 0.73 \times 10^{-5}$$

where Θ is the spectrometer solid angle in per cent of a sphere, N_a is the number of thorium atoms per cm^2 of converter and σ_K is the K photoelectric absorption cross section (2 K electrons per atom). From the experimental upper limit for this step, indicated by the short horizontal lines in Fig. 19, one gets

$$c < 2 \times 16 \text{ counts per } 77 \times 6.24 \times 10^{12} \text{ protons}$$

or

$$c < 0.67 \times 10^{-13} \text{ counts/proton}$$

$$Y(0.95) = \frac{c}{N} < \frac{0.67 \times 10^{-13}}{0.73 \times 10^{-5}} \frac{\gamma}{\text{proton}} = 0.92 \times 10^{-8}\ \gamma/\text{proton}$$

The corresponding yield of the 7.1 Mev radiation is 0.34×10^{-7} γ/proton. Then

$$\frac{Y(0.95)}{Y(7.1)} < \frac{0.92 \times 10^{-8}}{0.34 \times 10^{-7}} = 0.27$$

or

$$\frac{Y(0.95)}{Y(7.1) + Y(6.1)} < \frac{0.92 \times 10^{-8}}{1.5 \times 10^{-7}} = 0.06$$

from which it is apparent how rough the survey of the low energy radiation was. Because σ_K decreases with energy approximately as $m_0c^2/h\nu$ and the "effective" converter thickness increases with energy (very roughly linearly) one may extend this estimate and say that there are no γ-ray lines in the range 0.4 to 3 Mev of intensity greater than 5 to 10% of the known radiation at 6 and 7 Mev.

Table IV

$E_{res.}$ (kev)	E_{max} (Mev)	E_γ (Mev)	E_{level} (Mev)	I_6/I_7**	Y x 10^8†	y x 10^{10}††
					Disintegrations per proton	
γ 873.5	5.906 6.756	6.151 ± .04 *7.002 ± .06	6.14 ± .04 *6.99 ± .06	*2.5		
γ 939	5.906 6.854	6.151 ± .04 7.100 ± .06	6.14 ± .04 7.09 ± .06	3.3	15	120
γ 1353		(6.10 ± .06) (7.05 ± .1)	(6.09 ± .06) (7.03 ± .1)	1		
γ 1381	5.906 6.735	6.151 ± .04 *6.981 ± .06	6.14 ± .04 *6.96 ± .06	*4.7		
π 843					0.49	1.1
π 1236	5.018 ± .03	—	6.04 ± .03	—	1.42	3.7

* These values represent two unresolved high energy components.

** Relative intensity of 6 and 7 Mev radiation.

† Yield from CaF_2 target 50 kev thick for 900 kev protons.

†† Estimated thin target yield from one kev of CaF_2, using the excitation functions of Bennett, et al(40). (One kev measured at E_R in question.)

Table V

Yields for CaF_2 Target - Summary

$E_{res.}$ (kev)	Y x 10^8	Y(∞) x 10^8	y x 10^{10}	$Y^K(\infty)$ x 10^8	y^K x 10^{10}	y(B) x 10^{10}	$Y^B(\infty)$
γ 873.5 (Γ = 5.2)	26	26	320[a]	36	440	210	17
γ 939 (Γ = 8.0)	15	15	120[b]	20	160	80	10
γ 1381 (Γ = 15)	59	59	250[a]	77	326	220	52
π 843 (Γ = 28)	0.49	0.5	1.1	—	1	.57	
π 1236 (Γ = 85)	1.42	4.6	3.71	—	3.8	1.85	

Y = yield for CaF_2 target 50 kev thick at 900 kev.
Y(∞) = thick CaF_2 target yield.
y = thin target yield per kev of CaF_2.
K = previous Kellogg Laboratory measurements.
B = Bonner's measurements (Ref. 51).
(a) From excitation curve against monitor counter and Comptons at 939 kev (neglecting change in I_6/I_7).
(b) From Comptons.

E. Discussion

The yields obtained agree reasonably well with the results of others.[52] The relative intensities of the 6 and 7 Mev radiation agree with those predicted from the α-groups by Burcham and Freemen[46] and are not inconsistent with the thick target work of Walker and McDaniel.[3]

The γ-ray energies observed at the 873.5 and 1381 kev resonances agree well with those of Walker and McDaniel, while the results at the 939 kev resonance are not inconsistent with the assumption that a higher energy component exists, as suggested by Burcham and Freeman. The resolution and statistical accuracy of individual points obtained in the present experiment are such that one can say only that the difference between the results at the 939 kev resonance and the other resonances is somewhat outside the probable error. However, Chao, et al[47] have clearly separated two α-groups corresponding to γ-ray states in O^{16} at around 7 Mev. They find that at the 939 kev resonance only the short range group is of significant intensity but that at the 873.5 and 1381 kev resonances the two groups are of roughly equal intensity. Using this information, our results may be interpreted as indicating levels in O^{16} that decay by γ-ray emission at 7.09 ± 0.06, ≈ 6.9, and 6.14 ± 0.04 Mev.

The nuclear pair level is at 6.04 ± 0.03 Mev, 100 ± 30 kev below the lowest γ-ray level. The close agreement between the experimental and theoretical pair distributions confirms that these pairs are of nuclear origin, and are not ascribable to internal conversion of γ-radiation. It may be noted, however, that the pair state may also decay by the emission of two quanta in successive electric dipole transitions.[42] Whether or not such two-quantum decay can compete successfully with pair emission depends principally upon the nuclear matrix elements. Since the two quanta would have a continuous energy distribution, and since it is clear from the work of others[39,40] that their intensity is at most one or two times that of the nuclear pairs, they would be difficult to detect, and would not have been observed in the present experiments.

V. Radiation from the Deuteron Bombardment of Beryllium*

A. Possible reactions. Survey of γ-radiation

The bombardment of beryllium with deuterons of 0 to 2 Mev energy is known to lead to the following reactions:(5,6)

a. $Be^9 + D^2 \longrightarrow B^{10} + n^1 + 4.31$ Mev

b. $\longrightarrow Be^{10} + H^1 + 4.52$

c. $\longrightarrow Be^8 + T^3 + 4.53$

d. $\longrightarrow Li^7 + He^4 + 7.09$

In cases a, b, and d, particle groups which leave the residual nucleus in excited states have been observed. These states subsequently decay by the emission of γ-radiation which has been the subject of considerable experimental investigation in this laboratory.

The first observation of this radiation with a magnetic lens spectrometer is reported in Ref. (53). A preliminary model for the present spectrometer was used. The secondary electron spectrum, up to the maximum energy that this spectrometer would focus, is shown in Fig. 20, where the γ-ray energies obtained are also listed. As seen in this figure, the photoelectrons and Compton electrons were distinguished by obtaining the spectra with converters of both large Z (Pb, Th) and small Z (Be), the former giving both photoelectrons and Comptons, the latter giving, with observable intensity, only Comptons. Also described in this reference are experiments that show that 717 kev radiation is observed at the narrow 1087 kev resonance in the reaction $Be^9(p,\gamma)B^{10}$ but not at the wide 998 kev resonance (see also

---

* Some of the material in this section has previously been reported in Refs. (53) to (57).

Ref. 37). The secondary electron spectra involved are given in Fig. 21.

The next work on this reaction was done with a spectrometer using two of the four large coils for the final model, separated by 24 inches (between inner faces). The vacuum chamber was the same as that used in the final model, and "point" focusing was used to give a resolution of 3% and a solid angle of the order of 1.5% of a sphere. This arrangement was used for a quite careful survey of the secondary electrons from ~100 kev to 4 Mev. A thick beryllium metal target was bombarded with deutorons of ≈ 1.1 Mev. Monitoring was by means of a lead-shielded γ-ray counter 23 inches from the target. The spectra obtained are shown in Figs. 22, 23, and 24. In Fig. 22, the experimental points are omitted because they are too close together--an enlarged section is shown in Fig. 23, where the vertical lines are equal in length to the statistical standard deviations of the various points. (The rapid falling off in counts below 200 kev is a result of the finite counter window thickness.) The higher energy portion of the spectrum is shown in Fig. 24. The spectrum was essentially flat in the region not shown, from ~3.55 to ~4 Mev, the counts obtained here being attributed at the time to neutron background. It might be mentioned at this point that the large neutron yield from this reaction gave a large and troublesome background of counts that were independent of the spectrometer field. At the K-photoelectron peak from the 3.6 Mev line, for example, ≈ 3/4 of the recorded counts were attributable to neutron background. The energies obtained for the various γ-rays are listed in Table VI. Calibration of the spectrometer was in terms of the ThB F and I lines and photoelectrons ejected from a thorium converter by positron annihilation radiation and the 411.1 kev radiation from the decay of Au^{198}. An approximate correction for the component of the earth's magnetic field along the spectrometer axis was

determined by intercomparison of these several calibrations. Corrections for the finite converter thickness were made according to Fig. 50 of Ref. (17).

It is estimated from the data of Fig. 22 that under these conditions of bombardment there is no γ-radiation from ~120 to 400 kev of more than about 5% the intensity of the 411 kev line. The structure in the curve just above the L photoelectrons from the 718 kev line is ascribed either to oxygen contamination of the target,* or to Compton electrons from the 1022 kev line. Points on the lower (Compton) curve of Figs. 22 and 23 were not taken close enough together to make details certain, and later work with much better resolution (Fig. 27) failed to resolve the structure any further.

The data of Fig. 24 alone are not sufficient to establish the 3.6 Mev line entirely unambiguously. This part of the spectrum was therefore re-examined later, using the two separated coil, ring focus, configuration described in Sec. II E. With a resolution of 2%, the data of Fig. 25 were obtained. The photoelectron spectrum from the known single γ-ray from $C^{12}(d,p)C^{13*}$ was also obtained to check on possible scattering or other effects that might give spurious counts at the high energy side of the (unresolved) K and L photo-peaks. The 3.6 Mev line is clearly established by Fig. 25.

---

* Unpublished work at this laboratory indicates that the $O^{16}(d,p)O^{17*}$ reaction gives an 871 kev γ-ray.

Table VI

Peak millivolts (K-line from Th)	$B\rho$ (g.cm)	Electron energy (Mev)	Converter shift (Mev)	E_γ [e] (Mev)	Error in locating peak (Mev)	Total error [f] (Mev)
[a] 37.61	2084.7	.2964	[c] .0047	.4109	± .0027	± .004
[a] 42.36	2348.0	.3589	[c] .0057	.4744	± .0029	± .004
[a] 59.41	3293.1	.6007	[c] .0097	.7202	± .0043	± .006
[b] 15.65	3250.5	.5906	[d] .011	.7115	± .0055	± .008
[b] 21.16	4395	.9022	[c] .0088	1.0208	± .0072	± .009
[b] 27.78	5770	1.2928	[d] .026	1.429	± .0100	± .013
[b] 39.64	8233	2.009	[d] .031	2.150	± .022	± .026
[b] 51.59	10,724	2.742	[d] .030	2.884	± .017	± .024
[b] 59.78	12,416	3.247	[d] .030	3.387	± .014	± .024
[b] 63.51	13,191	3.476	[d] .030	3.616	± .034	± .040

a. 100 mV = 10 A. Corrected for earth's field by subtracting 0.14 mV from potentiometer reading. 1 mV = 55.43_2 gauss-cm.

b. 100 mV = 75 A. Corrected for earth's field by subtracting 0.04 mV from potentiometer reading. 1 mV = 207.7_0 gauss-cm.

c. 25 mg/cm^2 thorium.

d. 78 mg/cm^2 thorium.

e. E_K for thorium = 0.1098 Mev.

f. Includes ± ≈0.6% for calibration errors, earth's field correction and converter shifts.

B. Energy determination

Advantage was taken of the careful calibration made by Hornyak for the work reported in Refs. (4) and (17) to make a more accurate determination of the energy of the γ-ray lines found. This work was done with the "thin lens" configuration using all four coils and ring focus, the stops being set to give a resolution of 1.47 ± .05%. Thinner converters than before were used for the lower energy lines in order to get the full benefit of the higher resolution. A deuteron energy of 1.19 Mev and a thick beryllium metal target were used. The total γ-ray yield was monitored by a γ-ray counter. Particular care was taken not to change the position or shielding of this counter during the course of the experiments. The results are shown in Figs. 26 to 29. Here most of the points are averages for two or more runs, this procedure being useful in eliminating variation in the neutron background which, as a result of the somewhat smaller solid angle and poorer neutron shielding, was even more troublesome in this work than in the survey reported above. At the K photo-peak from the 3.6 Mev γ-ray, for example, 7/8 of the total counts were attributed to neutrons.

The γ-ray energies obtained from both the peak and the extrapolated front (high-energy) edge calibrations are given in Table VII. It is pointed out in Ref. (4) that if the high energy side of a photoelectron peak is extrapolated linearly to the background, the intercept is independent of the converter thickness over a considerable range, and no correction for converter thickness is required if the calibration is in terms of the extrapolated front edge (either for converter or internal conversion photoelectrons). The qualification is made that the effect of source size on the resolution might have to be considered--in the present case, this effect is

negligible. Another qualification that was not made is that the effect of Doppler broadening of the primary γ-radiation (see below) due to the motion of the excited nucleus must also be considered. This is not negligible in the present case, and may introduce an additional error of unknown but appreciable extent in the extrapolated edge determinations.*

---

* If the shape of the photoelectron line for the unbroadened γ-ray and the given converter were known, the exact effect of broadening could be obtained. In some cases, this shape can be obtained experimentally (Sec. V F). If it could be calculated generally, then a fit of the calculated to the observed curves would, of course, give a more accurate γ-ray energy than either the peak or extrapolated edge.

Table VII

K-photo peak (mV [a])	$B\rho$ (g.cm)	E_e (kev)	t [e]	Converter shift [f] (kev)	E_γ (kev)	Extrapolated edge (mV [a])	$B\rho$ (g.cm)	E_e (kev)	E_γ (kev)
[b] 43.97	2107.2	301.6	7.0	2.3	413.7 ± .9	[b] 44.67	2115.1	303.4	413.2 ± 1.9
[b] 49.04	2350.2	359.4	7.0	2.2	471.4 ± 1 [g]				
[b] 69.07 [d]	3310.1	605.3	7.0	1.7	716.8 ± 1.1	[b] 70.00	3314.4	606.4	716.2 ± 1.1
[b] 69.08 [d]	3310.6	605.4	7.0	1.7	716.9 ± 1.1				
[c] 12.28_7	4426.4	911.0	7.0	1.5	1022.3 ± 1.9	[c] 12.461	4435.2	913.5	1023.3 ± 2
[c] 12.21_7	4401.2	903.9	24.9	7.8	1021.5 ± 1.9	[c] 12.431	4424.6	910.3	1020.5 ± 2
[c] 16.26	5857.7	1318.1	24.9	7.1	1435.0 ± 3	[c] 16.54	5887	1326.2	1436.0 ± 4
[c] 16.11	5803.6	1302.6	57	15.7	1428.1 ± 5	[c] 16.54	5887	1326.2	1436.0 ± 4
[c] 22.97	8274.9	2022	57	19	2151 ± 16	[c] 23.48	8357	2046	2156 ± 15 [h]
[c] 29.58	10,656	2724	113	34	2868 ± 12	[h]			
[c] 34.30	12,357	3229	113	39	3378 ± 13	[h]			
[c] 36.32	13,084	3445	113	39	3594 ± 32	[h]			

a. Includes correction for axial component of earth's field.
b. 10A = 100 mV shunt. 1 mV = 47.92_4 g. cm peak. 1 mV = 47.34_9 g. cm extrapolated edge.
c. 75A = 100 mV shunt. 1 mV = 360.2_5 g. cm peak. 1 mV = 355.9_3 g. cm extrapolated edge.
d. Independent determinations at the beginning and end of this series of experiments.
e. Converter thickness in mg/cm^2 of Th.
f. From Ref. (17), Fig. 44.
g. See comments in text, especially Sec. V F.
h. K and L lines not well enough resolved for determination of extrapolated edge.

What we are interested in, of course, is not the γ-ray energy but the level energy, or difference in level energies, ΔE_ℓ. There are two correction terms involved. One results from the fact that we are, usually, not observing an excited nucleus at rest in the laboratory but one that has a certain kinetic energy T, as a result of being formed in a nuclear reaction. T is easily calculated for a given case by standard formulas (Ref. 36, p. 276). The corresponding velocity is, in the non-relativistic approximation

$$\frac{v}{c} = \sqrt{\frac{m_0}{M}\,\frac{2T}{m_0c^2}} \qquad (31)$$

where c is the velocity of light and m_0 and M are the electron and nuclear masses respectively. For the nuclear reactions with which we are concerned, v is at most a few per cent of c. The non-relativistic Doppler formula then gives the γ-ray energy

$$E_\gamma = E_\ell \left(1 + \frac{v}{c}\cos\epsilon\right) \qquad (32)$$

where ϵ is the angle between the γ-ray direction and the velocity. The second correction results from the recoil of the emitting nucleus. If we use p = momentum times c, then the equations for the conservation of momentum and energy, for a system in which the radiating nucleus is originally at rest, are

$$p_\gamma = E_\gamma = p = Mvc = \sqrt{2Mc^2T}$$

$$E_\ell = E_\gamma + T \approx E_\gamma$$

or

$$T \approx \frac{E_\gamma^{\,2}}{2Mc^2} \qquad (33)$$

This correction is usually small, much less than 0.1% except for very energetic γ-radiation from the lightest nuclei (e.g., in the $T^3(p,\gamma)He^4$

reaction, 20 Mev quanta are emitted, and the recoil energy of the He^4 is ~100 kev).

The Doppler effect may be considered in two parts. The first is that due to the motion of the center of mass of the whole system we are observing, this motion resulting from the initial momentum of the bombarding particle.* As long as the velocity of the center of mass is less than a few per cent that of light, this may be taken as a shift of the observed γ-energy

$$\Delta E_\gamma = E_l \frac{v_{cm}}{c} \overline{\cos \epsilon} \tag{34}$$

where $\overline{\cos \epsilon}$ corresponds to the mean direction of the observed γ-radiation. The second effect is due to the velocity of the excited nucleus. In the center of mass system, the magnitude of this velocity is constant for constant bombarding energy. Using primes (') to designate quantities in this system, and assuming isotropic distribution of both the reaction products and radiation and random correlation between the direction of motion of the excited nucleus and the γ-radiation it emits, we have

$$dN'_\gamma = N_0 \sin \alpha' \, d\alpha' \, d\Omega'_0.$$

Here dN'_γ is the number of quanta observed in the small cone $d\Omega'_0$ and α' is the angle between the direction of the nucleus and the direction of observation. The energy of the γ-ray, on the other hand, is given by

$$E'_\gamma = E_l \left(1 + \frac{v'}{c} \cos \alpha'\right). \tag{35}$$

Then

$$dE'_\gamma = E'_l \frac{v'}{c} \sin \alpha' \, d\alpha' \tag{36}$$

---

* It is assumed throughout that this momentum is along the spectrometer axis.

and $$dN'_\gamma = \text{const.} \times dE'_\gamma \qquad (37)$$

This is a rectangular distribution in energy, of width $2E'_\ell \; v'/c$. We note further that as long as purely relativistic effects (terms in v^2/c^2) are negligible, the transformation from the center of mass system to the laboratory system will only shift the distribution without changing its shape or width, and that the distribution does not depend upon the direction of observation.

Further consideration is required for cases where the isotropy or random correlation conditions do not hold. Such a case is discussed in Sec. V F.

In general, this broadening is somewhat less than the resolution and the unknown width due to energy loss in the converter; it therefore cannot be easily untangled from these effects and is practically an unobservable except in the unusual case where we can compare the broadened line directly with one of the same energy from a nucleus we know is stationary (from radioactive beta decay, for example). If the broadening can be observed, there is the possibility of learning two things from it. Since the amount of broadening depends on the energetics of the reaction, we may compare the results with the total energy available in the reaction and possibly decide to which of several residual nuclei the γ-ray may be assigned or whether it represents a transition between low-lying or high levels in a given nucleus. On the other hand, if the lifetime of the excited state is comparable to the time it takes the residual nucleus to be stopped in the target material, we may estimate the lifetime of the state by observing the broadening for targets of different stopping powers.(58)

There is very little experimental evidence as to the angular distribu-

tion of γ-radiation except in a few simple cases where only small*(10 to 15%) departures from spherical symmetry have been found.(59) In general, one is forced to assume that the broadening is symmetric around the center of mass shift so that the additional correction to the level energy is zero. A fore and aft asymmetry may give shifts from the level energy up to $\sim 0.5\%$ before the asymmetry becomes apparent from the shape of the photoelectron distribution.

The correction for the center of mass motion is given by Eq. (34), where $\bar{v}_{cm}$ is along the spectrometer axis. One may obtain an approximate value of $\overline{\cos \epsilon}$ for the case where one is observing photoelectrons by noting that it follows from Eq. (20), Sec. III B, that

$$\overline{\cos \epsilon} = \frac{\sqrt{\beta^2 - \sin^2 \theta_0}}{1 + \frac{1}{2} \frac{t}{x_m} \frac{\cos \theta_0}{\beta^2 - \sin^2 \theta_0}} \tag{38}$$

When the Compton effect is being used, the maximum energy electrons are ejected in the direction of the primary quantum. For these electrons, $\overline{\cos \epsilon}$ is the cosine of the mean spectrometer acceptance angle. For lower energy electrons, the converter geometry will give a slightly smaller value of $\overline{\cos \epsilon}$. This is a negligible effect in the cases considered in this paper.

The magnitude of the Doppler shift may be established experimentally by varying the bombarding voltage (rather precise experiments are required since the effect is proportional to $E^{1/2}$), or by examining the γ-ray when the level is excited in a different manner (e.g.--in a different nuclear reaction or in radioactive decay).

Eq. (38) has been used to calculate values of $\overline{\cos \epsilon}$ for the γ-rays of Tables VI and VII. The values, and the corresponding Doppler shifts and

---

* With the notable exceptions of the $H^2(p,\gamma)He^3$ and $H^3(p,\gamma)He^4$ reactions.

level energies (or differences in level energies) are given in Table VIII. Because of the smaller probable errors, the γ-ray energies are taken basically from Table VII. Because of the unknown effect of Doppler broadening, the extrapolated edge determinations are ignored. The breadth and asymmetry of the 472 kev peak are such as to make this useless for an accurate energy determination (see Sec. V F). The 717 kev line can be unambiguously assigned, at least in large part, to the transition from a state in B^{10} at 700 kev to the ground state. The Doppler broadening can thus be calculated as 1.88% (total width), and even if the transition were between the 3.6 and 2.9 Mev levels, the broadening would be 1.1%. Rather rough graphical integration shows that the combination of this broadening and a 1.45% Gaussian window is another approximate Gaussian of 2.3% or 1.8% in these two cases. The observed width of the K photo-peak is 1.60 $\pm$ .05%, the slight increase over the window width being more than adequately accounted for by energy loss in the converter. This discrepancy may be the result of an angular distribution that reduces the Doppler broadening very markedly, or it may indicate that the excited B^{10} nucleus is stopped, on the average, before it radiates, in which case the Doppler correction for the center of mass motion should not be made. The latter explanation is preferred, since this radiation, as discussed later, is presumed to be electric quadrupole. The half-life would then be of the order of 10^{-11} sec or greater, while the stopping time for the B^{10} nucleus in beryllium may be estimated as of the order of

10^{-13} sec.*

The photo-peaks from the 413 and the 1022 kev lines are also somewhat sharper than might be expected, but the discrepancy is not enough to do more than suggest that these lines be assigned to highly excited states in the residual nucleus. However, one notes that the extrapolated edge and peak determinations of energy for these two γ-rays agree, which also suggests that the nucleus is stopped before it radiates. It is quite possible that the Doppler shift correction should not be made for these lines. Similar, although more inconclusive, arguments for not making this correction for the 1430 kev line may be adduced.

---

* In Fig. 38 of Ref. (17), Hornyak has "unfolded" the K-photo-peak from this γ-ray, thus removing the effect of the finite instrument resolution. That this unfolded curve shows none of the expected Doppler broadening was first brought to my attention by R. G. Thomas. Since this was responsible for the consideration of the width of the original curve discussed above, I am much indebted to Mr. Thomas. It may be pointed out that the original of the unfolded curve was obtained with a thicker converter, and that the unfolding process is somewhat inexact, so that the width considerations given here are probably more convincing.

Table VIII

E_γ [a] (kev)	t [c] (mils)	x_m [d] (mils)	$\beta = v/c$ for electron	$\frac{\theta}{\cos \epsilon}$	$\Delta_{Dop.}$ [f] (kev)	ΔE_{level} [g] (kev)	$\overline{\Delta E_l}$
413.5 ± .9	.25	.355	.777	.459	-1.2 (0)	412.3 ± 1 (413.5 ± .9)	
(472) [b]	.25	.47	.813	.548	-1.7	—	
716.6 ± .9	.25	1.03	.887	.738	0 (-3.4)	716.6 ± 1 (713.2 ± 1)	
1022.3 ± 1.9	.25	1.95	.932	.841	-5.6 (0)	1016.7 ± 2 (1022.3 ± 2)	1017 ± 2 (1022 ± 2)
1021.5 ± 1.9	.90	1.95	.932	.741	-4.9 (0)	1016.6 ± 2 (1021.5 ± 2)	
1435.0 ± 3	.90	3.35	.960	.811	-7.5 (0)	1425.5 ± 3 (1435.0 ± 3)	1424 ± 3 (1432 ± 3)
1428.1 ± 5	2.04	3.35	.960	.696	-6.5 (0)	1421.6 ± 5 (1428.1 ± 5)	
2151 ± 16	2.04	6.8	.979	.820	-11	2140 ± 16	
2871 ± 15	4.05	11.7	.987	.812	-15	2856 ± 15	
3380 ± 15	4.05	15	.990	.843	-19	3361 ± 15	
3604 ± 30	4.05	16.5	.991	.866	-20	3584 ± 30	

a. Best values from all determinations.
b. The reaction $Be^7(X)Li^{7*}$ gives 476.7 ± 0.9 kev for this level energy. See Ref. 4 and Section V F.
c. Thorium metal converter
d. Scattering length, x_m, as calculated by Cohen and Christy (unpublished).
e. From Eq. 38
f. From Eq. 34
g. The possibility that anything from no Doppler shift to the full calculated shift may correspond to the actual physical situation has been ignored in determining the probable errors given.

C. Relative intensities and yields of γ-radiation

From the various photoelectron peaks one can estimate the relative intensities of the various γ-rays. On a counts per unit momentum interval vs. momentum curve, the area, A, under the peak is proportional to the intensity of the γ-radiation. If only the converter thickness is changed in going from one γ-ray to another, the relative intensities of various lines are given by Eq. (20), which may be rewritten as

$$I_\gamma = \frac{A}{\frac{t}{\overline{\cos \epsilon}} \frac{\phi_K}{\phi_o}} \tag{39}$$

Intensities calculated from this for the various peaks obtained with 1 1/2% resolution (Figs. 26 to 29) are given in Table IX. Values of $\overline{\cos \epsilon}$ are taken from Table VIII, and ϕ_K/ϕ_o is evaluated from the curves of Hulme, et al.[23] The work at 3% resolution is not useful for determining intensities, since the converters used were made too thick for many of the γ-lines, and since the position or shielding of the monitor γ-ray counter was apparently changed during the course of the experiments.

These relative intensities were checked, and absolute intensities were obtained for various lines by using Compton secondaries. The four-separated-coil configuration of the spectrometer was used, the various apertures being set to give a resolution of 1.9% for very small sources and $\approx$ 2.3% for the source sizes actually used. Beryllium metal foils of such thickness that the mean square scattering angle was less than $\sim$.01 radian^2 were used as targets and as Compton converters. Counts were taken for a fixed number of microcoulombs to the target. The deuteron bombarding energy, frequently checked against the electrostatic analyzer, was 1.19 $\pm$ .010 Mev, the same as used for the work at 1.5% resolution. The target was kept at a potential

of +300 V. with respect to the rest of the spectrometer, and a 3/8-inch diameter wire loop (3 times the deuteron beam diameter) at -300 V. was placed around the beam and about 1 inch from the target to eliminate the effect on the current measurement of secondary electrons from the target or residual gas. During all runs, the vacuum in the spectrometer was better than $\approx 5 \times 10^{-5}$ mm of Hg. The current measurement under these conditions is expected to be good to ± 5%, this was verified by comparing the current to the target with that measured in a standard Faraday cage just outside the spectrometer, the observed loss of ~ 5% being attributable to defining slits between the Faraday cage and the target.

For the 717 kev line, a beryllium converter of 19.2 mg/cm^2 superficial density (20.8 mg/cm^2 when divided by the mean cosine of the spectrometer acceptance angle) was used. The energy loss and straggling in this converter were determined experimentally by observing the K photoelectrons ejected from 7.0 mg/cm^2 of thorium by the same γ-ray through the beryllium converter, as shown in Fig. 30. The peak of the curve was shifted by 26.8 ± 1 kev, which is to be compared with the most probable energy loss of 23.3 kev given by the unpublished calculations of Cohen and Christy and the average energy loss of 35.5 kev calculated from the formula given by Heitler (Ref. 25, p. 219).* It is noted that both peaks are slightly asymmetric and that the one observed through the beryllium is wider. Both the window curve and the theoretical straggling in energy loss around the most probable energy

---

* The area under this curve was increased by about 10%, which is about the probable error in measuring it. This has bearing on the discussion of the variation of the photo-peak area with converter thickness given in Sec. III. Here there is no question of any increase in the total number of photoelectrons ejected. The increase in area, if real, must then be attributed to scattering in the beryllium, a predominence of scattering into the spectrometer acceptance over scattering out being indicated.

loss are Gaussian in form, this experiment indicating that the straggling is asymmetric (even excluding the "tail" of large energy losses). If it is assumed that the widths of these Gaussians can be added as if they were complete (i.e., $c = \sqrt{a^2 + b^2}$), then the straggling in the beryllium foil is found to be +6.9 kev and -11.7 kev (half-widths at half-maximum).

The primary Compton spectrum for this γ-ray was calculated from Eq. (22) and a 2.3% wide Gaussian window was folded in. The distribution in energy loss for electrons originating throughout the converter was assumed to be given by the lower curve in Fig. 31 (zero energy loss is at the right-hand edge of this distribution). The width of the triangular part of this distribution is roughly equal to the straggling, the most probable and average energy losses for the whole foil being noted. This distribution was taken as constant in width on a momentum scale over the whole range of integration, which gives a negligible error, the width being correct where the primary distribution is changing rapidly. The exact shape of the distribution is given by considerations of convenience in folding it into the Compton spectrum by numerical integration. The final calculated Compton distribution, with optimum values for p_{max} and the height, and added to an assumed constant background, is shown in Fig. 31, together with the experimental points. The discrepancy at lower energies is attributed to electrons originally directed along a radius of the converter and scattered into the acceptance angle. In support of this, it may be noted that for the distribution in energy loss in the converter, the moment of area around one-half the average energy loss (i.e., the average energy loss for one-half the foil thickness) is approximately zero, as it should be according to the definition of the average energy loss. One cannot, therefore, add to the tail of this distribution if it is to represent electrons whose original direction

corresponded to the acceptance angle of the spectrometer. The fit in the important part of the curve--the front edge to somewhat past the peak--is considered quite satisfactory, especially in view of the fact that the experimental points represent single runs--usually two or three runs at a given magnetic field setting are required to average over fluctuations in background and beam position.

The yield of the 717 kev radiation can be obtained by comparing the calculated and experimental curves. This may be done either in terms of the area under the two curves down to some reference momentum, or in terms of the ordinates at some reference momentum, the choices being obviously equivalent as long as the two curves match. When there is a discrepancy, reasons for it must be investigated before a choice can be made. In the present case, it seems fairly certain that the extra electrons observed are not included in calculations based on Eq. (22). The peak ordinates of the two curves were therefore compared.

Eq. (22) gives dN''/dp, the number of counts per unit momentum interval for one γ-quantum per steradian for zero energy loss in the converter and infinite resolution. The converter thickness (along the spectrometer axis) is included in the constant term, and the spectrometer acceptance angle in steradians is included in the final term (the definite integral). In folding in the converter distribution, we therefore take the area as equal to unity, and in folding in the window curve we take the height as equal to unity. The angles θ_1 and θ_2 used in the calculation corresponded to $\Theta = 3.58\%$ of 4π. As described in Sec. II F, the measured value of Θ_o for this configuration is 3.06%, for a resolution of 2.05%; the larger source used in the present experiments gave a resolution of 2.3%. Correcting Θ_o according to Eq. (24), we get a correction factor

$3.58\ [3.06\ (2.05/2.3)]^{-1} = 3.58/2.71$. We note also that the unit momentum interval (which we now take in momentum units) is given by the units used for $\mu/c = m_0c = 1703.9$ g. cm. and finally have counts per millivolt = $c/mV = dN/d(mV)\ I/4\pi$ where I is the total number of quanta emitted into 4π steradians, and is to be divided by the total number of incident deuterons to give the thick target yield, Y, of quanta per deuteron. In this way, one gets for the thick target yield of 0.717 Mev quanta

$$Y = (1.37 \pm 0.3) \times 10^{-5}\ \gamma/D.$$

The probable error given is possibly somewhat pessimistic, as is required by the absence of any extended experience with this type of yield measurement.

The yield of 2.87, 3.38, and 3.60 Mev γ-radiation was similarly determined. The beryllium metal target--Compton converter had a superficial density of 58.7 mg/cm^2 (63.7 mg/cm^2 when divided by cosine of the acceptance angle). The energy loss for 3 Mev electrons in this converter was measured experimentally by observing the photo-peak from a thorium converter and the 3.09 Mev γ-radiation from the reaction $C^{12}(d\,p)C^{13*}$ both directly and through the Be converter. As is clear from Fig. 32, the separation between the photo-peak and the Compton electrons was not sufficient to allow anything more than measurement of the energy loss as 78 $\pm$ 8 kev. The most probable energy loss, as given by Cohen and Christy's unpublished calculations, is 64 kev, the average energy loss calculated from the formula given by Heitler (Ref. 25, p. 220) is 96 kev.

Because these three γ-rays from Be + D are quite close together, it was found desirable to run the Compton electrons from the single C^{13} γ-ray and fit the calculated curve to these experimental points. A 15 mg/cm^2

carbon target was added to the beryllium converter, and the carbon was bombarded with 1.52 Mev deuterons. The primary Compton distribution was taken from Fig. 53 of Ref. (17)* and the 2.3% instrument window was folded in. The various distributions for the energy loss in the converter that were folded into this are shown in Fig. 33, and the calculated curves, with slightly different values of p_{max} to give the "best" fits, are shown in Figs. 34 and 35, together with the experimental points. The calculated distribution designated as ψ_8 agrees with these points very satisfactorily.**

When the energy loss in the carbon is subtracted from the converter distribution used to calculate ψ_8, the dashed curve of Fig. 36a is obtained. ψ_{10} was obtained using the solid curve of this figure (instead of the dashed curve, for reasons of expediency in the numerical integration), and an attempt was made to fit it to the three Be + D γ-rays. This was fairly successful for the 2.87 Mev line, as shown in Fig. 37. The background here is due to Comptons from the higher energy lines, to carbon contamination of the surface of the beryllium target, and to internal conversion pairs from the 3.60 Mev γ-ray (the rise in the positron spectrum just below the Compton peak is in the right position and of the right order of magnitude for these pairs).

The distribution given by ψ_{10} did not, however, fit the experimental points for the other two lines, as shown in Fig. 38. Some approximations were used in calculating the exact curve to use, and a slightly larger value

---

* It was verified that the variation in the definite integral of Eq. (22) was negligible over the range of p/p_{max} used.

** From these data, the thick target yield for 3.09 Mev quanta produced in the $C^{12}(d\,p)C^{13*}$ reaction by 1.52 ± .02 Mev deuterons is calculated as 3.33×10^{7} γ/μ coulomb or 5.4×10^{-6} γ/D.

of p_{max} for the 3.38 Mev line would give a slightly better fit. The overall discrepancy is, however, definitely larger in the case of the 3.38 Mev line than can be accounted for by experimental errors or by the approximate nature of the calculations. The 3.60 Mev line is not well enough resolved to allow any definite conclusions to be drawn.

Experimental error is definitely ruled out as a cause of this discrepancy, since the Comptons from the 2.87 Mev line were obtained in the same series of runs, without any changes in the experimental set-up, many points on this curve being obtained both before and after the higher energy curves were obtained.

If one assumes approximate isotropy of the γ-radiation and approximately random correlation between the direction of motion of an excited nucleus and that of the γ-ray it emits, Doppler broadening may also be ruled out as a cause. This broadening would be largest for the 3.4 Mev γ-ray, and even then is only 1.4% (total width), which is small compared to the width of the Compton distribution from other causes. Its effect is thus only to smooth out the sharpest curvatures, and is almost imperceptible, as can be shown by folding in a rectangle 1.4% wide. Fig. 36b, furthermore, shows how the converter energy loss distribution is changed if rectangles 1% and 2% wide, to represent the Doppler broadening, are folded in--it is clear from this, also, that the effect of the broadening will be apparent only in quite fine detail.

A strong forward and backward distribution of either the residual nuclei with respect to the deuteron beam or the γ-radiation with respect to the direction of motion of the residual nucleus would, on the other hand, give a distribution in energy of the γ-radiation strongly peaked at the extreme values of the Doppler broadening and would account for the observed curve.

A third possible explanation, and perhaps the one to be considered most favorably, is that there are actually two γ-rays, of roughly equal intensity and separated by something like 20 to 40 kev, in the neighborhood of 3.4 Mev.

None of these possible explanations could be easily investigated with our β-ray spectrometer, because of the small separations involved. They will be discussed further in Sec. V E, and for the present, we will assume that only a single γ-ray is present at 3.38 Mev (and also at 3.60 Mev). It is then appropriate to calculate a theoretical distribution that will fit the observed points, as shown in Fig. 39. The combined converter energy loss--Doppler broadening distribution used in calculating these curves is shown at the bottom of Fig. 39.

Yields for these γ-rays have been calculated in the same manner as those for the 0.717 Mev line, and are given in Table IV. The probable errors, as before, are estimated as roughly $\pm$ 25%.

Table IX

Relative intensities and thick target yields for γ-radiation from Be + D

E_d = 1.19 Mev

ΔE_{level} (Mev)	$\frac{t}{x_m}$ [a]	Photo-peak area (arb. units)	$\frac{\phi_k}{\phi_o}$ [b]	I_γ [c] $\times \frac{2.42}{15.5}$	Y_γ [d] $\gamma/D \times 10^6$	$\frac{d\sigma(\pi/2)}{d\sigma(\omega_o)}$ [f]	I'_γ [g]	Y [h] $\gamma/D \times 10^6$
0.4123 (0.4135)	.70	730	73	2.8		.0538	1.2	1.2
(0.472)	.53	490	50	3.3		.0341	1.6	1.6
0.7166 (0.713)	.24	860	20	19.8	13.7	.0111	13.7	13.7
1.017 (1.022)	.13	78	9.5	4.3		.0049	3.5	3.9
	.46	370		5.0			4.2	
1.424 (1.432)	.27	95	5.3	2.5				2.5
	.61	280		2.8				
2.140	.30	58	3.0	1.2				1.2
2.856	.35	170	2.2	2.42	2.42	.00043		2.4
3.361	.27	110	1.8	2.0[e]	2.07[e]			2.1
3.584	.25	28	1.6	0.6	0.89			$\frac{0.9}{\Sigma\ 29.4}$

a. From Table VIII.

b. $\phi_o = \frac{8\pi r_o^2}{3}$

c. $I_\gamma = \frac{A}{\frac{t}{\cos\epsilon}\ \frac{\phi_k}{\phi_o}}$ = relative intensity from photo-peaks. Isotropy of γ-radiation assumed.

d. From Compton secondaries. Isotropy assumed.

e. If there are really two γ-rays here, the intensity given will be somewhat less than the sum of the two intensities.

f. From Sauter's photo cross section (Eq. 1).

g. $I'_\gamma = \frac{I_\gamma}{1 + b\ \overline{\cos\epsilon}\ \frac{d\sigma(\pi/2)}{d\sigma(\omega_o)}}$, b determined to match I_γ and Y_γ for the .717 Mev line.

h. "Best" values.

The disagreement between relative intensities measured by the photoelectric effect and the Compton effect for the .717 and 2.86 lines is believed to be more than the possible experimental errors, although the measurement of the area of the photo-peak from the high energy lines is uncertain because of difficulties in deciding on the proper background and the contribution of L- and M-photoelectrons.* A correction for photoelectrons emitted at large angles to the quanta was therefore made for the low energy lines in the form suggested in Eq. (21). The arbitrary constant b was determined for the .717 Mev line, and the results are given in the column headed "I'_γ" in Table IX.** It may easily be that this correction is too large. However, these values are used for the "best" values in the last column. Where these values are obtained from Compton secondaries, they are probably reliable to ± 25% in absolute value and ± 15% in relative value. Where they are obtained from photoelectron peaks they are probably reliable to ± 40% for energies above 1 Mev. Below this value, errors up to a factor of two may occur. All these estimates of error are in themselves questionable because of the lack of any extended experience with such intensity measurements.

To get some indication of how the relative intensities of the various lines changed with bombarding voltage, certain relative yields were obtained

---

* It may also be noted that the calculated scattering lengths, x_m, may be considerably in error. This should not be important unless their variation with energy is also incorrect, since comparable values of t/x_m are found for these two lines.

** Because of the finite thickness of the Be target, the maximum path length of a γ-ray in the 0.00025-inch thorium converter was ~ 0.025 inches. Attenuation of the γ-radiation is therefore negligible.

at four different voltages. The total γ-ray yield was measured at the same time with a γ-ray counter at 21.7 inches from the target. This counter was shielded by 1.45 cm of aluminum completely surrounding it, and by 3.8 cm of lead except in the direction of the target. The geometric factor for this arrangement was determined by observing the counting rate with a Co^{60} source of known activity* in the spectrometer source position. An "effective" counting efficiency ϵ' for both the Co^{60} γ-rays (1.17 and 1.33 Mev) and the Be + D γ-rays was calculated by taking the product of the attenuation of a particular γ-ray in $(1.45-R_0)$ cm of aluminum times the counter efficiency ϵ for the γ-ray times the relative intensity of the γ-ray (as compared to the whole spectrum). The attenuation was calculated from curves given by Heitler (Ref. 25, p. 216). R_0, the maximum range of secondary electrons, and ϵ, the counter efficiency, were taken from curves given by Fowler, et al[37]. This correction is very approximate (Heitler's curves, for example, give only the number of primary quanta remaining after traversal of a given thickness of aluminum, and make no correction for the secondary quanta that may appear. Attenuation in the .145-inch wall of the spectrometer vacuum chamber was also neglected) but is more or less justified by the observation that the total yield of the Be + D γ-radiation calculated in this manner is not changed if the attenuation correction is neglected entirely.

Another source of error in this determination is that neutrons, as well as γ-rays, may be counted. Glass-wall counters such as those used will count slow neutrons by the $B^{10}(n\,\alpha)Li^{7*}$ reaction; and neutron capture or inelastical scattering by matter around the target—principally the spectrometer

---

* Compared with a calibrated Co^{60} source obtained from the Bureau of Standards.

field coils--will give rise to γ-radiation that may be counted. The slow neutron group that appears at a threshold energy of E_D = 900 kev, as discovered by Evans, Malich, and Risser[60] seems to be especially effective in this regard. It may be noted that Evans, et al, placed their γ-counter much closer to their target, so that there is no reason for questioning their assumption that they did not count neutrons to any extent.

The results are given in Table X, where the third column gives the result of integrating the thin target γ-ray yields of Evans, et al. Because of the long bombardments necessary in some cases, surface layers of carbon causing an error of ~10% in yield is possible.

Table X

Be^9 + D Thick target yields as a function of E_D

E_D [a] (kev)	Mon. counts per μcoulomb (arb.scale)	Total [b] γ-yield (arb.scale)	Rel. yield 2.9 Mev γ		Rel. yield 0.72 Mev γ	
			per μcoulomb	per total γ-yield	per μcoulomb	per total γ-yield
802	46	46	16.9	36.8	45.5	99
1004	95	92	39	42.5	94	102
1188[c]	161	151	65	43	165	109
1403	264	220	99	44.9	234	106

a. Referred to electrostatic analyzer.

b. Integrated thin target yield of Evans, Malich, and Risser,[60] and assuming our monitor counts only γ's at 802 kev.

c. Assuming 10/161 of our monitor counts are due to neutrons, the Co^{60} calibration of the monitor described above gives $Y = 32.2 \times 10^{-6}$ γ/D for the total thick target yield of γ-radiation at E_D = 1.19 Mev.

D. Higher energy lines

As noted above, Evans, et al, in Ref. (60), report finding a new neutron group, corresponding to a Q of -0.74 Mev, from the $Be^9(d\ n)B^{10}$ reaction. A search was made for the γ-radiation, which was expected at around 5 Mev. The target consisted of several beryllium foils, agregating $\approx$300 kev energy loss for the 1.435 Mev deuterons used, 50 mg/cm^2 of thorium foil to stop the deuterons, and 1.6 gm/cm^2 of copper to serve as a source of Compton electrons. The results are shown in Fig. 40. The most noticeable point is that the high energy radiation is very weak, although Evans, et al, reported that if isotropy is assumed, the slow neutrons represented 30% of all the neutrons from a thin target at 1.4 Mev. Two new γ-rays are indicated, and there are two low points just above the Comptons from the 3.6 Mev γ-ray that were later found to result from a third new γ-ray.*

The principle difficulty in obtaining the curves of Fig. 40 was the high background. The field-insensitive neutron and γ-ray background at the highest energy line (at a potentiometer reading of 47 mV) was about ten times the counting rate due to that line, and fluctuations in this background were such that each point in this region had to be taken 8 to 10 times before they were well averaged out. The converter was also much too thick compared to the separation of the lines.

An attempt was made to reduce this neutron background by additional shielding. A reduction of approximately a factor of two was attained by adding sheet cadmium and 3 inches of paraffin containing boric acid to the 3.5 inches of lead already around the spectrometer counter (outside of the spectrometer vacuum chamber), by putting cadmium sheet inside the spectro-

---

* The slope of the curve above 5 Mev is attributed to an underestimate of the field-independent background and to scattering and inadequate shielding in the spectrometer.

meter when it could be shielded from the counter by at least 2 inches of lead, and by putting a plate of pyrex glass (which contains a few per cent of boron) against the spectrometer end plate where such lead shielding was not feasible.* Similar shielding was also put around the monitor counter. To increase the number of Compton electrons counted, the ring focus aperture was opened, increasing the resolution from 2.4% to 2.8% (although this did not give much increase in the window curve height, there was an approximately 30% increase in area). The net result of these changes was a gain of about a factor of three in the ratio of Compton electrons to background at 47 mV (5 Mev γ-ray).

The target used in these later experiments consisted of $\approx$ 300 kev of Be foil, 25 mg/cm^2 of Th foil and 250 mg/cm^2 of Be. The beryllium converter was substituted for the copper because of the possibility that some of the γ-rays observed might be resulting from neutron capture (or inelastic scattering) in the copper. With this converter, the ratio of electrons from the 5 Mev line to background was about 1/6. The various γ-rays are, however, much better defined, as is apparent from Fig. 41. The energies of the various γ-rays were obtained from these curves by assuming that the momentum given by extrapolating the front edge of the curve linearly to the background (including electrons from higher energy lines) is 0.6% greater than the true maximum electron momentum. This rule is justified by the observation of 0.5% to 0.7% for this quantity for both 3.1 Mev (C^{13*}) and 6.1 Mev (O^{16*}) γ-radiation, provided only that the converter thickness is somewhat

---

* It would seem from the attempts that were made to reduce the background that the counter was responding both to slow neutrons that actually reached it, and to capture radiation from other parts of the spectrometer.

greater than the instrument resolution and the "width" of the primary spectrum.*

Rough relative intensities for the various lines were obtained by estimating the magnitude of the step in the Compton distribution due to each of the lines and assuming that this step (in a counts per unit momentum interval vs. momentum plot) is proportional to the total Compton cross section and the intensity of the γ-ray. This very approximate procedure is justified by the following considerations. First, the distributions due to the several lines overlap so badly that it is very difficult to determine the height of a particular distribution--the data obviously do not justify the labor of trying to fit each of these distributions with a calculated curve. Second, at the peak of an observed Compton distribution, one may assume roughly that all electrons of the primary distribution from those of maximum energy to those of maximum energy minus the converter thickness are being counted, and no others. One notes that the primary distribution is peaked at the maximum energy and that this peak becomes sharper as the initial quantum energy is increased, while the converter

---

* This can be explained, in general terms, as follows: It can be easily shown that if a function that rises essentially linearly from zero is observed with a symmetric window narrow compared to the length of the linear portion of the curve, the zero intercept and the slope of the linearly extrapolated edge are not changed. For the Compton distribution, the extrapolated edge intercept is determined, for small window width, by the fold of the converter distribution into the primary distribution and, for converters thicker than a certain minimum, the front edge will not change with converter thickness (see, for example, Fig. 5d of Ref. 17). It is also found, for resolutions of 2 to 3% and converters 3 to 5% thick, that this extrapolated end point does not change much with energy from 0.7 to 7 Mev. On the other hand, the extrapolated edge is not well enough defined for either experimental or calculated distributions to give energy determinations of the maximum accuracy.

thickness, in units of energy loss, is almost constant. To a first approximation, then, one is counting a constant fraction of the total number of Compton electrons, the total number being given by the integrated Klein-Nishina formula (Heitler, Ref. 25, p. 157).

The results are given in Table XI. The relative intensities given may be in error by as much as a factor of two. However, it still seems certain that the total intensity of these three high energy lines is less than 2% that of the remainder of the γ-radiation under the conditions of this experiment, thus justifying their neglect in the yield calculations of the previous section.

Table XI

E_γ (Mev)	Relative Intensity	ΔE_{level} (Mev)
2.89 ± .04 [a]	2.9	—
3.35 ± .05 [a]	1.8	—
3.56 ± .06 [a]	1.0	—
3.97 ± .08	0.1	3.94
4.47 ± .07	0.14	4.44
5.20 ± .1	0.04	5.16

a. From this experiment only. Compare with Table VIII.

E. Assignment of γ-rays to residual nuclei.

Some of the γ-rays discussed above can be assigned immediately to levels in the various residual nuclei that are known from observation of particle groups. Buechner and Strait[61] have made the most accurate and

complete investigation of the various groups of charged particles resulting from the bombardment of beryllium with deuterons. They find two groups of immediate interest--a proton group corresponding to a level in Be^{10} at 3.375 ± .010 Mev and an α-particle group leaving Li^7 excited by 0.482 ± .003 Mev. They also state with some certainty that there are no other excited levels in these two nuclei between 0 and 3.4 Mev that are reached by heavy particle groups at the deuteron energies of 1 to 2 Mev that were used. The 3.36 ± .015 Mev γ-ray can thus clearly be assigned to Be^{10*} and the γ-ray at ~475 kev to Li^{7*}. This latter γ-ray is discussed in detail in the following section. At 90° to a 1.38 Mev deuteron beam and using a thin target, Buechner states in a private communication that he would infer from the curves of Ref. (61) a ratio of $Be^{10*}/Li^{7*} = 0.56$. The ratio of the corresponding γ-ray intensities (Table IX) is 1.3. The disagreement may result, in part, from the differences in bombarding energy and target thickness, or it may indicate errors in the procedure used to calculate the γ-ray intensities. It seems quite certain that it is not the result of anisotropy in the proton or α-particle distributions, since Resnick and Hanna[62] report that the proton group is spherically symmetric and (in a private communication amplifying their published report) that although they could not adequately separate the α-groups to the ground and the excited states of Li^7, the combined groups are roughly spherically symmetric, and a partial resolution seems to indicate that they are separately spherically symmetric. Furthermore, the analysis of Sec. V F shows that if the α's are anisotropic, their distribution is given by $(1 - \cos\theta)$, so that yields measured at 90° to the deuteron beam would be an average value.

This disagreement in relative intensities may, on the other hand, result from anisotropy of either γ-ray, or it may also indicate that there

are two γ-rays in the neighborhood of 3.36 Mev, as mentioned in Sec. V C. In this latter case, the second γ-ray may also belong to Be^{10}, since the corresponding proton group may have been obscured by protons from the $O^{16}(d,p)O^{17*}$ reaction in the work of Buechner and Strait.

The third reaction* that yields charged particles is $Be^9(d,t)Be^8$. Bennett, et al[63] find a γ-ray of 4.9 ± 0.3 Mev from the $Li^7(d,n)Be^{8*}$ reaction. This level is energetically accessible in the present case.** One can calculate that if the true level energy is 4.44 Mev, Buechner, et al, should be able to observe the corresponding triton group. If the level is at 4.9 or 5.2 Mev, the triton group would be obscured by elastically scattered deuterons. At our request, Professor Buechner kindly re-examined some of their photographic plates and found a short range group that could be tritons from this reaction. The level in Be^8 corresponding to this group would be at 4.63 Mev, and appears to be about 70 kev wide, indicating that the state decays by α-particle emission rather than γ-radiation.

The remaining reaction is $Be^9(d,n)B^{10}$. The energy spectrum of the neutrons from this reaction has been investigated in some detail (as summarized in Ref. 5, p. 202) although unfortunately the methods used have poor resolving power. The earlier results give neutron groups corresponding to levels in B^{10} at 0.55, 2.15, and 3.45 Mev. The group corresponding to the slow neutron threshold of Evans, et al[60] has been verified by Whitehead

---

* Excitation of Be^9 by inelastic scattering of deuterons is neglected not only because it is expected to be improbable compared to the other modes of decay of the compound B^{11} nucleus--neutron or fast charged particle emission--but also because no energetically accessible levels in Be^9 are known and because the observed low energy γ-radiation can be easily accounted for in other ways.

** Although Be^8 is energetically unstable to α-particle decay, such decay may be forbidden by strict selection rules and the otherwise improbable decay by γ-radiation will be observed, as in the well known 17 Mev capture radiation from $Li^7 + p$.

and Mandeville[64] who obtain, at a bombarding energy of 1.62 Mev, a neutron spectrum corresponding to levels in B^{10} at 0.69 ± .10, 2.20 ± .10, 3.66 ± .10 and 5.13 ± .08 Mev. In no determination of this neutron spectrum so far published are fairly strong groups to levels at 0.4 and 1.02 Mev or weak groups to levels at 1.4, 2.8, 3.9 and 4.4 Mev ruled out. The work of Haxel and Stuhlinger[65] on the $Li^7(\alpha,n)B^{10}$ reaction (Q = -2.78 Mev) gives evidence for a level at 1.4 Mev. In a recent abstract, Bonner, Butler, and Risser[66] report five thresholds for slow neutron production from 920 to 1070 kev deuteron energy, corresponding to five levels in B^{10} at ~5.1 Mev and within 120 kev of each other.

Certain relations between the energies of these γ-rays (see Table VIII, p. 68) that are left may be noted. The most striking is, as first noticed by Hornyak,[56] that several of them are integral multiples of 717 kev to within 0.5%. It was noted in Sec. V B that it seemed very probable that no Doppler correction should be made for this γ-ray, so that the level energies should also be compared with multiples of 717 kev. Since it is not possible, in the other cases, to say definitely whether or not the Doppler correction, of ≈ 0.5%, should be made, the present data can only be used to conclude that the interval rule holds to at least this accuracy and may hold exactly. It may also be noted that the sum of the γ-ray energies, 413 kev plus 1022 kev equals 1435 kev, which compares closely with the 1432 kev observed for a third γ-ray. If we make the Doppler correction for all three γ-rays, we get 412 kev plus 1017 kev equals 1429 kev which differs from 1424 kev by slightly more than is consistent with the probable errors given. Since, as discussed in Sec. V B, there are other experimental observations that imply that these Doppler corrections should not be made, we assume that this is the case for all three of these lines.

Evidence from the neutron groups and γ-radiation can be combined to give an energy level diagram as shown in Fig. 42 where the vertical scale is proportional to the level energy. Levels demanded primarily by γ-rays, whose existence is also allowed by the low resolution of the neutron work are shown dashed, and a level at 2.86 Mev that is indicated solely by the 717 kev interval rule is shown lightly dashed. Other levels may also occur--an attempt has been made to fit the observed data with the minimum possible number. In Fig. 43, where the lower part of the diagram only is reproduced, the γ-ray and neutron relative intensities are noted. The latter are taken, as noted, from the calculations of Evans, et al[60] based on the experimental work of Bonner and Brubaker[67] (900 kev peak A.C. deuterons, thick target, observation at 90° to the deuteron beam) and from the results of Whitehead and Mandeville[64] (1150 kev deuterons, 100 kev target, observation at 0° to the deuteron beam). In neither case are the experimental conditions as close to those under which the γ-ray intensities were measured as is desirable. The three highest energy γ-rays are ignored in this discussion of intensities, since they are at most 2% of the total intensity. Further, it may be noted that the fast neutron and total γ-ray yields of Evans, et al, are parallel up to $\sim$1.4 Mev--i.e., the γ-ray yield does not reflect the production of slow neutrons corresponding to the 5 Mev states, so that it may be assumed that the γ-ray intensity from these states is negligible.*

---

* The net counting efficiency of a γ-ray counter would be roughly the same for one 5 Mev quantum as for any combinations of quanta (of at least several hundred kev energy) that add up to 5 Mev. Thus decay of the 5 Mev states by cascade transitions would not explain these excitation curves.

The arguments used to construct this level scheme may be outlined briefly. The 0.7 Mev level is established both by the neutron group and by observation of the $Be^9(p,\gamma)B^{10}$ reaction.(53) The levels at 2.14, 3.56 and 5.04 to 5.16 Mev are required by the observed neutron groups. A level at 1.43 Mev, indicated by the $Li^7(\alpha,n)B^{10}$ reaction is also indicated as permitting another possible cascade transition from the 2.14 Mev level, since the neutron intensity to this level is appreciably greater than the γ-intensity directly to the ground state. The observation that 0.413 Mev + 1.022 Mev = 1.435 Mev suggests that these two γ-rays represent a cascade through a state 0.413 or 1.022 Mev from any of the several states separated by 1.43 Mev. The excess of neutrons to the neighborhood of the 0.7 Mev state (see especially the curves of Ref. 64) and the difference in relative intensities of the 0.412 and 1.017 radiation then suggests putting the level at 0.412 or 1.017 Mev, the latter position being somewhat preferred both because the 1.017 Mev radiation is the stronger and because this location allows the simplest explanation of the three high energy lines discussed below.*

The correspondence between the original populations of the various levels as given by the γ-ray intensities and cascade scheme and as given by the neutron intensities is quite good when the uncertainty in the various intensities, the differences in experimental conditions, and the low resolution of the neutron work are considered. However, the non-uniqueness of this level scheme should be emphasized and in particular it is clear that

---

* In reference (53), the 0.42 Mev radiation observed when B^{10} is bombarded with protons is attributed to excitation of the .412 Mev level by inelastic scattering. Recent work by Brown, Chao, Fowler, and Lauritsen(68) and Lauritsen and Thomas(69) has shown that the reaction is $B^{10}(p,\alpha)Be^{7*}$, the radiation corresponding to a state in Be^7 at 0.430 Mev.

several cascade transitions not shown are allowed by the close additivity of the various γ-ray energies.

The 5.16 Mev γ-ray is clearly to be associated with the slow neutron threshold of Evans, et al. Since 0.72 + 4.44 = 5.16 and 1.02 + 3.94 = 4.96, one can use the results of Bonner, et al,(66) to minimize discrepancies (the maximum estimated errors must be taken, and in opposite directions) by assuming one level at 5.1 Mev that can decay to both the ground state and the 0.717 Mev state and another at 5.0 Mev that decays to the state at 1.022 Mev.* There is, of course, no over-riding reason for doing this—actually, the 4.44 and 3.94 γ-rays may belong to Be^{10} or even to Be^{8}, the triton group in the latter case escaping notice in Buechner's work because of its low intensity. At this excitation, Li^{7*} is unstable to heavy particle emission by 1.4 or 1.9 Mev so that the radiation is probably not to be attributed to Li^{7*}.

The 5.1 Mev state in B^{10} is unstable to $Li^{6} + He^{4}$ by 0.8 Mev. That this heavy particle reaction predominates over γ-decay is shown by the observation of Evans, et al, that although the slow neutrons to this level are prominent (they estimate 30% of the total neutrons at 1.4 Mev—Whitehead and Mandeville get 15% at 1.62 Mev), their total γ-ray yield does not reflect the presence of this group. This behavior is reasonable, as can be shown by calculating the widths, Γ_{α} and Γ_{γ}, for α-emission and γ-emission respectively. Using Bethe's formulas for s-wave α's (Ref. 35, p. 166), one

---

* Only preliminary results of the work of Bonner, et al, in which the number of levels near 5.1 Mev was uncertain, were available when Fig. 42 was prepared, so that only three of the five levels are shown.

gets, in the center of mass system

$$\Gamma_\alpha = .076\ G$$

where G is the specifically nuclear width, depending upon the exact characters of the initial and final states, and may have values from, say, 1 kev to 100 kev. This gives Γ_α = 76 to 7600 ev. For Γ_γ, one may use the formulas of Fowler, et al (Ref. 37, p. 274), which give for electric dipole radiation

$$\Gamma_\gamma = \left(\frac{r}{r_o}\right)^2 \frac{(h\nu)^3}{(0.7)^2} = 250 \left(\frac{r}{r_o}\right)^2 \text{ ev}$$

Here r/r_o represents a nuclear matrix element that can have values from, say, 1/16 to 1/2. This gives $\Gamma_\gamma \approx$ 1 to 60 ev.

Thus even with the small amount of energy available, α-decay can easily be ten times more probable than Γ-decay, and we assume that this state decays primarily by α-emission.*

It may be noted that this group of α-particles would have been obscured by scattered deuterons in Buechner's experiments, and further, that even if they were not so obscured, that two-step nature of the reaction would result in a roughly 15% spread (in the laboratory system) in momentum of the α's, thus making them difficult to observe at very high resolution, as used by Buechner.

Spins may be assigned to certain of the levels in B^{10}. The spin of the ground state has been shown to be 3,[70] and the parity is usually taken as even. Cohen[71] has then shown that experiments on the scattering

---

* This is, of course, a simple order of magnitude discussion of a situation that is undoubtedly quite complex, especially in view of the possible multiplet structure of the level.

of protons by Be^9 lead to an assignment of zero spin and even parity to the state at 7.47 Mev and a spin of two and odd parity to the state at 7.38 Mev. It has also been shown[53] that the 7.47 Mev state decays by cascade through the state at 0.72 Mev while the 7.38 Mev state goes primarily to the ground state. These observations are in agreement with an assignment of spin one and even parity to the 0.72 Mev state, provided one makes very plausible assumptions as to the relative dipole moments for the 7.38 Mev to ground and 7.38 Mev to 0.72 Mev transitions. It is not possible to make definite spin assignments to any of the other levels in B^{10}. However, one experimental observation that such an assignment must explain may be pointed out. This is that the 413 and 1022 kev radiation appear only in combination with the 1432 kev radiation, i.e.—that there is no observed γ-ray corresponding, for example, to a direct transition from the 2.14 Mev level to that at 1022 (or 413) kev.

F. The first excited state of Li^7.

In the work at 1.5% resolution, the breadth and asymmetry of the photo-peak from the radiation at 475 kev is most noticeable (Fig. 26). This radiation is assigned to the $Be^9(d,\alpha)Li^{7*}$ reaction both on the basis of Buechner's investigation of the α-groups[61] and because of the broadening, which is attributed to Doppler effect, the latter being much larger for the (d,α) reaction than for the other possible reactions (because of the large Q and the large mass of the emitted α-particle).

In order to compare this observed shape with that of the unbroadened line, and to establish the level energy, the photo-peak was obtained when the state in Li^7 was excited in two other ways; by the decay of Be^7,

$Be^7(K)Li^{7*}$[(†)] and by the inelastic scattering of protons in lithium, $Li^7(p,p')Li^{7*}$. The same thorium metal photoelectron converter (7.0 mg/cm^2) and essentially identical converter-source geometry were used throughout. The three K photoelectron peaks, normalized to equal areas, are shown in Fig. 44. The peak from Be^7 decay is 2.1 ± 0.1% wide (the increase over the instrument resolution of 1.47 ± .05% being completely attributable to energy loss in the converter), that from inelastic scattering is 2.2 ± 0.1% wide, and that from the $Be^9(d,\alpha)Li^{7*}$ reaction is 4.1 ± 0.1% wide. The peak from the inelastic scattering is 1.6 ± 0.5 kev higher than that from Be^7, and that from the (d,α) reaction is several kev lower and markedly asymmetric. The horizontal line below the curve in this and the following figures gives the limits of the Doppler broadening for the (d,α) reaction, as obtained from the location of the Be^7 curve and from Table XII below.

When Li^{7*} is formed by Be^7 K-capture, the maximum recoil energy of the Li^7 is 67 ev (neutrino and γ-ray in the same direction), and Doppler effects are negligible. As is seen from Table XII, this is not the case for the heavy particle reactions, and in particular it is seen that Doppler broadening is quite large for the (d,α) reaction.

---

† I am greatly indebted to Professor J. R. Richardson of the University of California at Los Angeles for making the Be^7, and to Professor D. M. Yost of the California Institute for performing the chemical separations involved.

Table XII

Reaction	E_D (Mev)	v_{cm}	Δ_{cm} † (kev)	v_{Li^7} (in cm coord.)	Δ (kev)
$Li^7(p,p')Li^{7*}$	1.05	0.0059c	2.8	0.00441c	2.0
$Be^9(d,\alpha)Li^{7*}$	1.19	0.0065c	3.1	0.029c	13.8

† The observed peak shift will be given by $\delta = \Delta_{cm}\ \overline{\cos\epsilon}$. From Table VIII, $\overline{\cos\epsilon} = 0.548$ for this radiation and converter, giving $\delta = 1.5$ kev.

The behavior of this asymmetry with variation in bombarding energy was considered to be of interest. For satisfactory results, it was necessary to increase the spectrometer solid angle as much as possible by using the four separated coil arrangement. The instrument resolution was kept the same ($\approx 1.47\%$) and the same 7.0 mg/cm^2 thorium photo-converter was used. The target was an ~ 0.14 mg/cm^2 beryllium metal foil (~ 40 kev for the deuterons used), separated from the thorium by ~ 0.01 to 0.02 inch. The K photo-peaks obtained for the 717 and 413 kev γ's are shown in Fig. 45. They are essentially identical with the corresponding curves from the earlier work. The 475 kev line was run with this source at deuteron energies of 1180 and 1485 kev (curves III and IV of Fig. 46). The beryllium foil was replaced by one of 8.9 mg/cm^2 and the curve run at 1210 and 510 kev (curves I and II of Fig. 46). All the solid curves of Fig. 45 are taken from Fig. 44, which represents the earlier work on this line. Although the statistical errors in these various sets of data are not as small as desirable, because of the low intensity available, and although there is some difficulty with changes in the background, it is clear that the general character of the asymmetry does not change.

There are four possible reasons for the asymmetry of this line. First, several γ-rays (separated from one another by several kev), rather than only one, may be involved. This additional radiation would have to be both lower in energy and considerably more intense than that attributed to Li^{7*}. Consideration of the relative intensities of the γ-radiation and the corresponding α-particles (see Sec. V E) and of the observation that the shape of the line does not change with bombarding voltage both make this an unlikely explanation. A second possibility is that the lifetime of the state is slightly longer than the stopping time for the recoil nucleus. The nuclei in the forward direction are then mostly stopped in the target material before they radiate, those in the backward direction, on the other hand, escape from the target before they lose much velocity (the exponential variation of the reaction yield with deuteron energy is significant here), the net result being a "red shift" of the radiation. Aside from the fact that this mechanism cannot quantitatively account for our observations, it is ruled out by Elliott and Bell's measurement[72] of the lifetime of the state as $0.75 \pm 0.25 \times 10^{-13}$ sec—the stopping time for the Li^{7*} in Be metal may be estimated as $\sim 10^{-12}$ sec—and by our observation of the asymmetry with a thin target separated from the converter.

A third possibility is that the recoil Li^{7*}'s are primarily in the backward direction, the radiation being isotropic, and a fourth is that the radiation is primarily backwards with respect to the Li^{7*} velocity, the Li^{7*}'s being distributed isotropically.

With some simplifying assumptions, the effect of anisotropy in the Li^{7*} distribution or the γ-ray distribution may be calculated (both may be contributing simultaneously to the observed result, of course). These assumptions are that we can neglect the effect of the transformation from the

center of mass system to the laboratory system on the angular distributions and that we observe only that γ-radiation at a mean angle ϵ_o with the spectrometer axis.

We note that the deuteron beam is along the spectrometer axis and define angles as follows:

θ = angle between the Li^{7*} velocity and the spectrometer axis,

ϵ = angle between the γ-quantum and the spectrometer axis,

α = angle between the γ-quantum and the Li^{7*} velocity,

ψ = angle between θ and α, in spherical triangle.

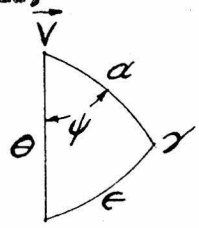

Then if $\Theta(\theta)$ is the number of radiating Li^{7*}'s per unit time per unit solid angle and $\Phi(\alpha)$ is the γ-distribution

$$dN(\theta,\alpha,\psi) = 2\pi\Theta(\theta) \sin\theta\, d\theta\, \Phi(\alpha) \sin\alpha\, d\alpha\, d\psi.$$

As in Eq. (6) we have

$$d\psi = \sin\epsilon\, d\epsilon \left\{[\cos(\epsilon - \alpha) - \cos\theta][\cos\theta - \cos(\epsilon + \alpha)]\right\}^{-1/2}.$$

Putting $x = \cos\theta$ and $\cos(\epsilon + \alpha) = b$, $\cos(\epsilon - \alpha) = a$ and noting that the limits on θ are given by $(\epsilon + \alpha)$ and $|\epsilon - \alpha|$, we can write

$$dN' = 2\pi\Phi(\alpha) \sin\alpha\, d\alpha \sin\epsilon\, d\epsilon\, (-2) \int_a^b \frac{\Theta(x)\, dx}{\left[(a-x)(x-b)\right]^{1/2}}$$

which is integrable by standard formulas if $\Theta(x)$ is a polynomial.

As shown in Sec. III B, if we take the photoelectron distribution as a δ-function at $\omega_o = \cos^{-1}\beta$, then $\overline{\cos\epsilon} \equiv \cos\epsilon_o$ is given by

$$\cos\epsilon_o = \sqrt{\cos^2\theta_o - \sin^2\omega_o} \qquad (11)$$

where θ_o is the mean acceptance angle of the spectrometer. If we include the effect of scattering in the converter (Sec. III B)

$$\cos \epsilon_o = \frac{\sqrt{\beta^2 - \sin^2 \theta_o}}{1 + \frac{1}{2} \frac{t}{x_m} \frac{\cos \theta_o}{\beta^2 - \sin^2 \theta_o}} \tag{38}$$

We can say to a fair order of approximation that we count secondaries only from γ-quanta at this angle ϵ_o with the spectrometer axis. Analytically, we take a detection factor $\delta(\cos \epsilon - \cos \epsilon_o)\, t\sigma_K / \cos \epsilon$. Integration over ϵ then gives

$$dN' = 2\pi \Phi(\alpha) \sin \alpha \, d\alpha \frac{\sigma_K t}{\cos \epsilon_o} (-2) \int_a^b \frac{\Theta(x)\, dx}{\left[(a-x)(x-b)\right]^{1/2}}$$

If V is the velocity of the radiating nucleus in the center of mass system, in units of the velocity of light, the Doppler shift is given by

$$E_\gamma = E_\ell \, (1 + V \cos \alpha)$$

or

$$\cos \alpha = \frac{E_\gamma - E_\ell}{E_\ell \, V} = \frac{\Delta E}{(\Delta E)_o} .$$

We also have

$$dE_\gamma = dE_{e^-} = -E_\ell \, V \sin \alpha \, d\alpha .$$

Thus we get

$$\frac{dN'}{dE} = \frac{4\pi \sigma_K t}{E_\ell \, V \cos \epsilon_o} \Phi\left(\frac{\Delta E}{(\Delta E)_o}\right) F\left(\frac{\Delta E}{(\Delta E)_o}, \epsilon_o\right) \tag{40}$$

From the general nature of the asymmetry of Fig. 44, an extreme distribution of the form $(A - \cos \alpha)$ or $(A - \cos \theta)$ is required. Taking the

γ-distribution as isotropic and the Li^{7*} distribution as $(A - \cos\theta)$, we get

$$\frac{dN'}{dE} = \frac{4\pi^2 \sigma_K t}{E_\ell V \cos\epsilon_o}\left(A - \frac{\Delta E}{(\Delta E)_o}\cos\epsilon_o\right)$$

Taking the Li^{7*} distribution as isotropic, and the γ-distribution as $(A - \cos\alpha)$ gives

$$\frac{dN'}{dE} = \frac{4\pi^2 \sigma_K t}{E_\ell V \cos\epsilon_o}\left(A - \frac{\Delta E}{(\Delta E)_o}\right)$$

Taking the acceptance angle of the spectrometer as 13°, we have $\cos\epsilon_o = 0.796$ or, if we use Eq. (38) to allow for scattering, we have $\cos\epsilon_o = 0.548$. The calculated primary distributions are shown in the lower part of Fig. 47. The K-photo-peak from Be^7 decay (Fig. 44) gives a "window" curve that includes both the instrument resolution and energy loss in the converter. The result of folding this "window" into two of the primary distributions is given in the second pair of curves. The low energy tail of the 412 kev L-line is taken from the $Be^7(K)Li^{7*}$ K peak. Addition of this background to the folded distributions gives the upper curves, the dashed curve corresponding to the dashed primary distribution.

The energy shift due to the center of mass motion has been taken as 2.8 kev in all cases. For $\cos\epsilon_o = 0.548$, this should really be 1.7 kev, which would improve the fit to the experimental points on the high energy side, but make it definitely poorer for lower energies. Actually, such details are somewhat uncertain anyway, especially for the sharply dropping low energy edge, because of approximations in the numerical integration.

The general correspondence between the calculated curves and the experimental points is good enough that one can say with some certainty

that the observed asymmetry can be explained either by a Li^{7*} distribution $\Theta(\theta) \sim (1 - \cos\theta)$ or a γ-ray distribution $\Phi(\alpha) \sim (1 - 0.8 \cos\alpha)$. A more detailed examination of the distribution is possible, but would not be too profitable because of the uncertainty in the experimental points and because of the approximations in the theoretical treatment. The principal error in the latter probably arises from neglect of the solid angle transformation from the center of mass system to the laboratory system, both for the heavy particles and for the radiation, which will increase the calculated number of high energy quanta by a few per cent.

The asymmetry of these distributions requires that they result from interference between two overlapping levels of opposite parity (see the general discussion of Devons and Hine[59]) in either the compound nucleus, B^{11}, which could give the required distribution of the Li^{7*} nuclei, or in the residual nucleus, Li^7, which could give the required distribution of the γ-radiation. In neither case are direct measurements of these distributions available. The work of Bosnick and Hanna on the Li^{7*} distribution (or, more exactly, the correlated α-particle distribution--see Sec. V E and Ref. 62) is not conclusive. However, it would then seem somewhat surprising that the general character of the asymmetry does not change noticeably in going from 16.15 to 16.95 Mev excitation in B^{11} (E_D = 510 to 1185 kev). On the other hand, the levels in Li^7, since they can decay only by γ-radiation, would certainly not be more than a few volts wide. It would therefore be really surprising if two such levels should be close enough together to give strong interference, especially since it would be required that only one be accessible in the $B^{10}(n,\alpha)Li^{7*}$ reaction, for which Elliott and Bell[58,72] observed a symmetric Doppler broadening.

REFERENCES

1. Buechner, Strait, Stergiopoulos, and Sperduto, Phys. Rev. 74, 1569 (1948).
2. C. W. Snyder, Thesis, California Institute of Technology, 1948.
3. R. L. Walker and B. D. McDaniel, Phys. Rev. 74, 315 (1948).
4. Hornyak, Lauritsen, and Rasmussen, Phys. Rev. 76, 731 (1949).
5. W. F. Hornyak and T. Lauritsen, Rev. Mod. Phys. 20, 191 (1948).
6. T. Lauritsen, National Research Council, Nuclear Science Series, Preliminary Report #5.
7. Deutsch, Elliott, and Evans, Rev. Sci. Inst. 15, 178 (1944).
8. C. M. Witcher, Phys. Rev. 60, 32 (1941).
9. K. Siegbahn, Phil. Mag. 37, 162 (1946).
10. H. Busch, Ann. Physik 81, 974 (1926); Arch. Elektrotech. 18, 583 (1927).
11. T. Lauritsen and R. F. Christy, Phys. Rev. 73, 536 (1948).
12. S. Frankel, Phys. Rev. 73, 804 (1948).
13. E. Persico, Rev. Sci. Inst. 20, 191 (1949).
14. J. W. M. DuMond, Rev. Sci. Inst. 20, 160 (1949).
15. Rutherford, Chadwick, and Ellis, "Radiations from Radioactive Substances" Cambridge University Press, London (1930).
16. C. D. Ellis, Proc. Roy. Soc. A138, 318 (1932).
17. W. F. Hornyak, Thesis, California Institute of Technology, 1949.
18. H. Slätis and K. Siegbahn, Phys. Rev. 75, 1955 (1949); Ark. f. Fys. 1, Nr. 17, 339 (1949).
19. Lauritsen, Lauritsen, and Fowler, Phys. Rev. 59, 241 (1941).
20. Fowler, Lauritsen, and Lauritsen, Rev. Sci. Inst. 18, 818 (1947).
21. N. Bohr, "D. Kgl. Danske Vid. Sel. Mathr. fys. Medd." XVIII, 8, 1-114 (1948).

22. F. Sauter, Ann. d. Ph. 11, 475 (1931).

23. Hulme, McDougall, Buckingham, and Fowler, Proc. Roy. Soc. 149, 131, (1935).

24. H. Hall, Phys. Rev. 45, 620 (1934).

25. W. Heitler, "The Quantum Theory of Radiation" (Oxford University Press, London, 1944).

26. W. Bothe, Zeits. f. Ph. 54, 161 (1929).

27. Bethe, Rose, and Smith, Proc. Am. Phil. Soc. 78, 573 (1938).

28. Rasmussen, Hornyak, Lauritsen, and Lauritsen, Phys. Rev. 77, 617 (1950).

29. R. L. Walker, Phys. Rev. 76, 1440 (1949).

30. M. E. Rose, Phys. Rev. 76, 678 (1949).

31. Dougherty, Hornyak, Lauritsen, and Rasmussen, Phys. Rev. 74, 712 (1948).

32. Ellis and Aston, Proc. Roy. Soc. 124, 180 (1930).

33. Owen and Primakoff, Phys. Rev. 74, 1406 (1948).

34. Bethe and Bacher, Rev. Mod. Phys. 8, 82 (1936).

35. H. A. Bethe, Rev. Mod. Phys. 9, 69 (1937).

36. Livingston and Bethe, Rev. Mod. Phys. 9, 245 (1937).

37. Fowler, Lauritsen, and Lauritsen, Rev. Mod. Phys. 20, 236 (1948).

38. Devons and Hereward, Nat. 162, 331 (1948).

39. Streib, Fowler, and Lauritsen, Phys. Rev. 59, 253 (1941).

40. Bennett, Bonner, Mandeville, and Watt, Phys. Rev. 70, 882 (1946).

41. S. Kojima, Proc. Imp. Acad. Tokyo 19, 282 (1943).

42. Oppenheimer and Schwinger, Phys. Rev. 56, 1066 (1939).

43. E. P. Tomlinson, Phys. Rev. 60, 159A (1941); Thesis, California Institute of Technology (1941).

44. Devons and Lindsay, Nat. 164, 539 (1949).

45. Devons, Hereward, and Lindsay, Nat. 164, 586 (1949).

46. Burcham and Freeman, Phys. Rev. 75, 1756 (1949).

47. Chao, Tollestrup, Fowler, and Lauritsen (to be published in Phys. Rev).

48. Herb, Snowden, and Sala, Phys. Rev. 75, 246 (1949).

49. J. R. Oppenheimer, Phys. Rev. 60, 164A (1941).

50. Rose and Uhlenbeck, Phys. Rev. 48, 211 (1935).

51. Bonner and Evans, Phys. Rev. 73, 666 (1948).

52. Fowler and Lauritsen, Phys. Rev. 76, 314 (1949).

53. Lauritsen, Fowler, Lauritsen, and Rasmussen, Phys. Rev. 73, 636 (1948).

54. Lauritsen, Dougherty, and Rasmussen, Phys. Rev. 74, 1566A (1948).

55. Rasmussen, Lauritsen, and Lauritsen, Phys. Rev. 75, 199 (1949).

56. Rasmussen, Hornyak, and Lauritsen, Phys. Rev. 76, 581 (1949).

57. Chao, Lauritsen, and Rasmussen, Phys. Rev. 76, 582 (1949).

58. Elliott and Bell, Phys. Rev. 76, 168A (1949).

59. Devons and Hine, Proc. Roy. Soc. A199, 56 (1949).

60. Evans, Malich, and Risser, Phys. Rev. 75, 1161 (1949).

61. Buechner and Strait, Phys. Rev. 76, 1547 (1949).

62. Rosnick and Hanna, Phys. Rev. 76, 168A (1949).

63. Bennett, Bonner, Richards, and Watt, Phys. Rev. 71, 11 (1947).

64. Whitehead and Mandeville, Phys. Rev. 77, 732 (1950).

65. Haxel and Stuhlinger, Zeits. f. Physik 114, 178 (1939).

66. Bonner, Butler, and Risser, Bul. Am. Phys. Soc. 25, No. 3, p. 49 (1950).

67. Bonner and Brubaker, Phys. Rev. 50, 308 (1936).

68. Brown, Chao, Fowler, and Lauritsen, Phys. Rev. 78, 88A (1950).

69. Lauritsen and Thomas, Phys. Rev. 78, 88A (1950).

70. Gordy, Ring and Burg, Phys. Rev. 74, 1191 (1948).

71. E. R. Cohen, Phys. Rev. 75, 1463A (1949).

72. Elliott and Bell, Phys. Rev. 74, 1869 (1948).

APPENDIX I

The experimental procedure used in setting up the ring focus for the four separated coil configuration (Sec. II F) is outlined here as a matter of possible interest to other experimenters.

Three 0.25-inch wide transmission zones, of mean radii 2.62, 3.87, and 4.87 inches, were defined by stops midway between the source and the counter. The source was a Th B deposit ~0.06 inch in diameter, and the counter opening used was 0.078 inch in diameter. Under these conditions, a single internal conversion line appeared as three distinct peaks, each about 1.7% wide, the peak at the highest magnetic field corresponding to the inner transmission zone.* Two movable stops, made from ~0.2-inch thick aluminum plate, were placed at the counter end of the spectrometer. One of these was a plug of 1.22 inches outside radius, and the other was a ring of 2.25-inch inside radius. By moving these stops along the spectrometer axis until the various peaks were reduced to half intensity, two points on the corresponding rays were located. The counter opening then gave a third point. By moving the counter 0.75 inches out along the z-axis, $\Delta I/\Delta z$ was determined for the three zones. If one then assumes that $\Delta I/\Delta z$ is constant over this range of Δz, and that the electron paths are displaced parallel to themselves, the positions of the three rays at a given magnetic field can be calculated, and the location of the ring focus becomes apparent. The results are shown in Fig. 48, where experimental points for the middle and outer paths are shown.

---

* Similar curves, obtained with the two separated coil configuration, are shown in Fig. 5.

Although one may get more accurate data from the obvious second approximation, the simple steps outlined above served in our case to locate the ring focus with sufficient accuracy. Appropriate thick conical stops, suitable for use with high energy electrons, were then installed in the spectrometer, as shown in Fig. 2. At first, both of these were made movable from outside the spectrometer because of anticipated difficulties in getting both the extreme rays into the counter. Once a suitable location for the hollow cone was found, it was left fixed. After the spectrometer solid angle desired had been selected by the ring stop on the source end, the appropriate ring focus aperture could be obtained by moving the conical plug.

It may be noted that although a mean diameter of 2.25 inches was selected for the ring focus aperture, it was found experimentally that any diameter between 2 and 2.5 inches gave almost as good resolution. As was previously noted, this was expected since the ring focus is, in reality, only a rather poorly-defined intersection of rays with a small divergence.

Somewhat more difficulty was encountered in locating the ring focus for the two separated coil configuration (Sec. II E) since the desired transmission zone corresponded to an annulus of four to five inches radius at the center of the spectrometer. It did not seem possible to get three well-defined peaks corresponding to the inner, middle, and outer parts of this zone. The following less satisfactory and much more tedious procedure was therefore used. After the four to five inch radius transmission zone was defined, the counter end of the spectrometer was completely closed by a movable aluminum disk. A 1/8-inch wide radial slot in the disk was covered by a sheet of aluminum in which was cut a 3/16-inch wide diagonal slot. The diagonal slot could be moved across the radial one, thus leaving a small

opening at any desired radius between two and four inches. Thus it was possible to determine, in a roundabout way, the width and location of the transmitted electron beam, and consequently the appropriate location for the ring focus aperture.

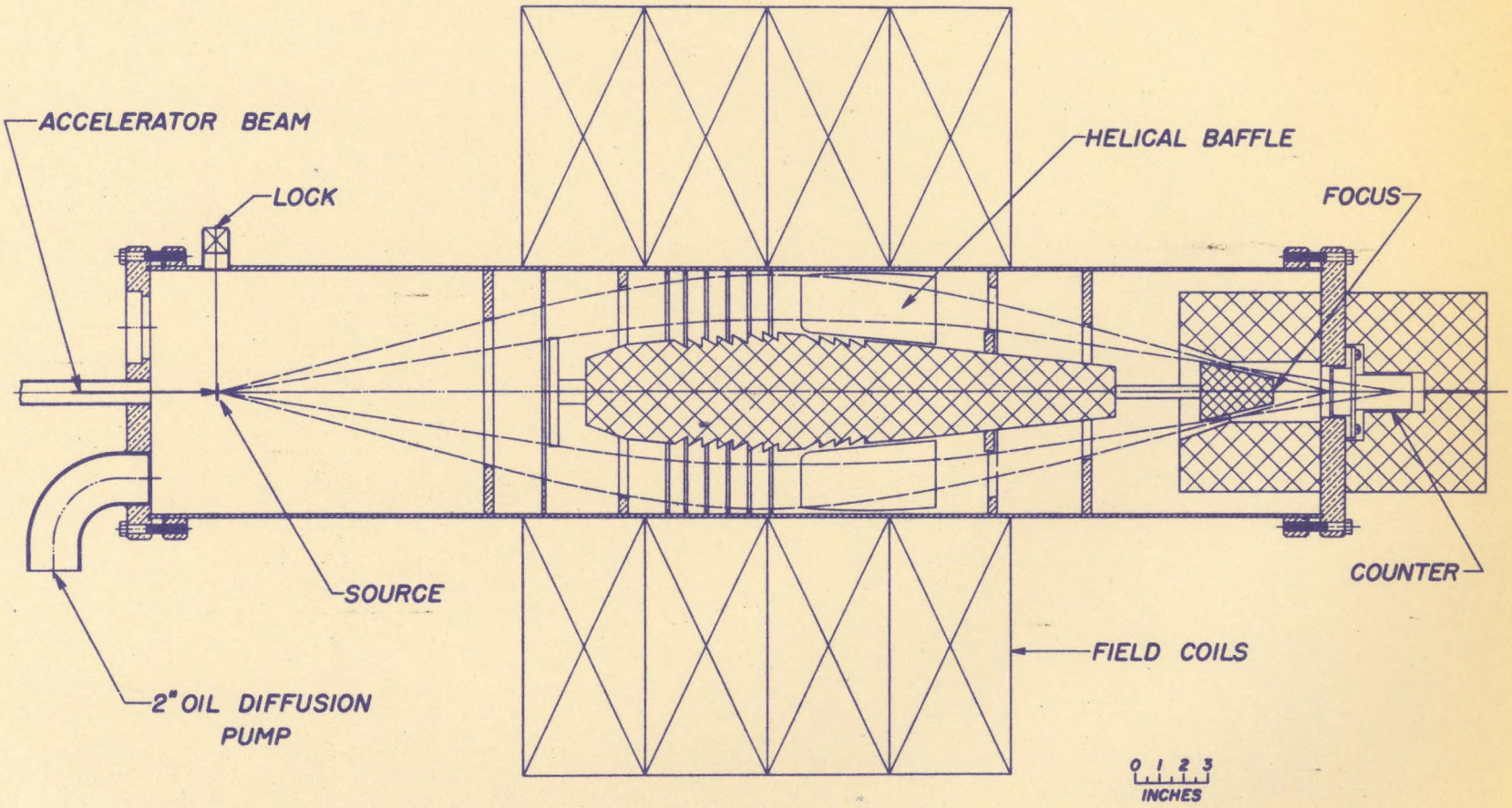
ACCELERATOR BEAM
LOCK
HELICAL BAFFLE
FOCUS
SOURCE
COUNTER
FIELD COILS
2" OIL DIFFUSION PUMP
0 1 2 3
INCHES

FIG. 1

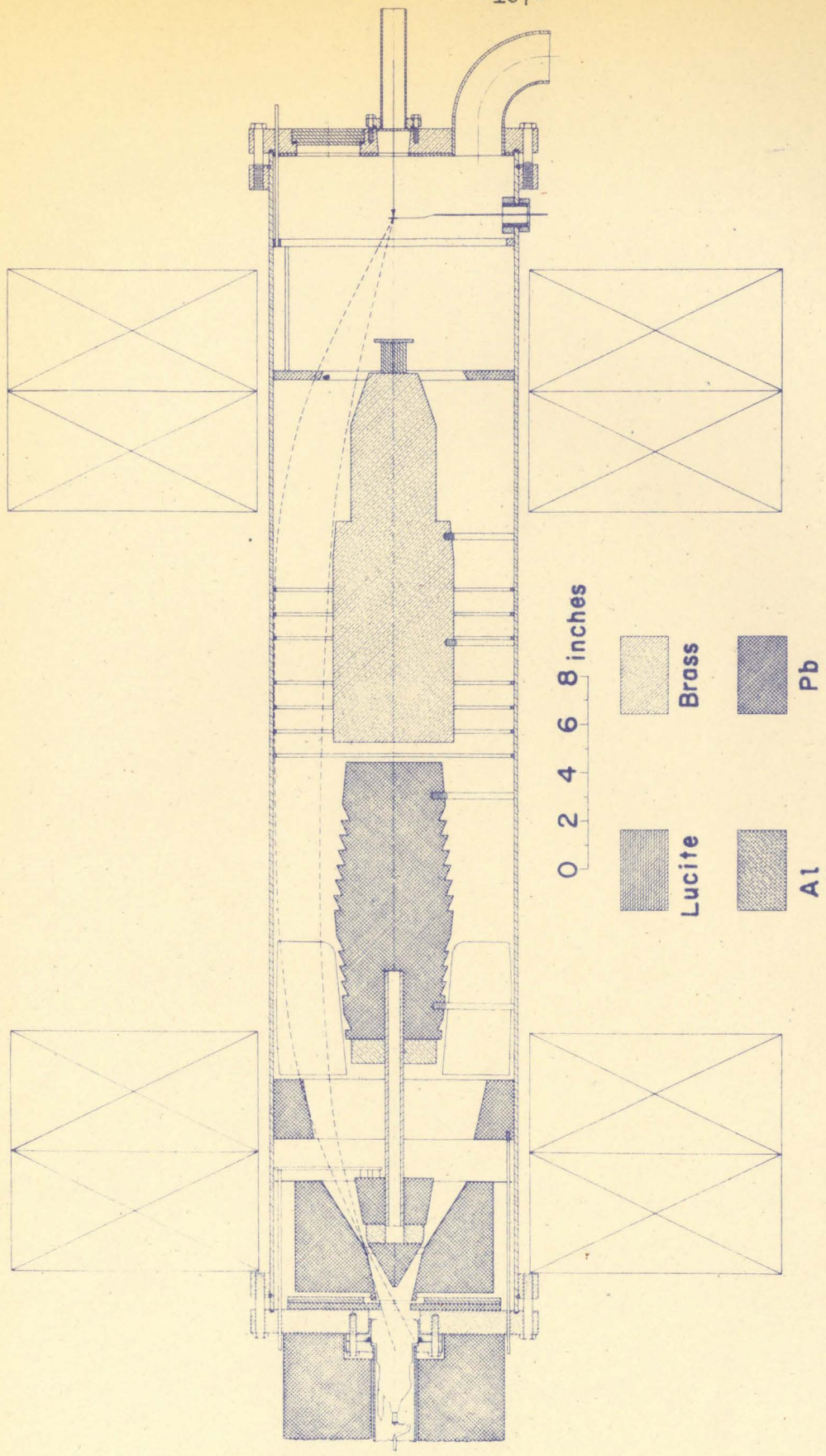

FIG. 2

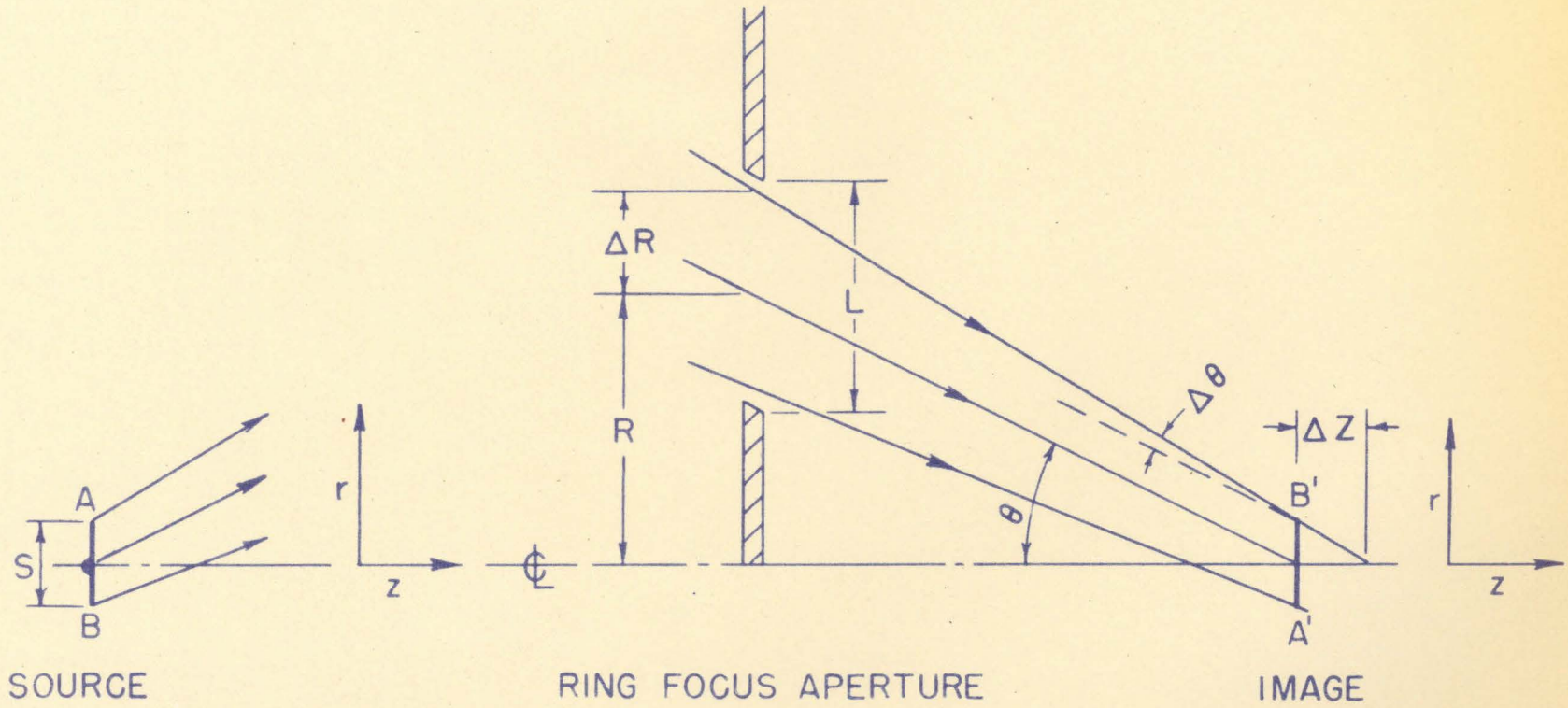

FIG. 3 ELECTRON PATHS (ROTATION NEGLECTED)

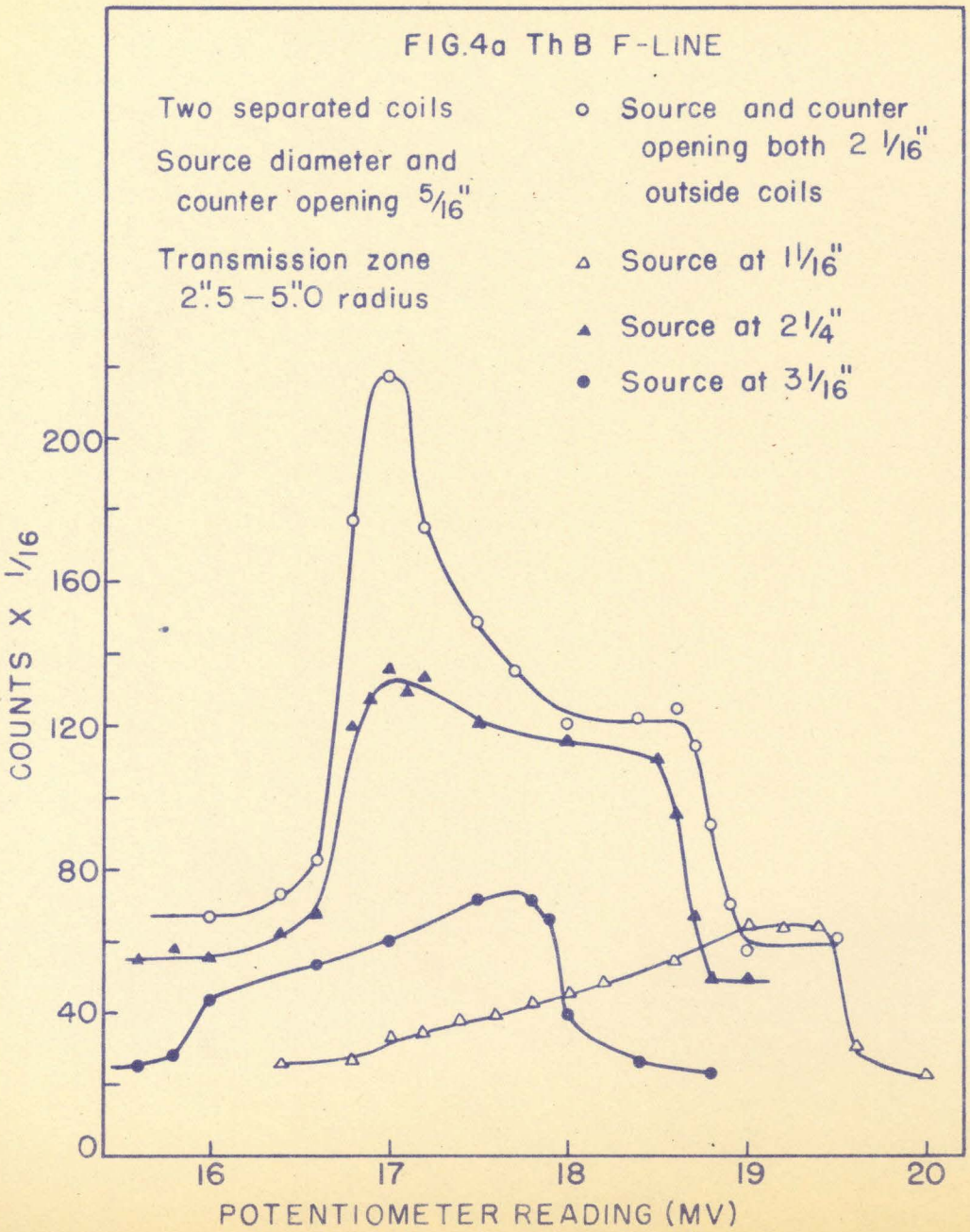
FIG.4a Th B F-LINE
Two separated coils
Source diameter and counter opening 5/16"
Transmission zone 2".5 – 5".0 radius
o Source and counter opening both 2 1/16" outside coils
Δ Source at 1 1/16"
▲ Source at 2 1/4"
● Source at 3 1/16"
COUNTS X 1/16
0
40
80
120
160
200
16
17
18
19
20
POTENTIOMETER READING (MV)

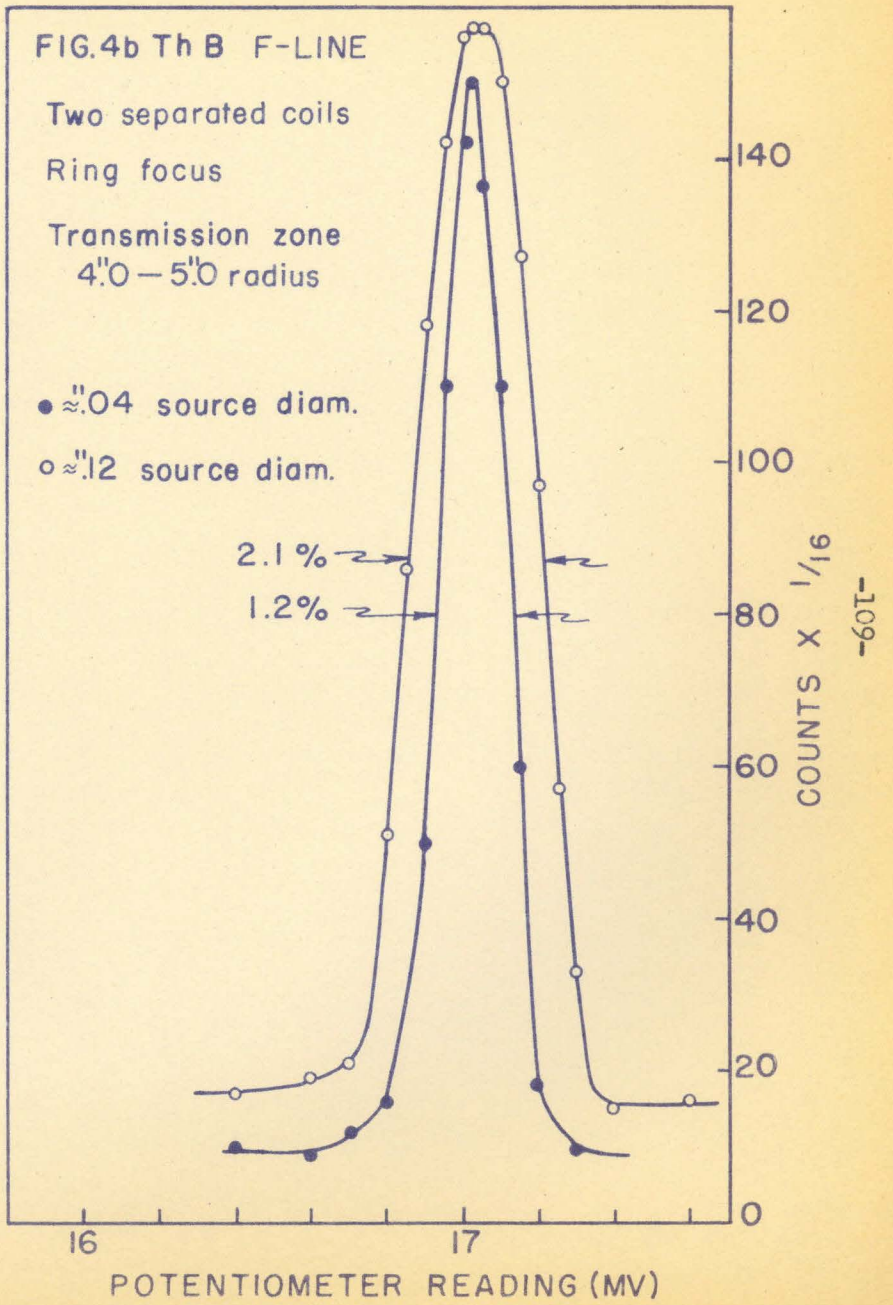
FIG.4b Th B F-LINE
Two separated coils
Ring focus
Transmission zone 4".0 – 5".0 radius
● ≈".04 source diam.
o ≈".12 source diam.
2.1%
1.2%
COUNTS X 1/16
0
20
40
60
80
100
120
140
16
17
POTENTIOMETER READING (MV)

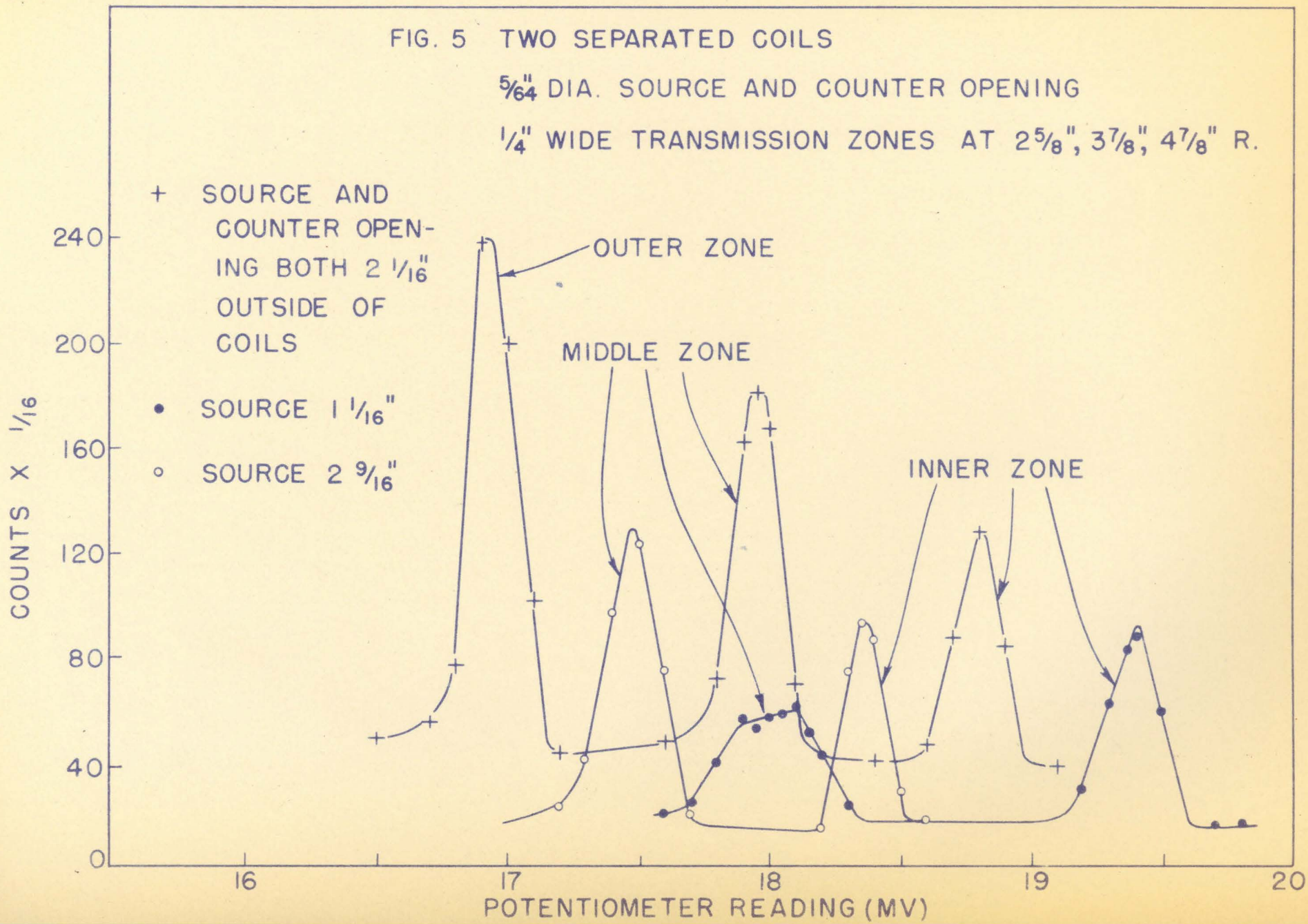
FIG. 5 TWO SEPARATED COILS
5/64" DIA. SOURCE AND COUNTER OPENING
1/4" WIDE TRANSMISSION ZONES AT 2 5/8", 3 7/8", 4 7/8" R.
+ SOURCE AND COUNTER OPENING BOTH 2 1/16" OUTSIDE OF COILS
• SOURCE 1 1/16"
○ SOURCE 2 9/16"
OUTER ZONE
MIDDLE ZONE
INNER ZONE
COUNTS X 1/16
0
40
80
120
160
200
240
16
17
18
19
20
POTENTIOMETER READING (MV)

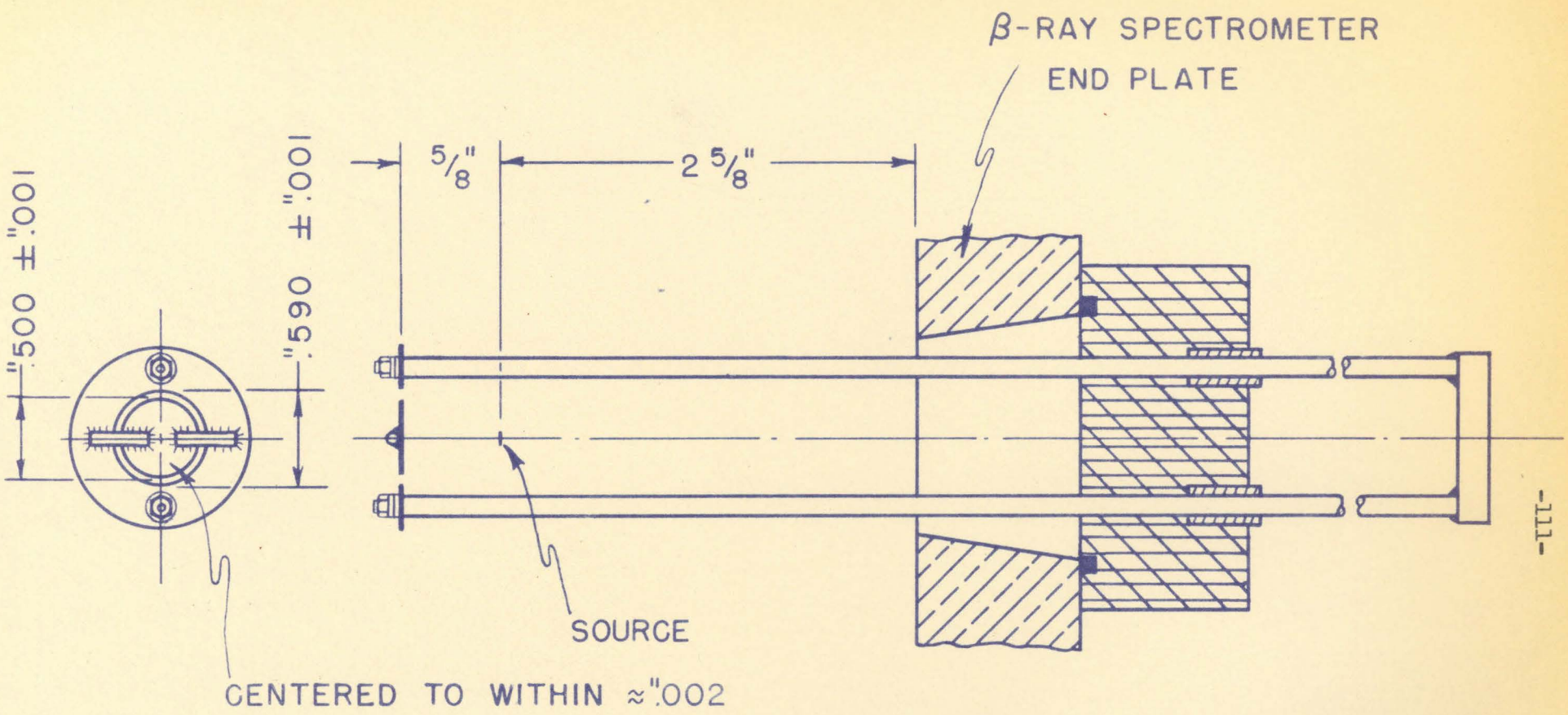

FIG. 6 ANNULAR SLIT FOR SOLID ANGLE MEASUREMENT

FIG. 7

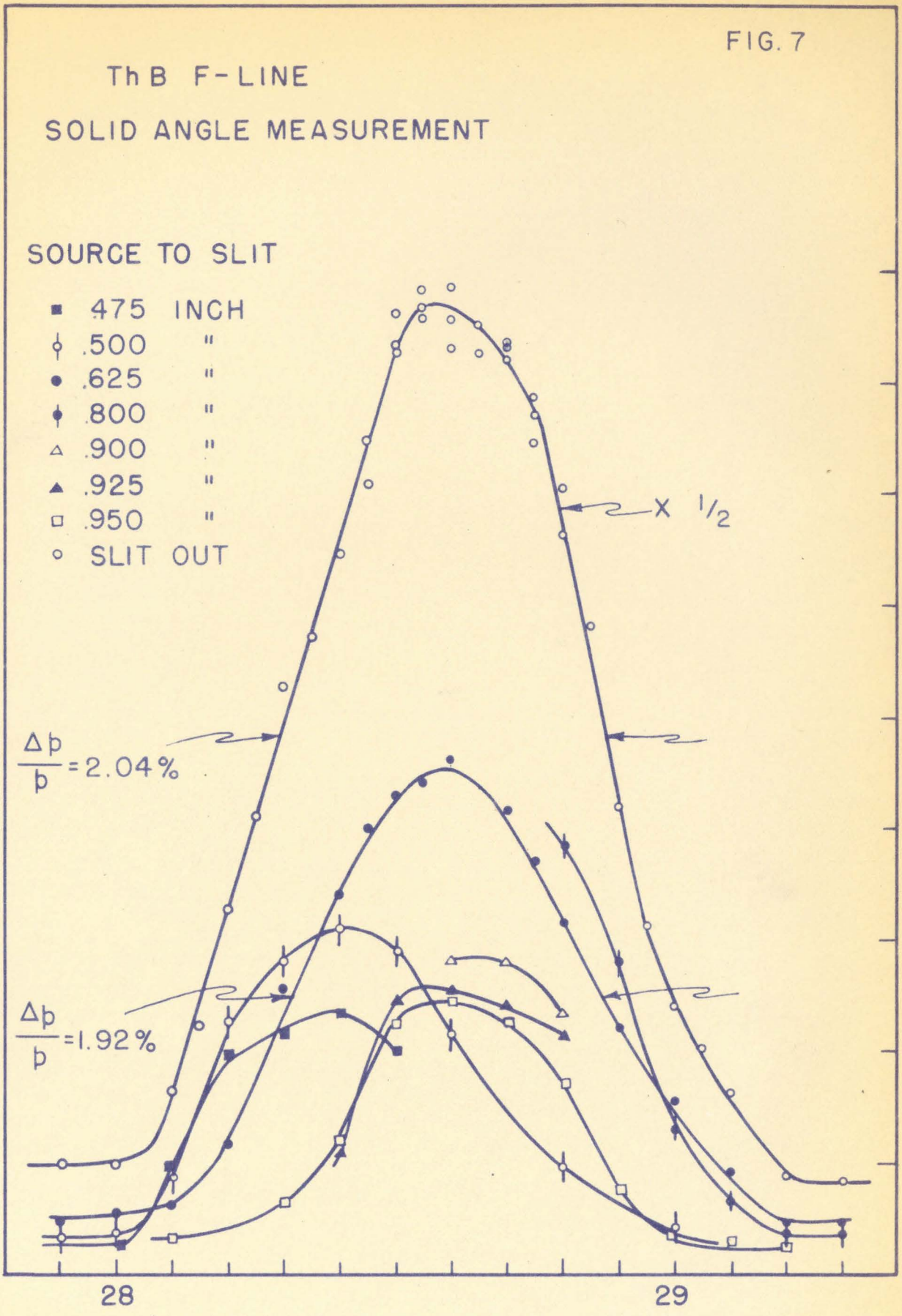
Th B F-LINE
SOLID ANGLE MEASUREMENT
SOURCE TO SLIT
■ .475 INCH
⊖ .500 "
● .625 "
⊕ .800 "
△ .900 "
▲ .925 "
□ .950 "
○ SLIT OUT
X 1/2
Δp/p = 2.04%
Δp/p = 1.92%
160
120
80
40
0
COUNTS X 1/16
28
29
POTENTIOMETER READING (MV)

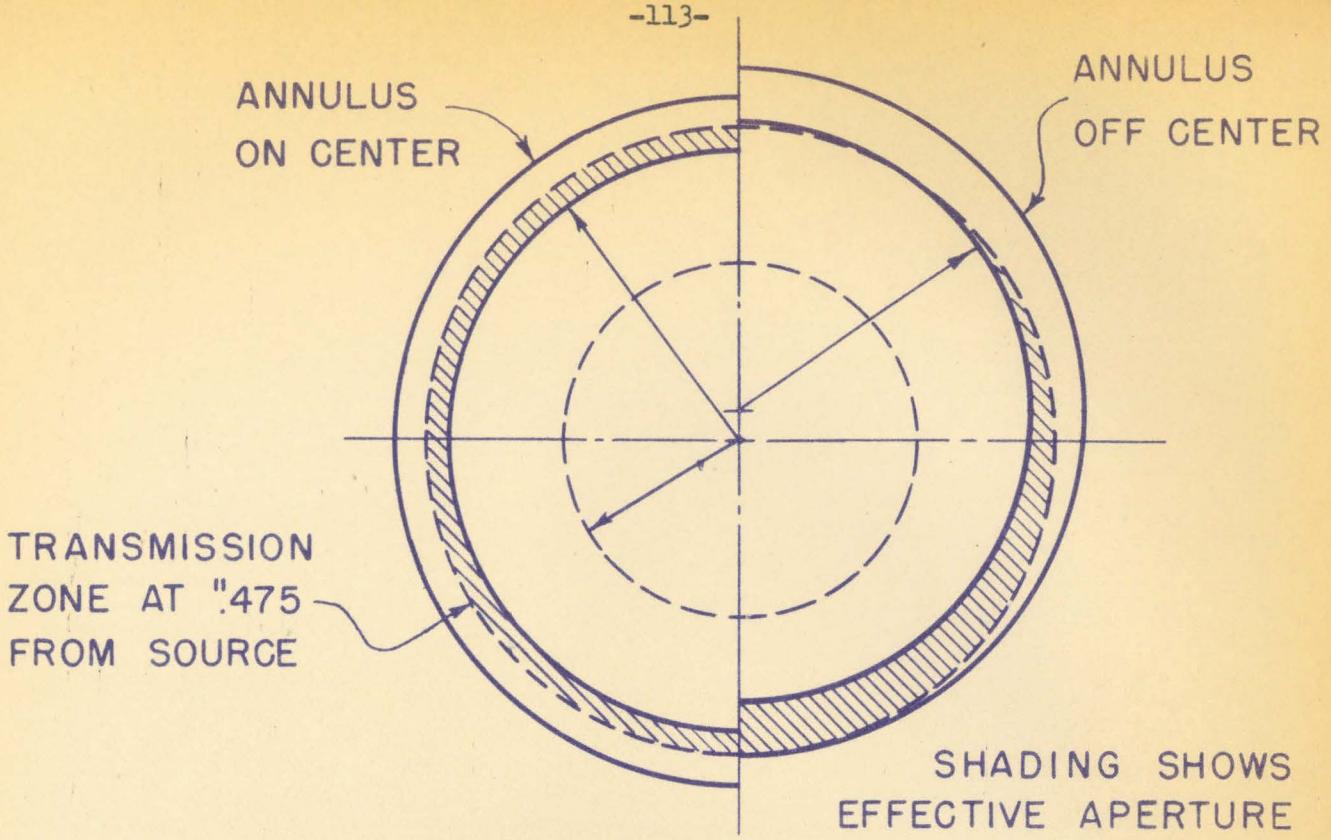

FIG.8b EFFECT OF MALALIGNMENT

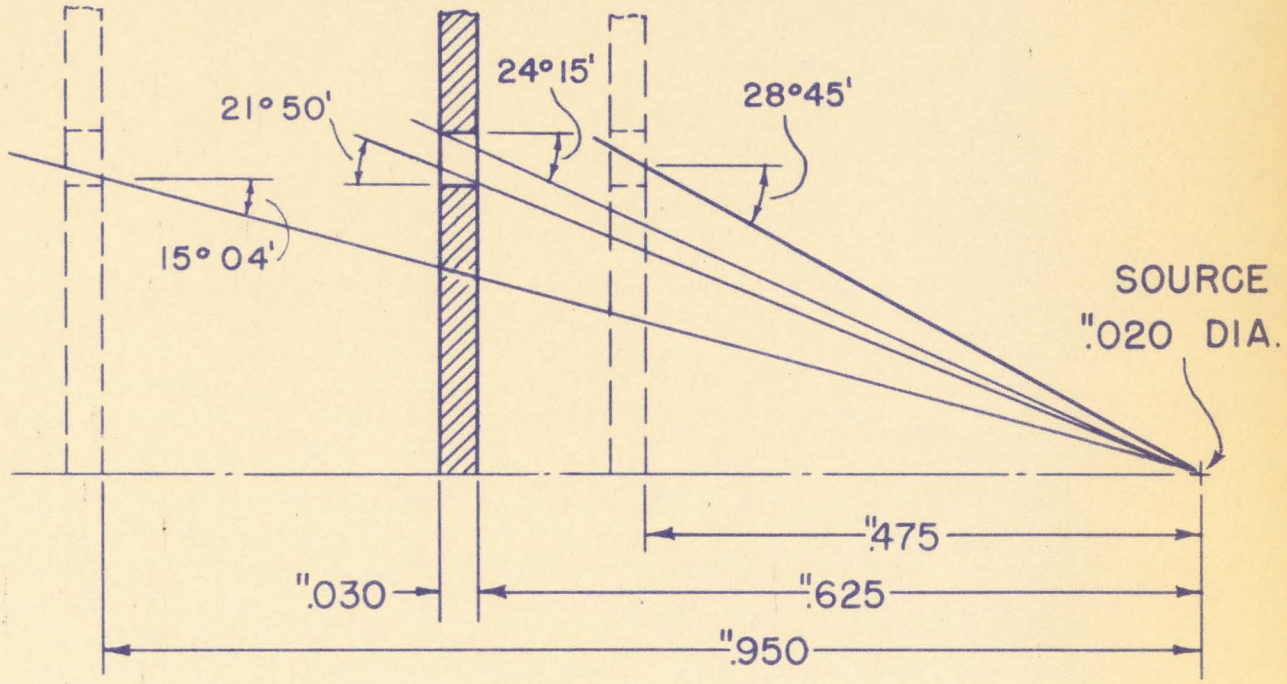

FIG.8a POSITIONS OF ANNULUS
SOLID ANGLE MEASUREMENT

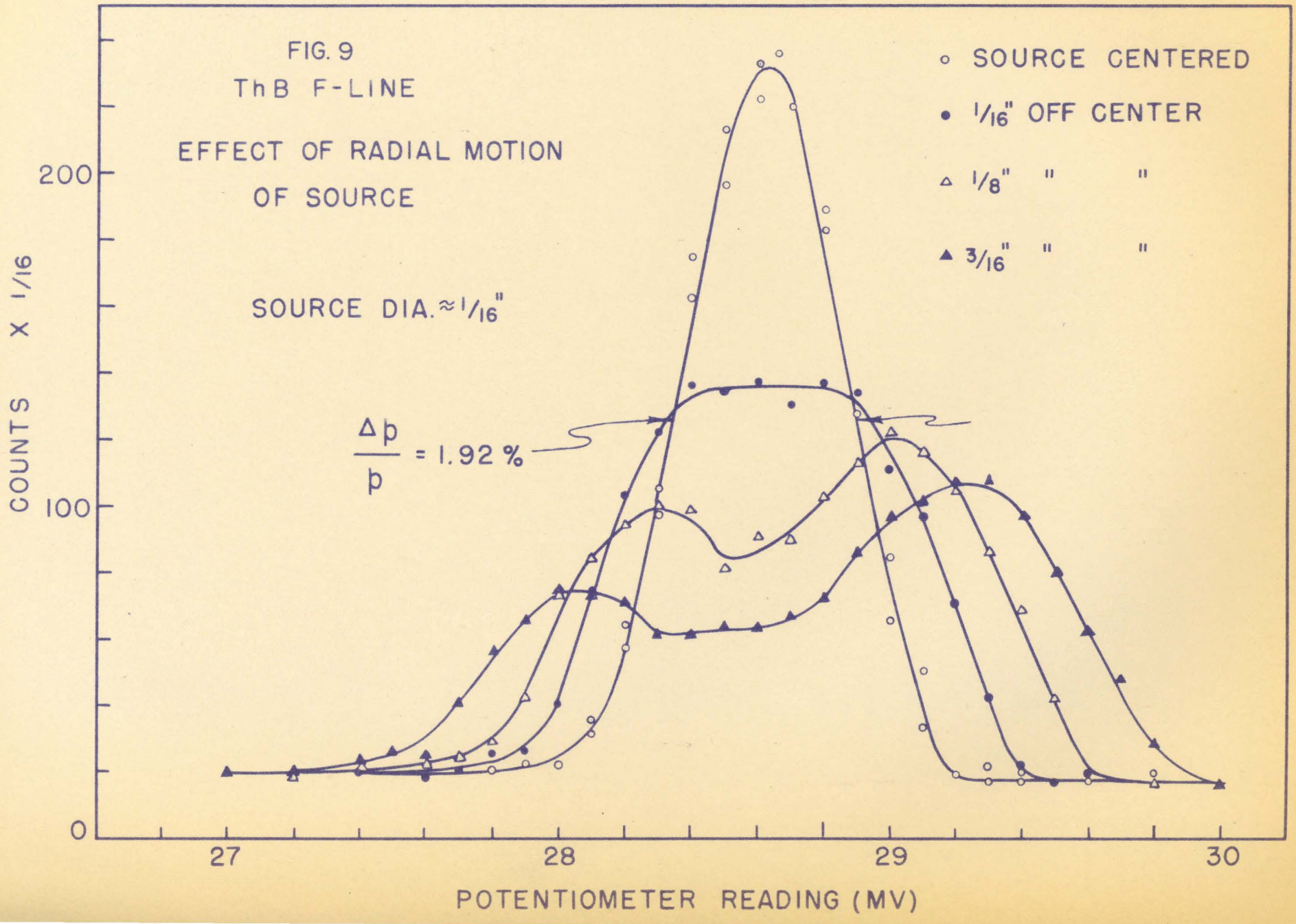
FIG. 9
ThB F-LINE
EFFECT OF RADIAL MOTION
OF SOURCE
SOURCE DIA. ≈ 1/16"
SOURCE CENTERED
1/16" OFF CENTER
1/8" " "
3/16" " "
Δp/p = 1.92 %
COUNTS X 1/16
0
100
200
27
28
29
30
POTENTIOMETER READING (MV)

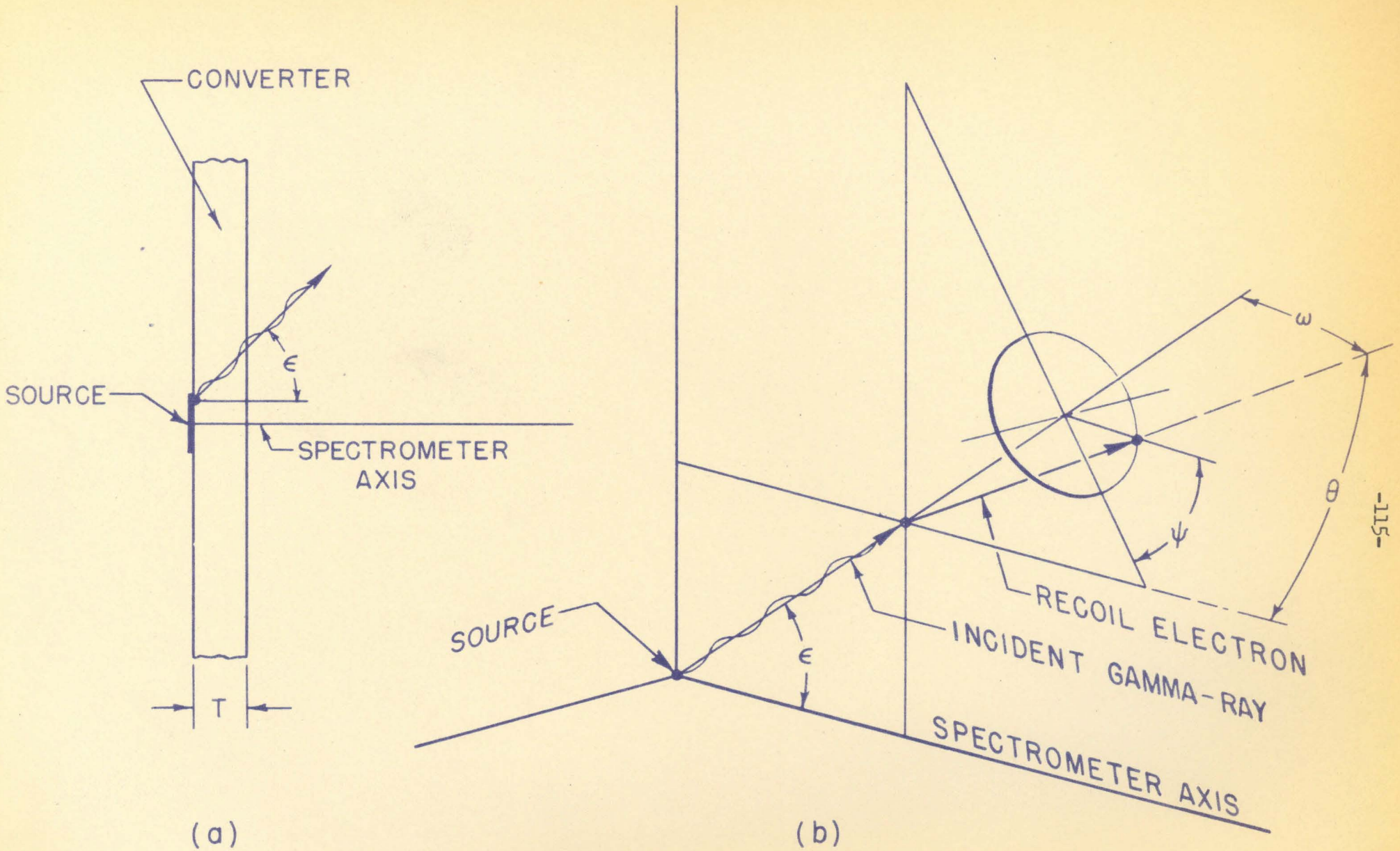

FIG. 10 SOURCE GEOMETRY

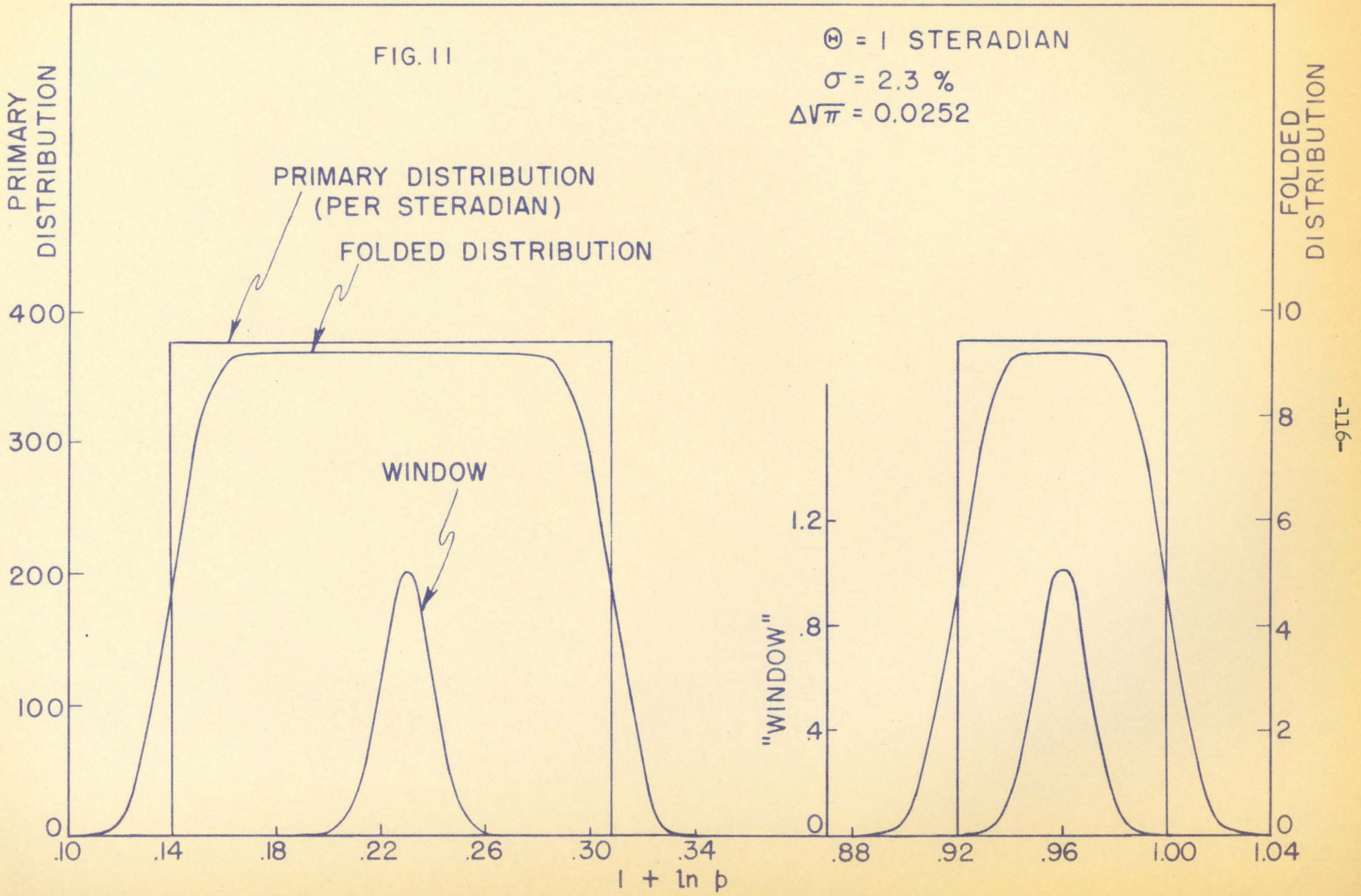
FIG. 11
Ω = 1 STERADIAN
σ = 2.3 %
Δ√π = 0.0252
PRIMARY DISTRIBUTION (PER STERADIAN)
FOLDED DISTRIBUTION
WINDOW
PRIMARY DISTRIBUTION
FOLDED DISTRIBUTION
"WINDOW"
400
300
200
100
0
10
8
6
4
2
0
1.2
.8
.4
0
.10
.14
.18
.22
.26
.30
.34
.88
.92
.96
1.00
1.04
1 + ln p

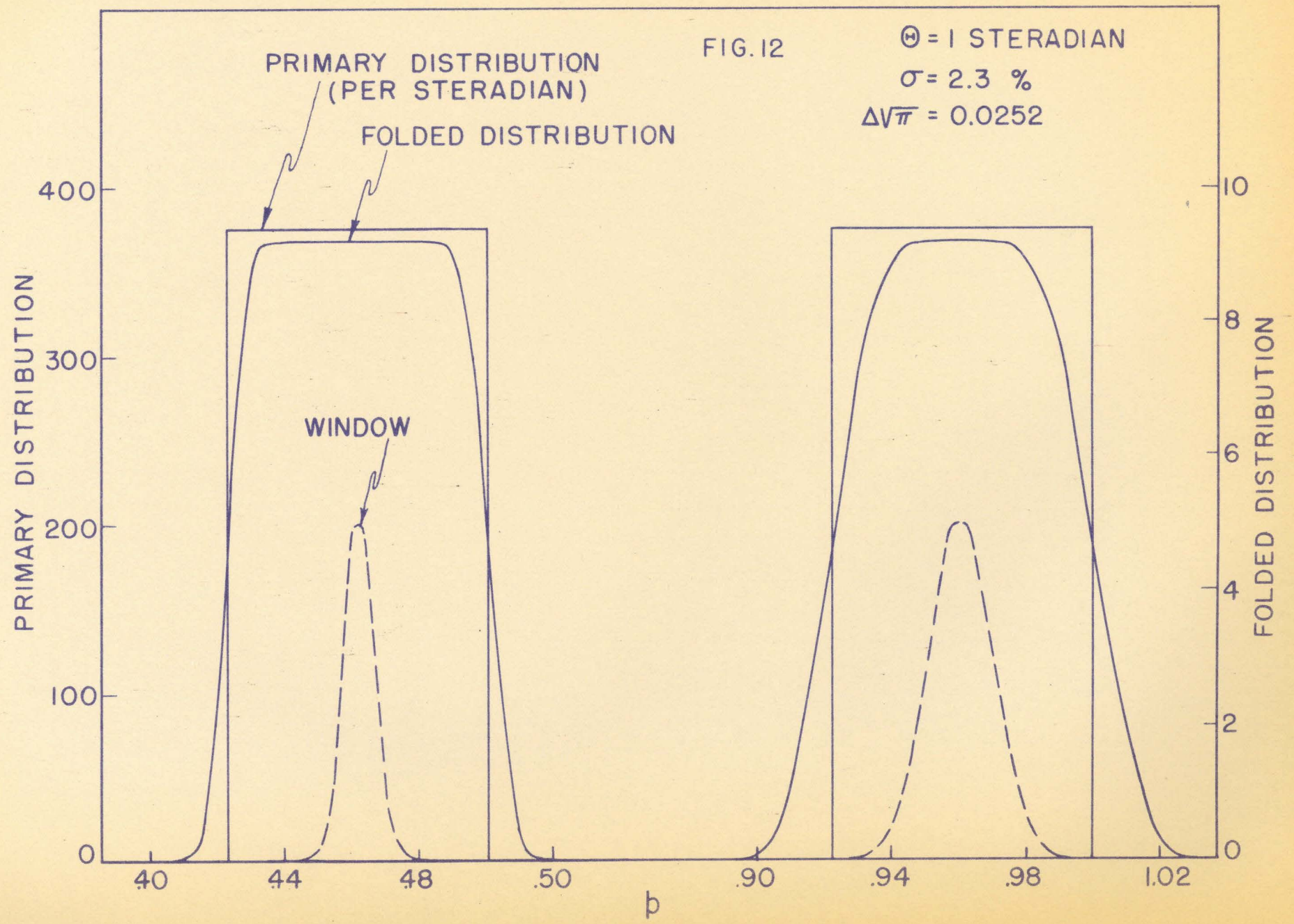
FIG. 12
Θ = 1 STERADIAN
σ = 2.3 %
ΔV̄π = 0.0252
PRIMARY DISTRIBUTION
(PER STERADIAN)
FOLDED DISTRIBUTION
WINDOW
PRIMARY DISTRIBUTION
FOLDED DISTRIBUTION
400
300
200
100
0
10
8
6
4
2
0
.40
.44
.48
.50
.90
.94
.98
1.02
b

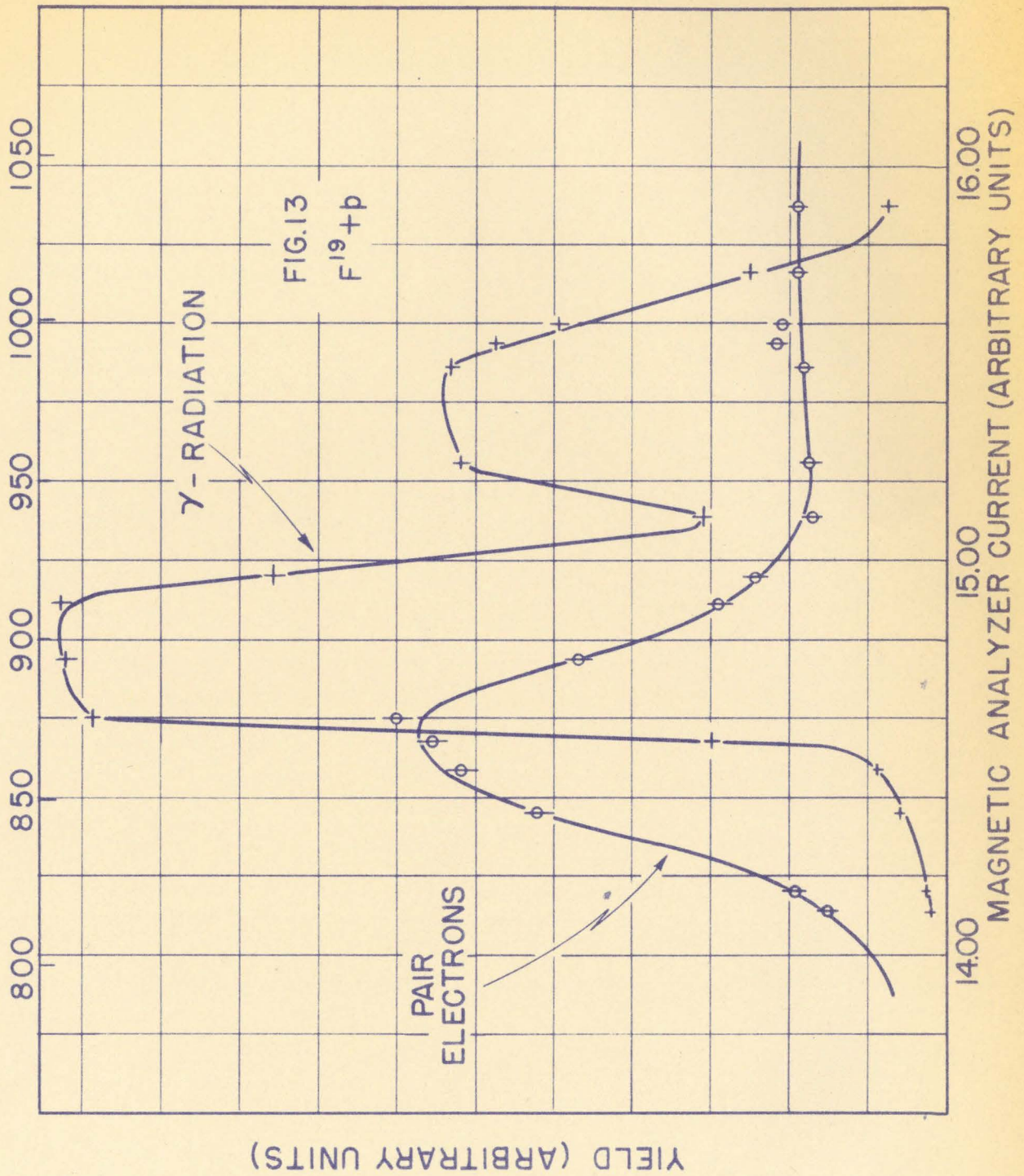
FIG.13
$F^{19}+p$
γ- RADIATION
PAIR ELECTRONS
YIELD (ARBITRARY UNITS)
800
850
900
950
1000
1050
14.00
15.00
16.00
MAGNETIC ANALYZER CURRENT (ARBITRARY UNITS)

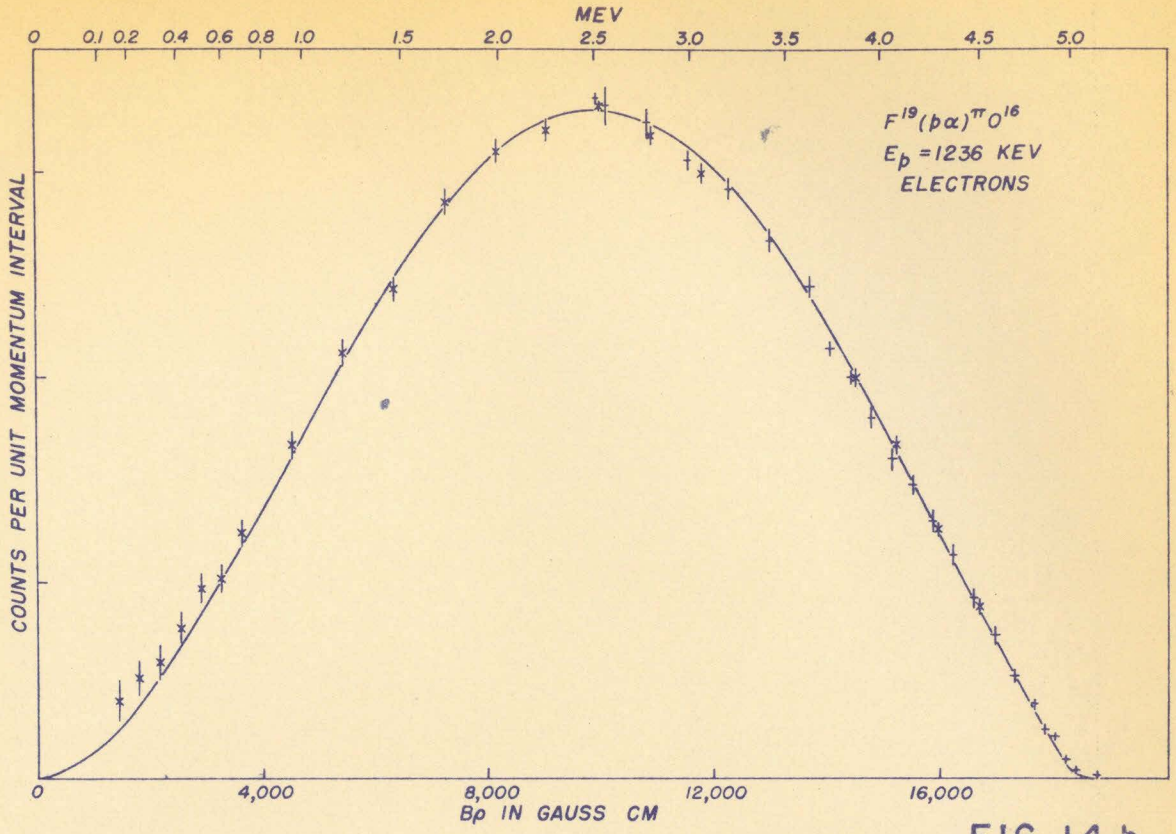

FIG. 14 b

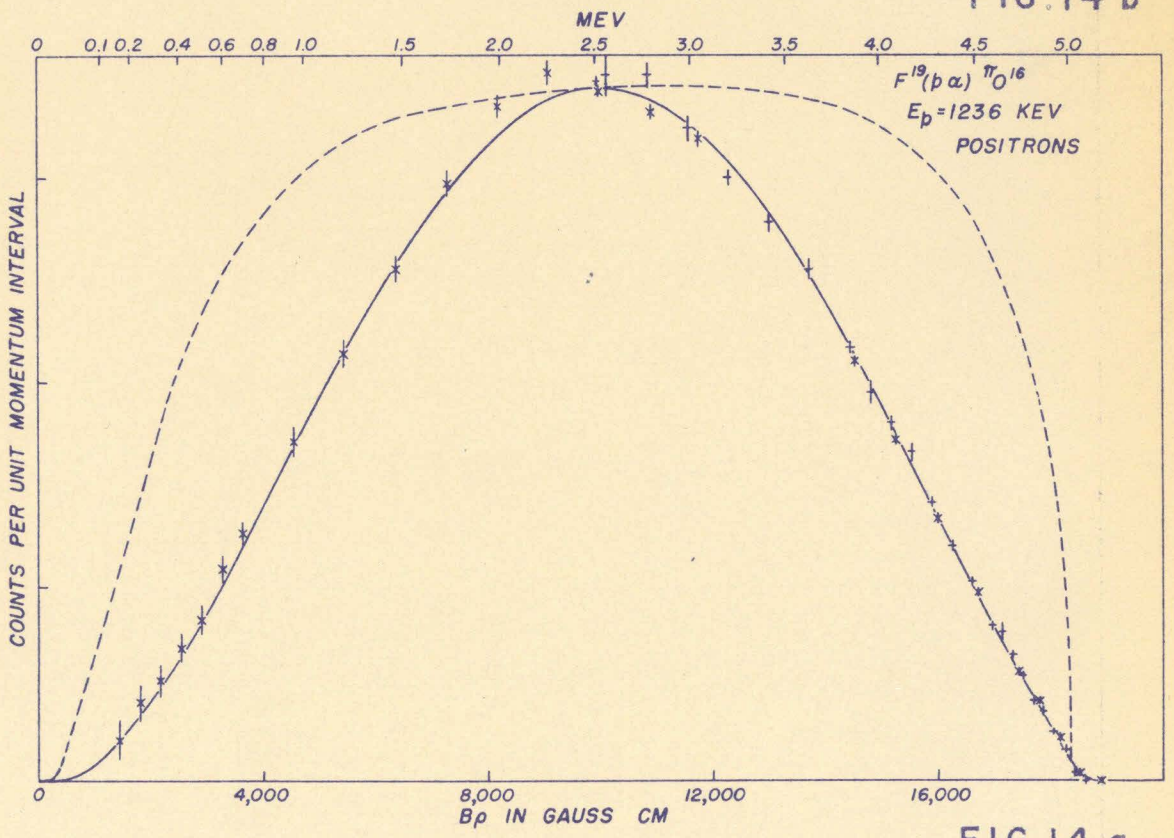

FIG. 14 a

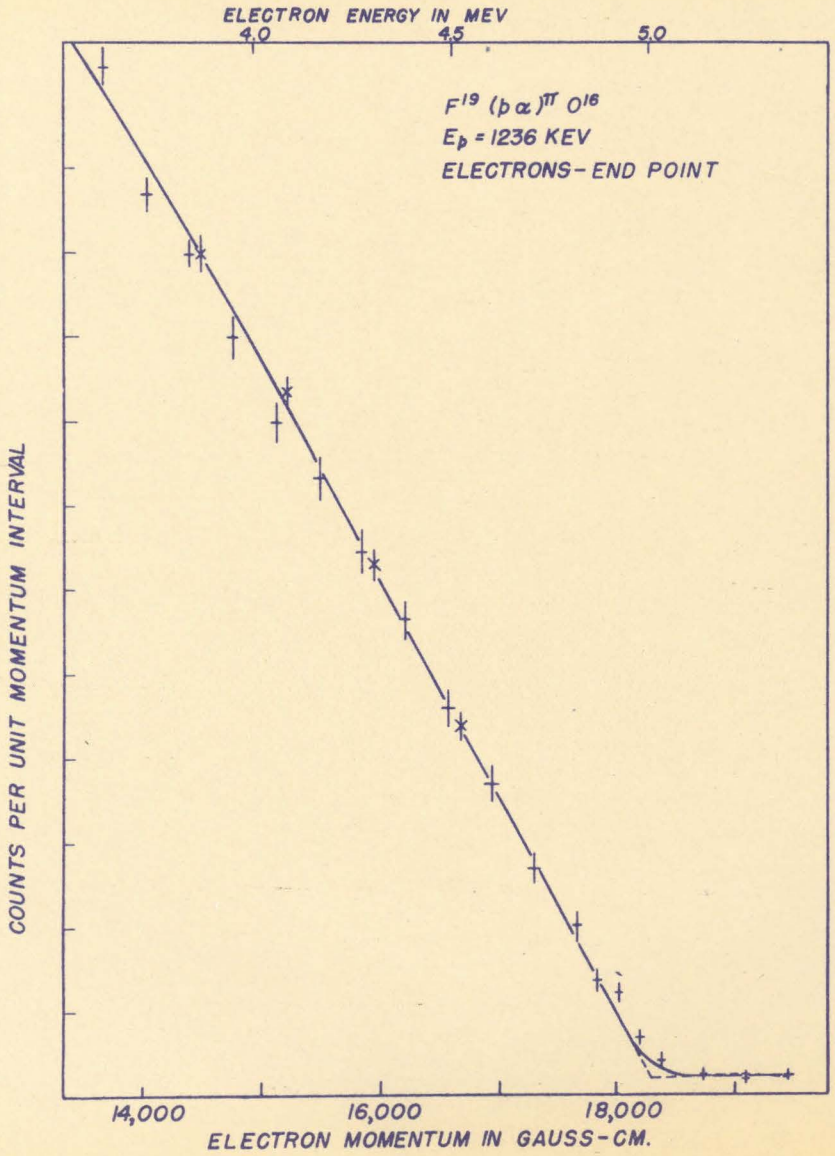

FIG. 15 b

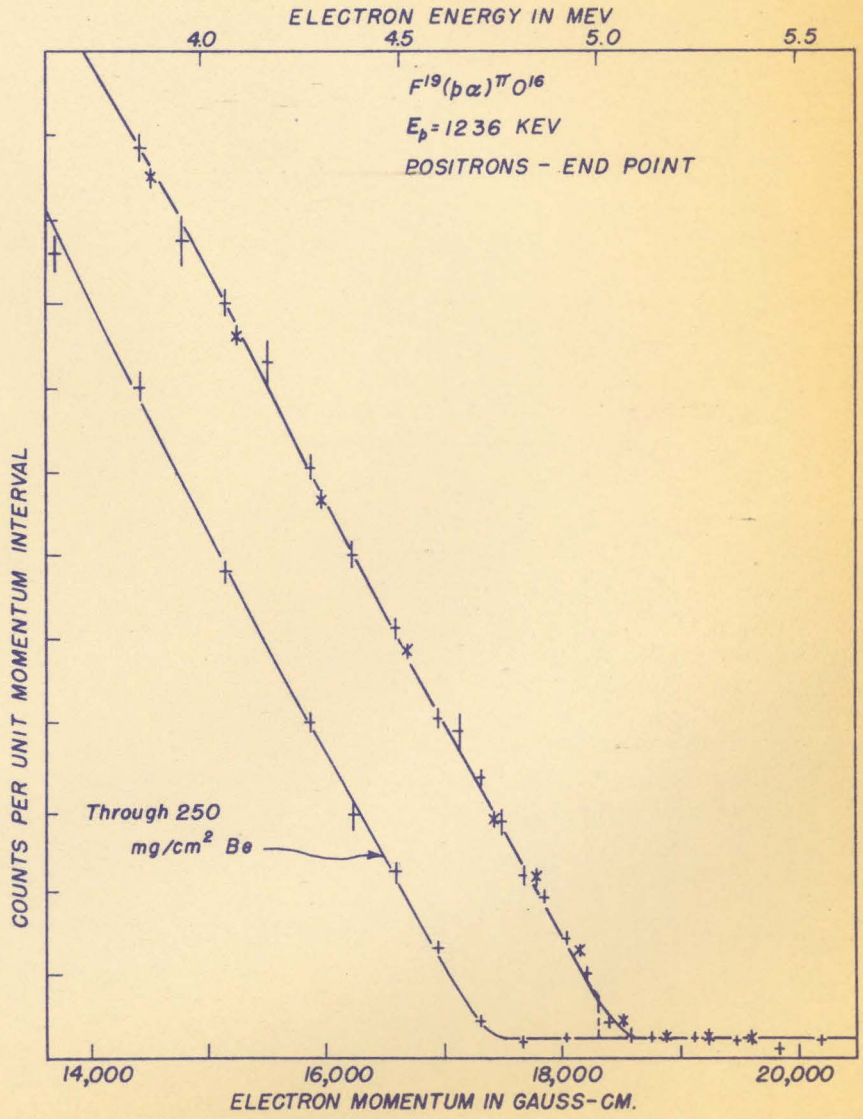

FIG. 15 a

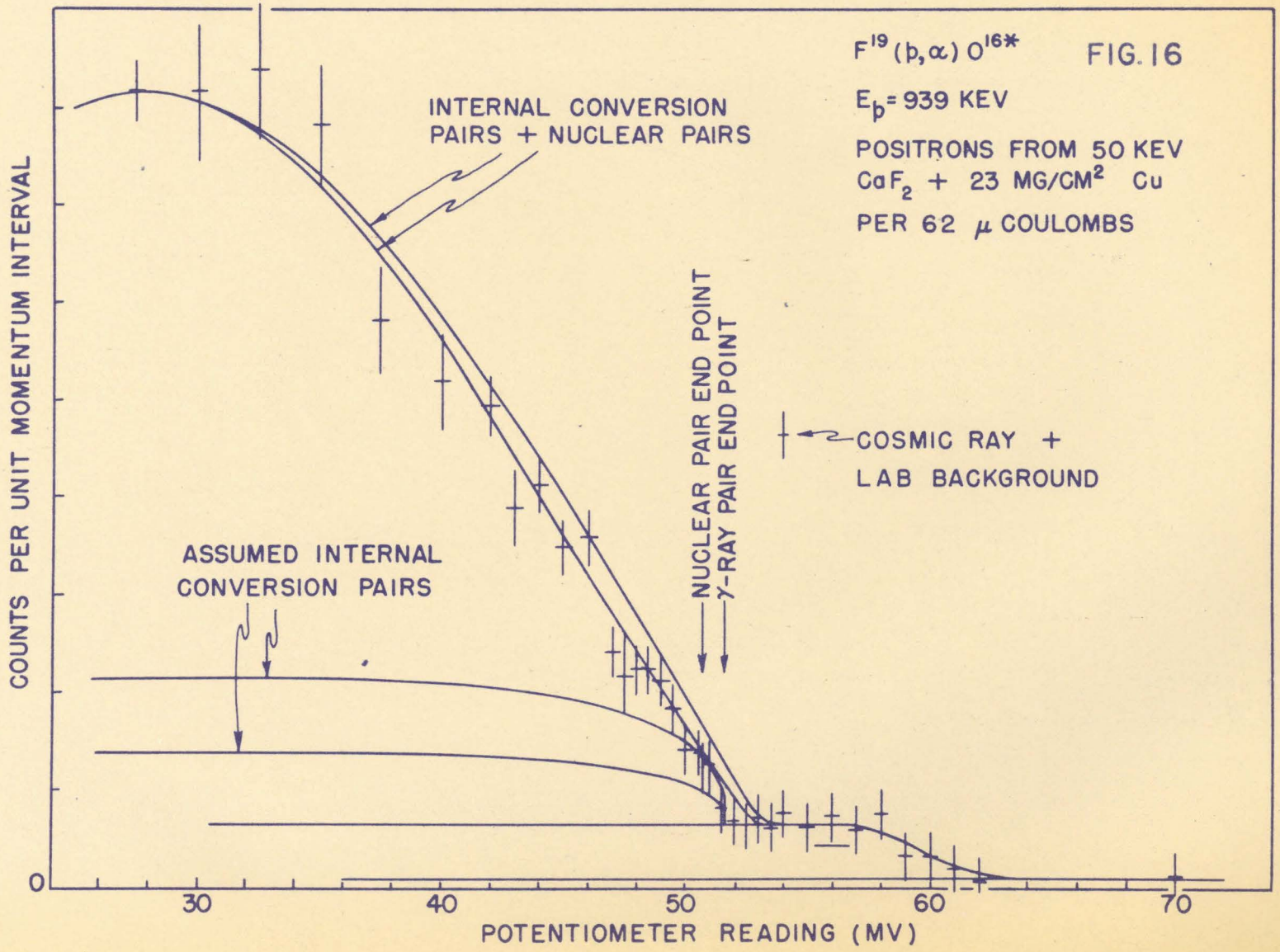
$F^{19}(p,\alpha)O^{16*}$
FIG. 16
E_p = 939 KEV
POSITRONS FROM 50 KEV
CaF_2 + 23 MG/CM^2 Cu
PER 62 μ COULOMBS
INTERNAL CONVERSION
PAIRS + NUCLEAR PAIRS
NUCLEAR PAIR END POINT
γ-RAY PAIR END POINT
COSMIC RAY +
LAB BACKGROUND
ASSUMED INTERNAL
CONVERSION PAIRS
COUNTS PER UNIT MOMENTUM INTERVAL
0
30
40
50
60
70
POTENTIOMETER READING (MV)

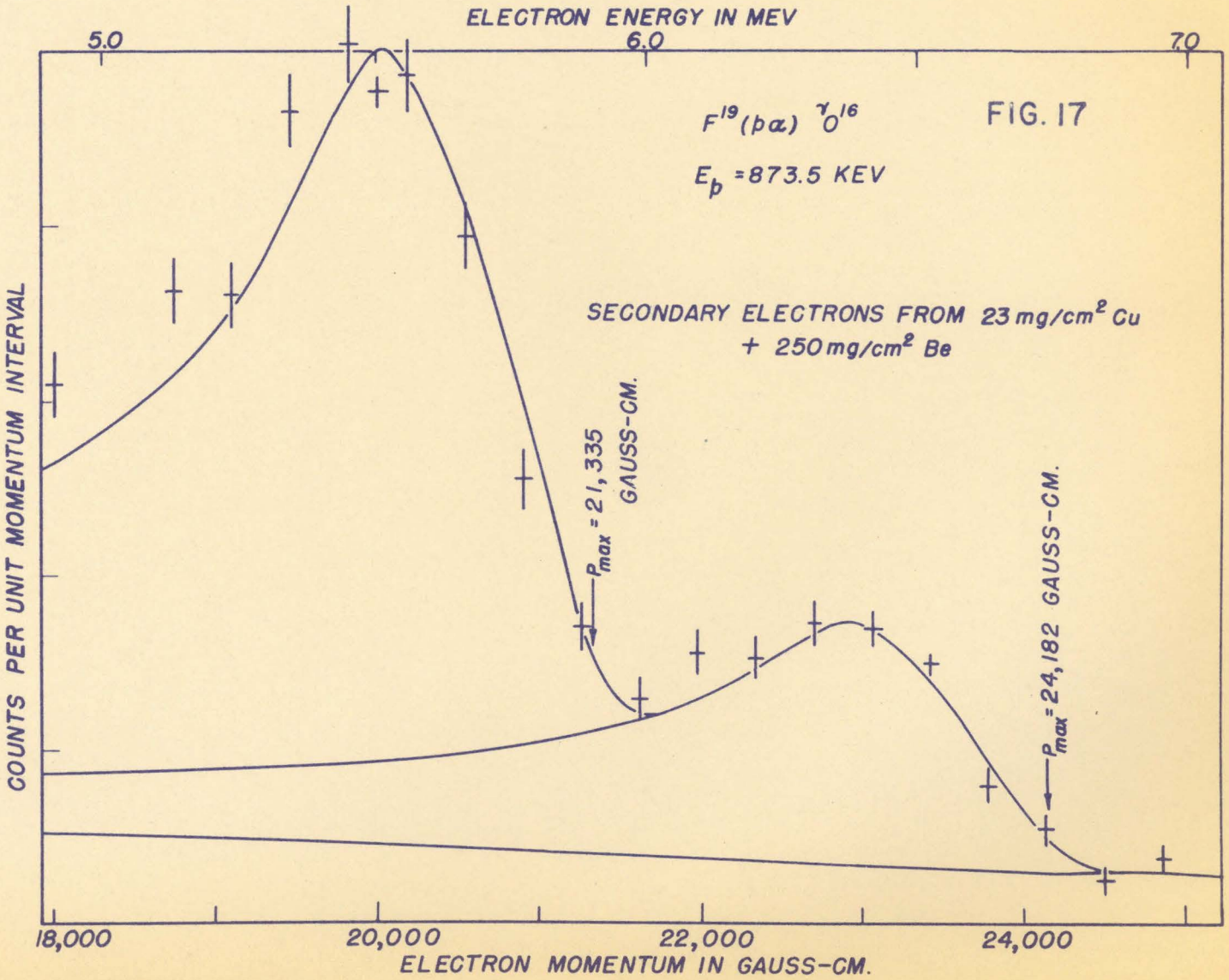
ELECTRON ENERGY IN MEV
5.0
6.0
7.0
$F^{19}(p\alpha)\,{}^{\gamma}O^{16}$
FIG. 17
E_p = 873.5 KEV
SECONDARY ELECTRONS FROM 23 mg/cm² Cu
+ 250 mg/cm² Be
P_{max} = 21,335 GAUSS-CM.
P_{max} = 24,182 GAUSS-CM.
COUNTS PER UNIT MOMENTUM INTERVAL
18,000
20,000
22,000
24,000
ELECTRON MOMENTUM IN GAUSS-CM.

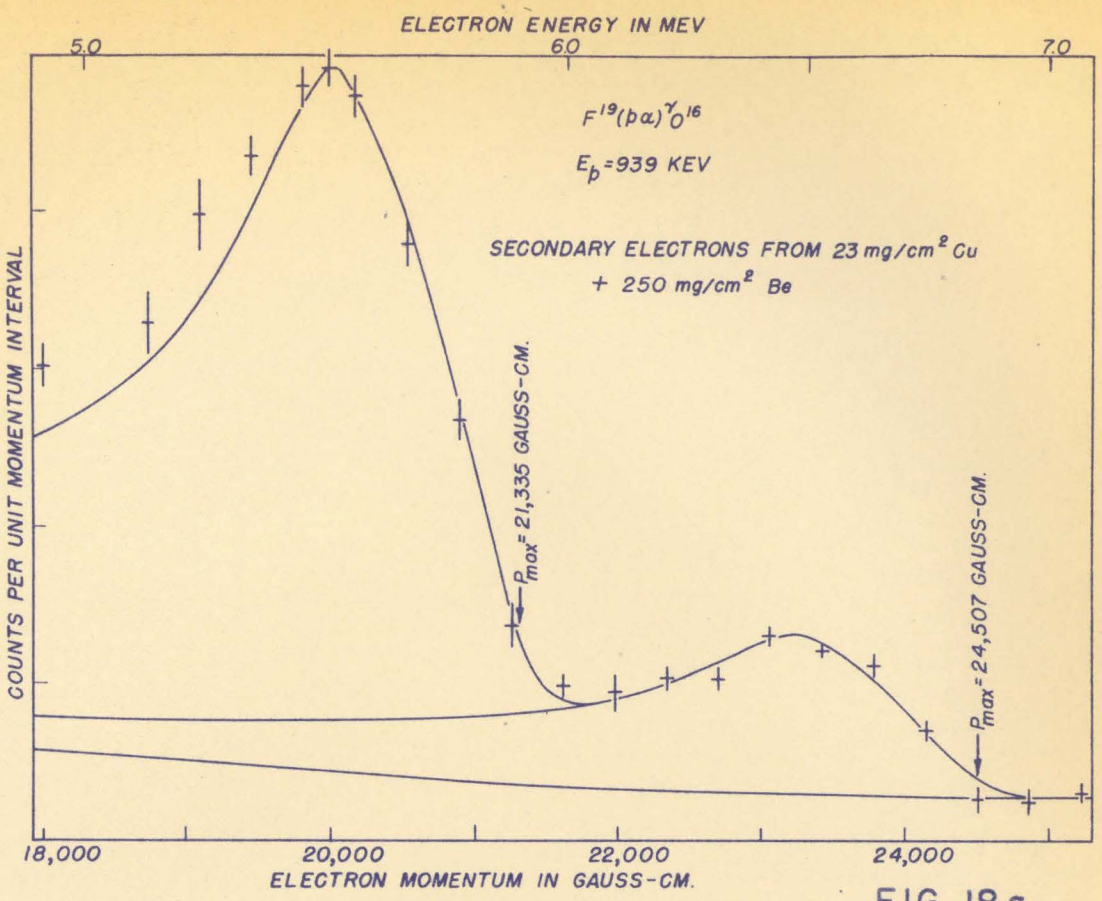

FIG. 18a

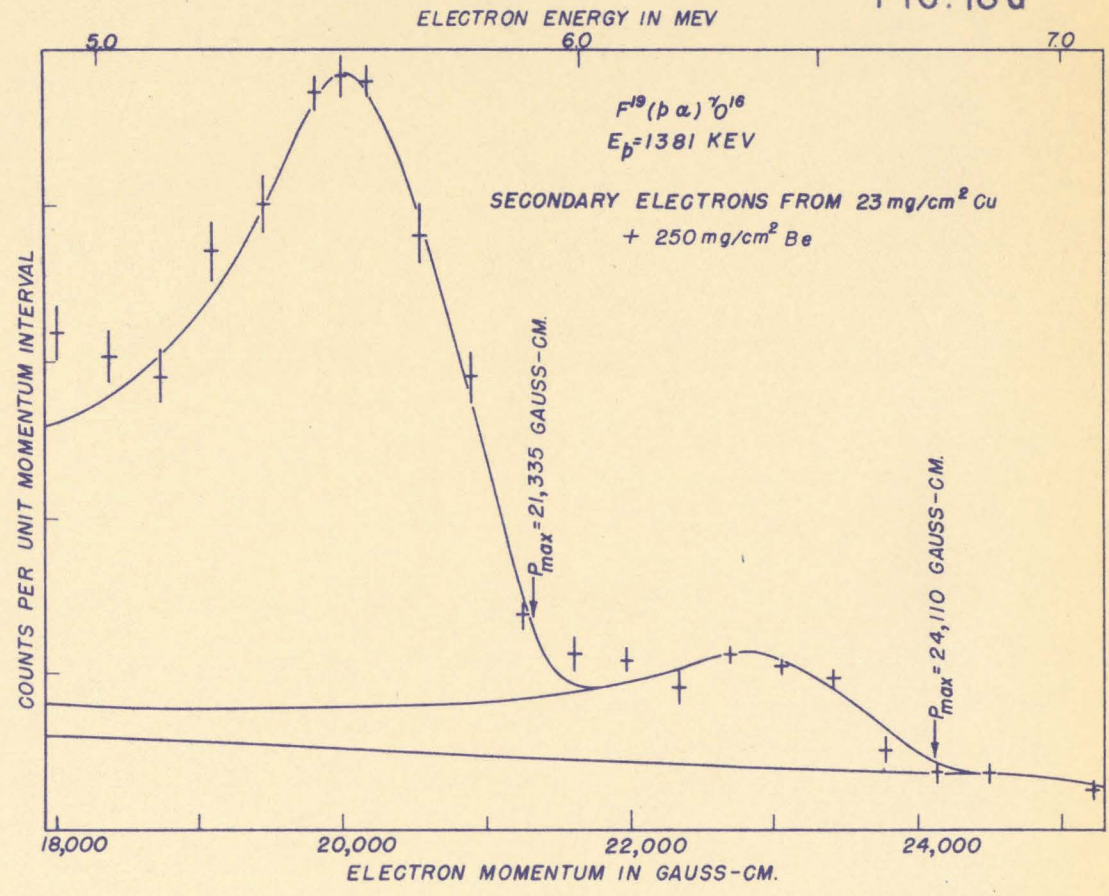

FIG. 18b

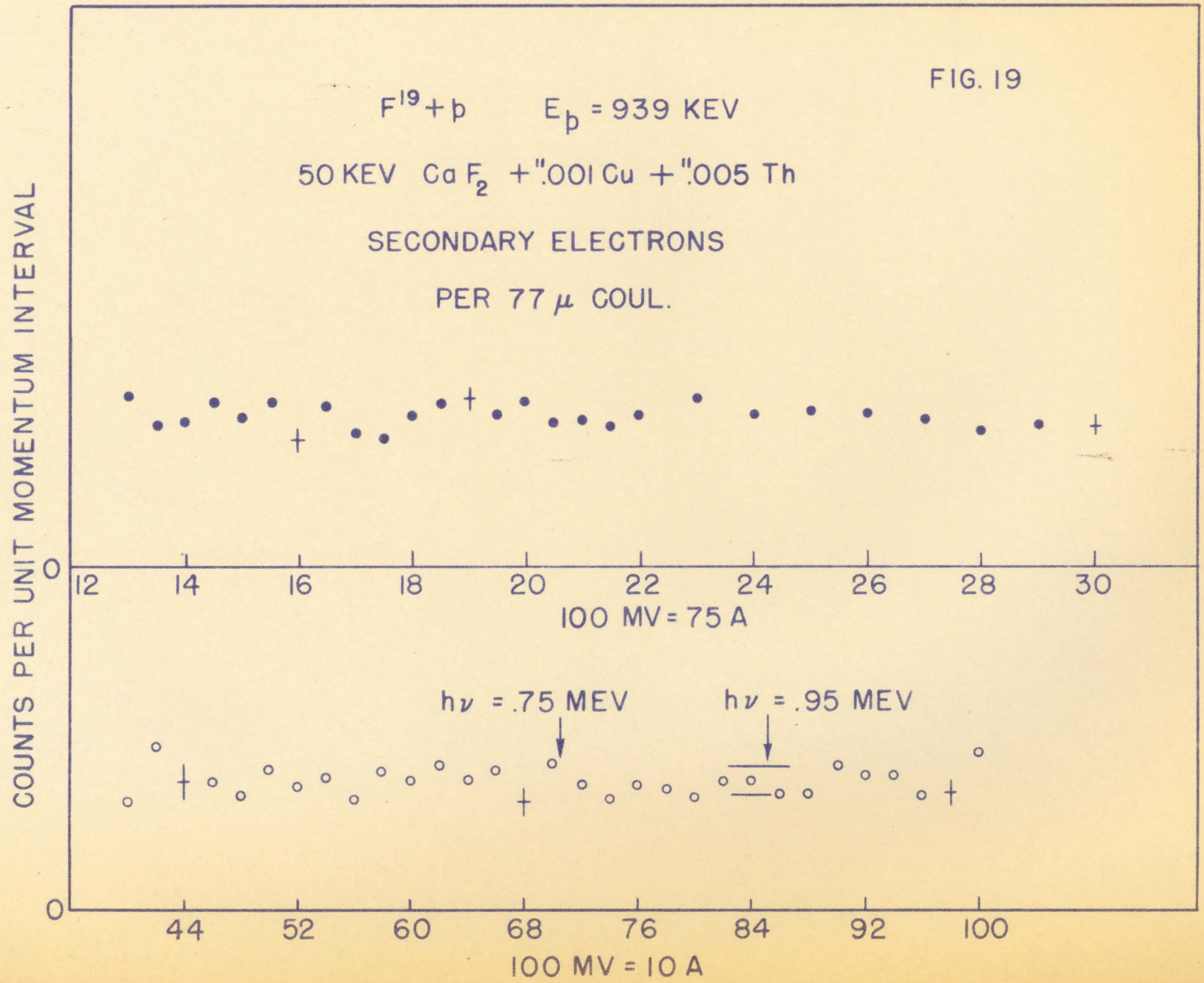
FIG. 19
$F^{19} + p$ $E_p = 939$ KEV
50 KEV CaF_2 + ".001 Cu + ".005 Th
SECONDARY ELECTRONS
PER 77 μ COUL.
COUNTS PER UNIT MOMENTUM INTERVAL
0
12
14
16
18
20
22
24
26
28
30
100 MV = 75 A
hν = .75 MEV
hν = .95 MEV
0
44
52
60
68
76
84
92
100
100 MV = 10 A

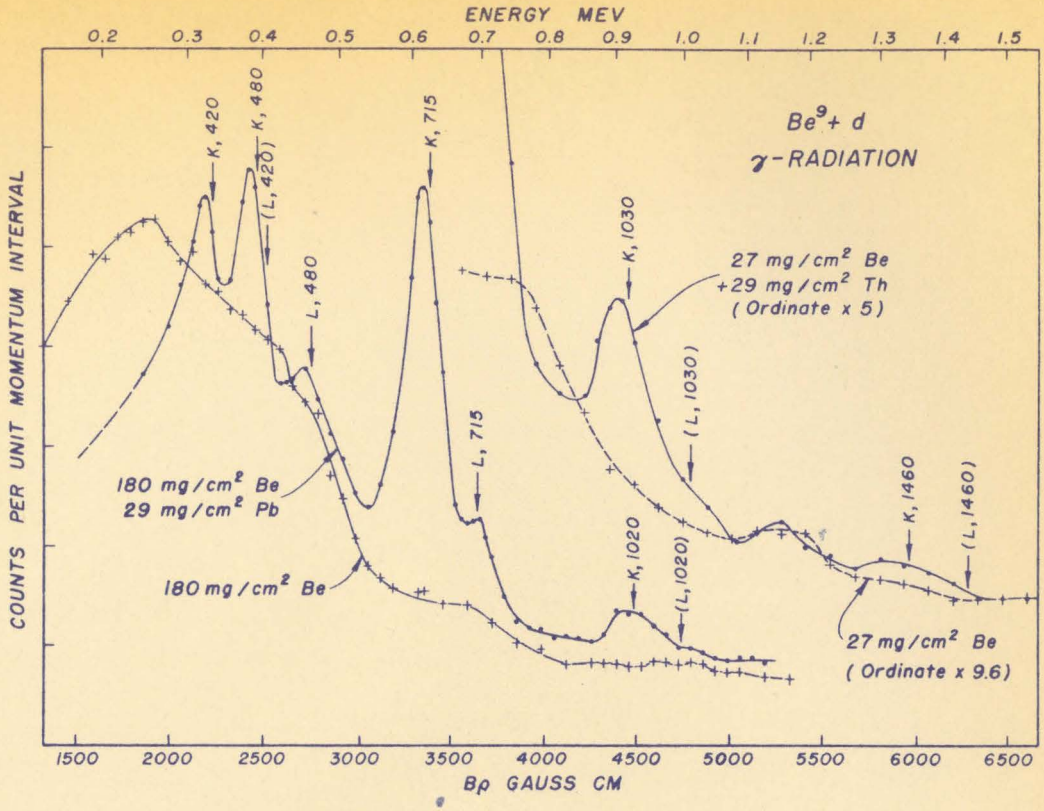
ENERGY MEV
0.2 0.3 0.4 0.5 0.6 0.7 0.8 0.9 1.0 1.1 1.2 1.3 1.4 1.5
COUNTS PER UNIT MOMENTUM INTERVAL
Be9 + d
γ-RADIATION
K, 420
K, 480
(L, 420)
L, 480
K, 715
L, 715
K, 1030
(L, 1030)
K, 1020
(L, 1020)
K, 1460
(L, 1460)
27 mg/cm² Be
+29 mg/cm² Th
(Ordinate x 5)
180 mg/cm² Be
29 mg/cm² Pb
180 mg/cm² Be
27 mg/cm² Be
(Ordinate x 9.6)
1500 2000 2500 3000 3500 4000 4500 5000 5500 6000 6500
Bρ GAUSS CM

FIG. 20

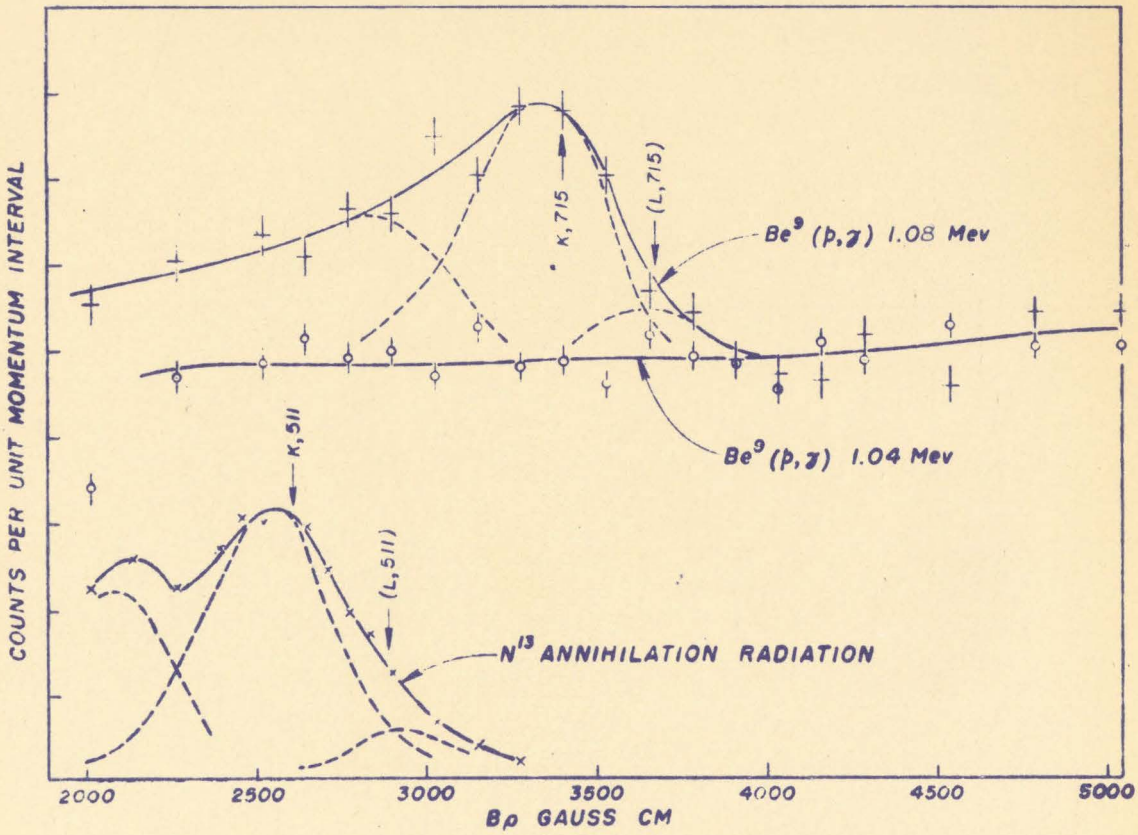
COUNTS PER UNIT MOMENTUM INTERVAL
K, 715
(L, 715)
Be9 (p, γ) 1.08 Mev
Be9 (p, γ) 1.04 Mev
K, 511
(L, 511)
N13 ANNIHILATION RADIATION
2000 2500 3000 3500 4000 4500 5000
Bρ GAUSS CM

FIG. 21

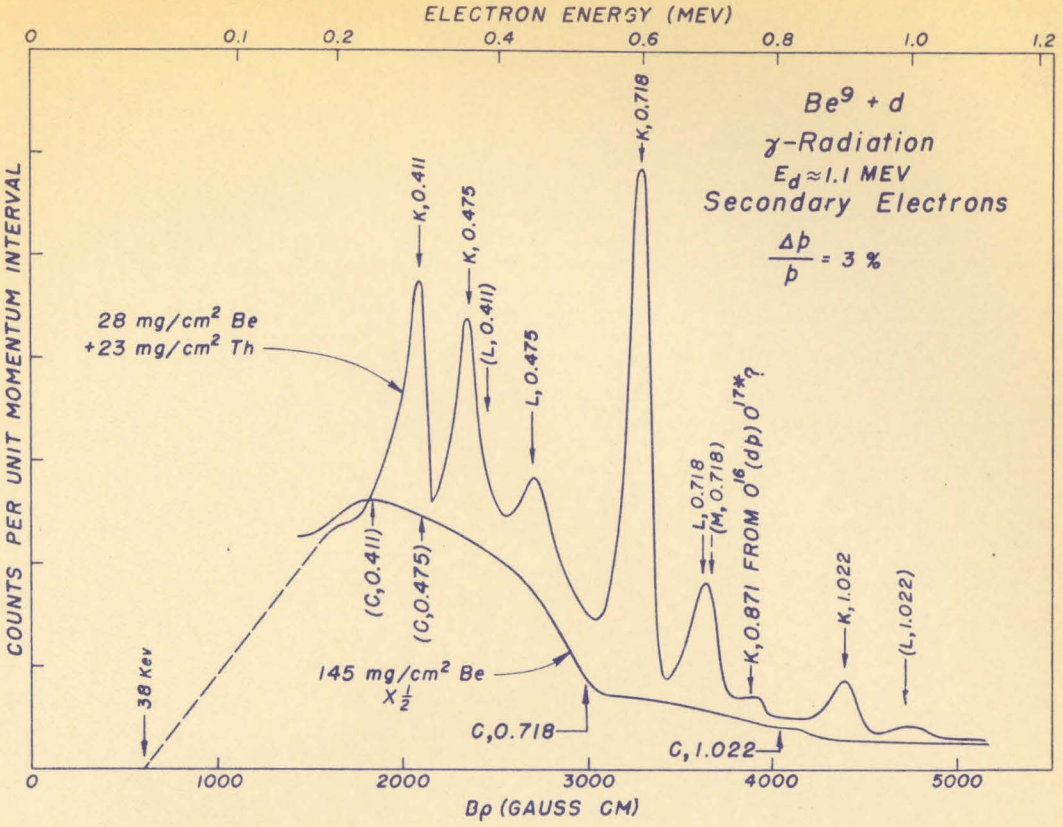
ELECTRON ENERGY (MEV)
0
0.1
0.2
0.4
0.6
0.8
1.0
1.2
COUNTS PER UNIT MOMENTUM INTERVAL
Be9 + d
γ-Radiation
Ed ≈ 1.1 MEV
Secondary Electrons
Δp/p = 3 %
K, 0.411
K, 0.475
(L, 0.411)
L, 0.475
K, 0.718
L, 0.718
(M, 0.718)
K, 0.871 FROM O16(dp)O17*?
K, 1.022
(L, 1.022)
28 mg/cm² Be
+23 mg/cm² Th
(C, 0.411)
(C, 0.475)
38 Kev
145 mg/cm² Be
X 1/2
C, 0.718
C, 1.022
0
1000
2000
3000
4000
5000
Bρ (GAUSS CM)

FIG. 22

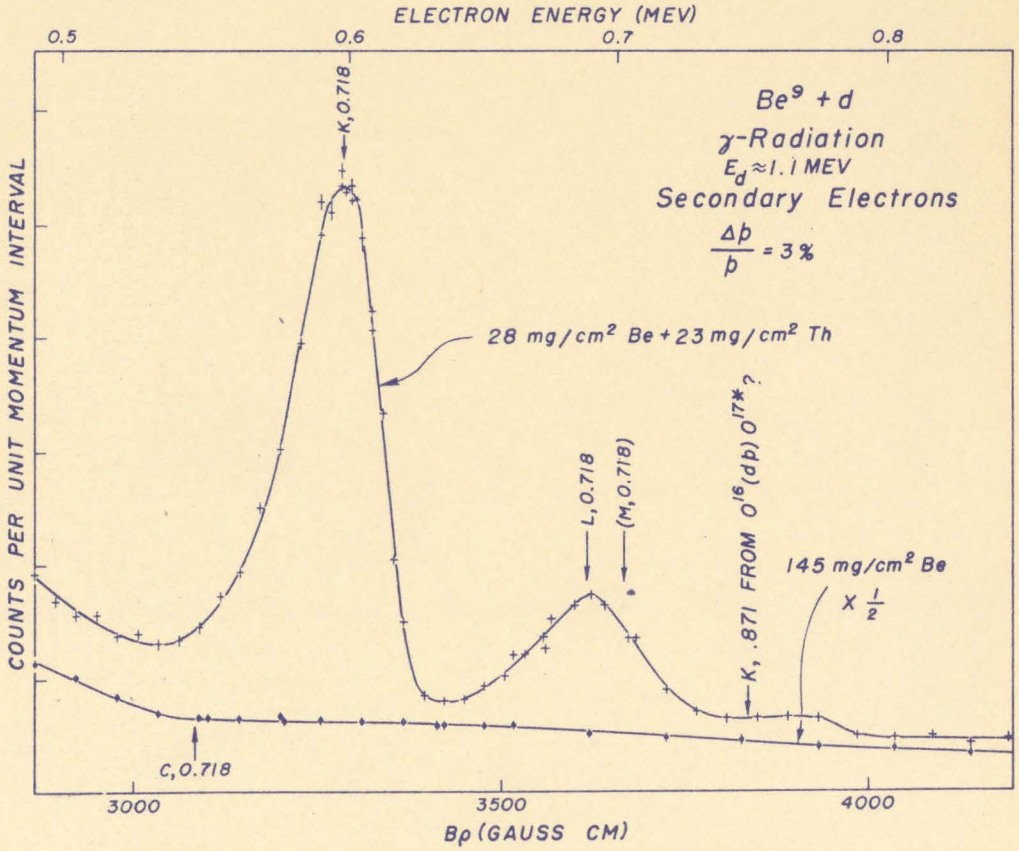
ELECTRON ENERGY (MEV)
0.5
0.6
0.7
0.8
COUNTS PER UNIT MOMENTUM INTERVAL
Be9 + d
γ-Radiation
Ed ≈ 1.1 MEV
Secondary Electrons
Δp/p = 3 %
K, 0.718
28 mg/cm² Be + 23 mg/cm² Th
L, 0.718
(M, 0.718)
K, .871 FROM O16(dp)O17*?
145 mg/cm² Be
X 1/2
C, 0.718
3000
3500
4000
Bρ (GAUSS CM)

FIG. 23

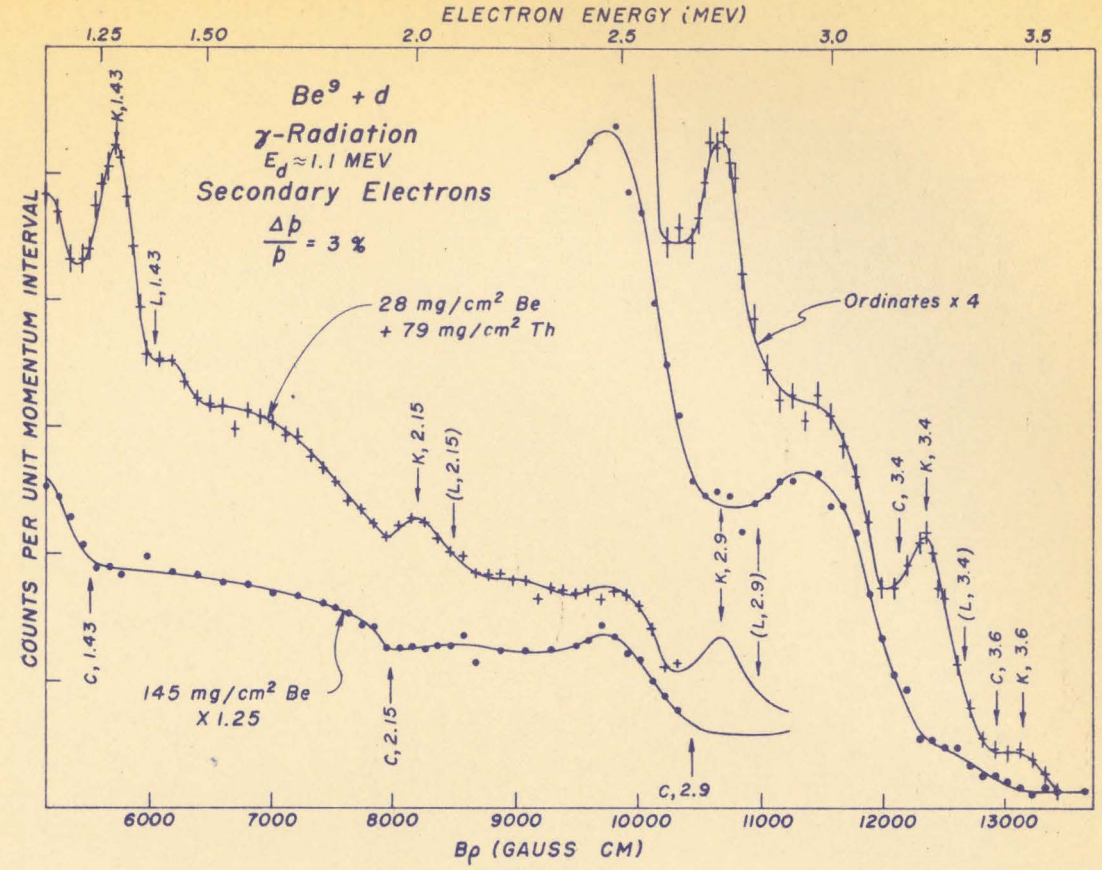
ELECTRON ENERGY (MEV)
1.25
1.50
2.0
2.5
3.0
3.5
Be⁹ + d
γ-Radiation
E_d ≈ 1.1 MEV
Secondary Electrons
Δp/p = 3 %
28 mg/cm² Be
+ 79 mg/cm² Th
Ordinates x 4
K, 1.43
L, 1.43
C, 1.43
K, 2.15
(L, 2.15)
C, 2.15
K, 2.9
(L, 2.9)
C, 2.9
C, 3.4
K, 3.4
(L, 3.4)
C, 3.6
K, 3.6
145 mg/cm² Be
X 1.25
COUNTS PER UNIT MOMENTUM INTERVAL
6000
7000
8000
9000
10000
11000
12000
13000
Bρ (GAUSS CM)

FIG. 24

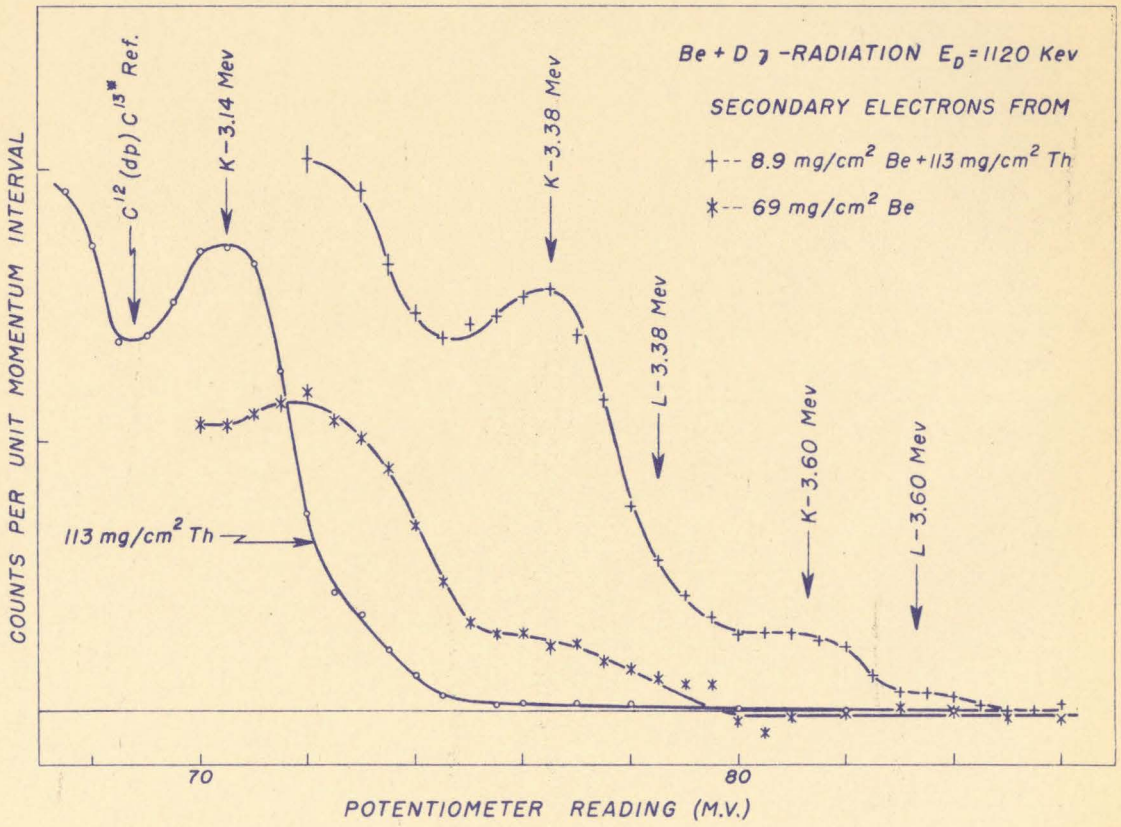
Be + D γ -RADIATION E_D = 1120 Kev
SECONDARY ELECTRONS FROM
+-- 8.9 mg/cm² Be + 113 mg/cm² Th
*-- 69 mg/cm² Be
C¹² (dp) C¹³* Ref.
K-3.14 Mev
K-3.38 Mev
L-3.38 Mev
K-3.60 Mev
L-3.60 Mev
113 mg/cm² Th
COUNTS PER UNIT MOMENTUM INTERVAL
70
80
POTENTIOMETER READING (M.V.)

FIG. 25

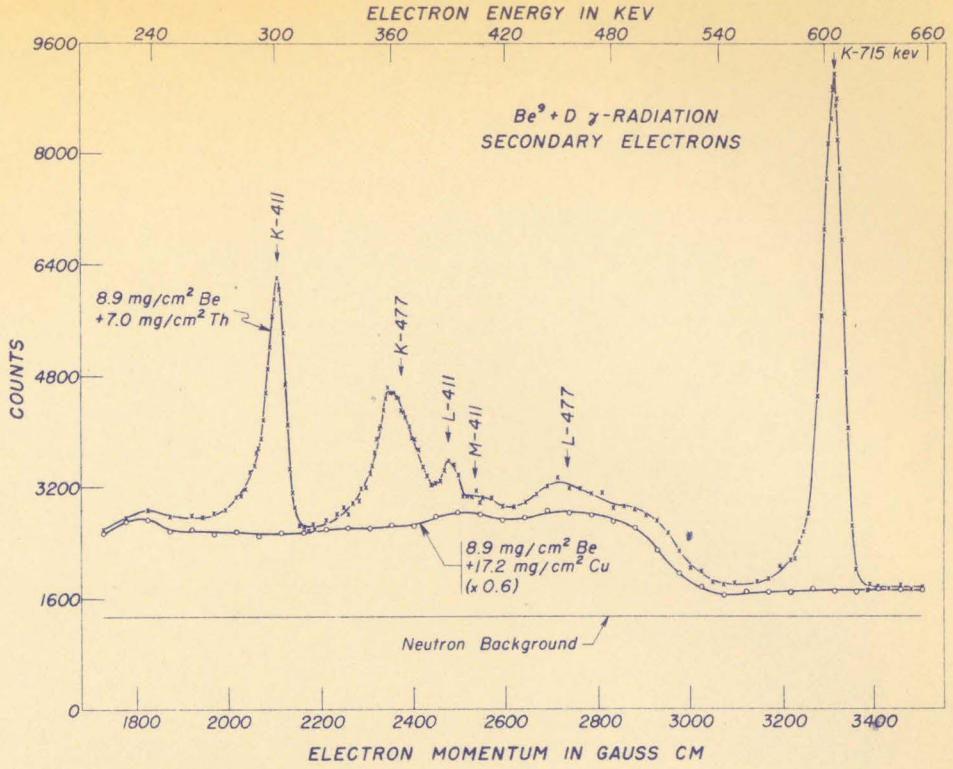
ELECTRON ENERGY IN KEV
240
300
360
420
480
540
600
660
9600
8000
6400
4800
3200
1600
0
COUNTS
K-715 kev
Be⁹ + D γ-RADIATION
SECONDARY ELECTRONS
K-411
K-477
L-411
M-411
L-477
8.9 mg/cm² Be
+7.0 mg/cm² Th
8.9 mg/cm² Be
+17.2 mg/cm² Cu
(x 0.6)
Neutron Background
1800
2000
2200
2400
2600
2800
3000
3200
3400
ELECTRON MOMENTUM IN GAUSS CM

FIG. 26

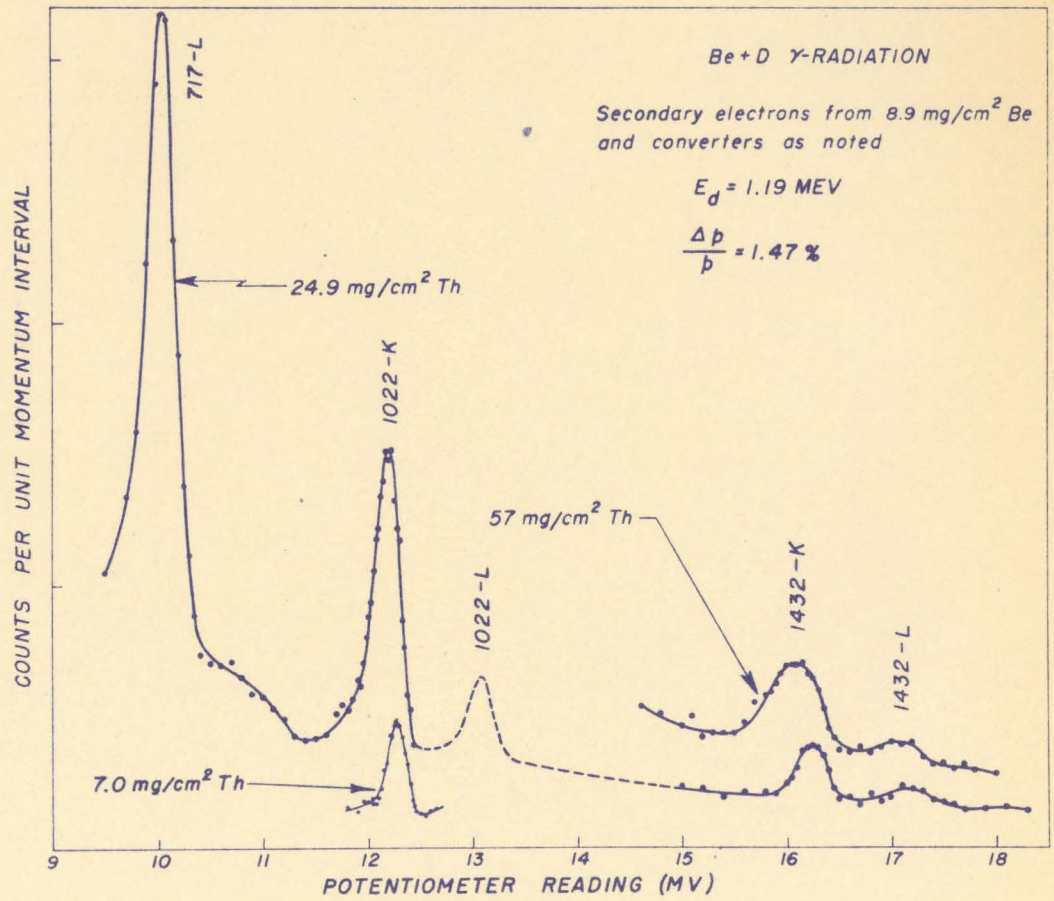
Be + D γ-RADIATION
Secondary electrons from 8.9 mg/cm² Be
and converters as noted
E_d = 1.19 MEV
Δp/p = 1.47 %
717-L
24.9 mg/cm² Th
1022-K
1022-L
57 mg/cm² Th
1432-K
1432-L
7.0 mg/cm² Th
COUNTS PER UNIT MOMENTUM INTERVAL
9
10
11
12
13
14
15
16
17
18
POTENTIOMETER READING (MV)

FIG. 27

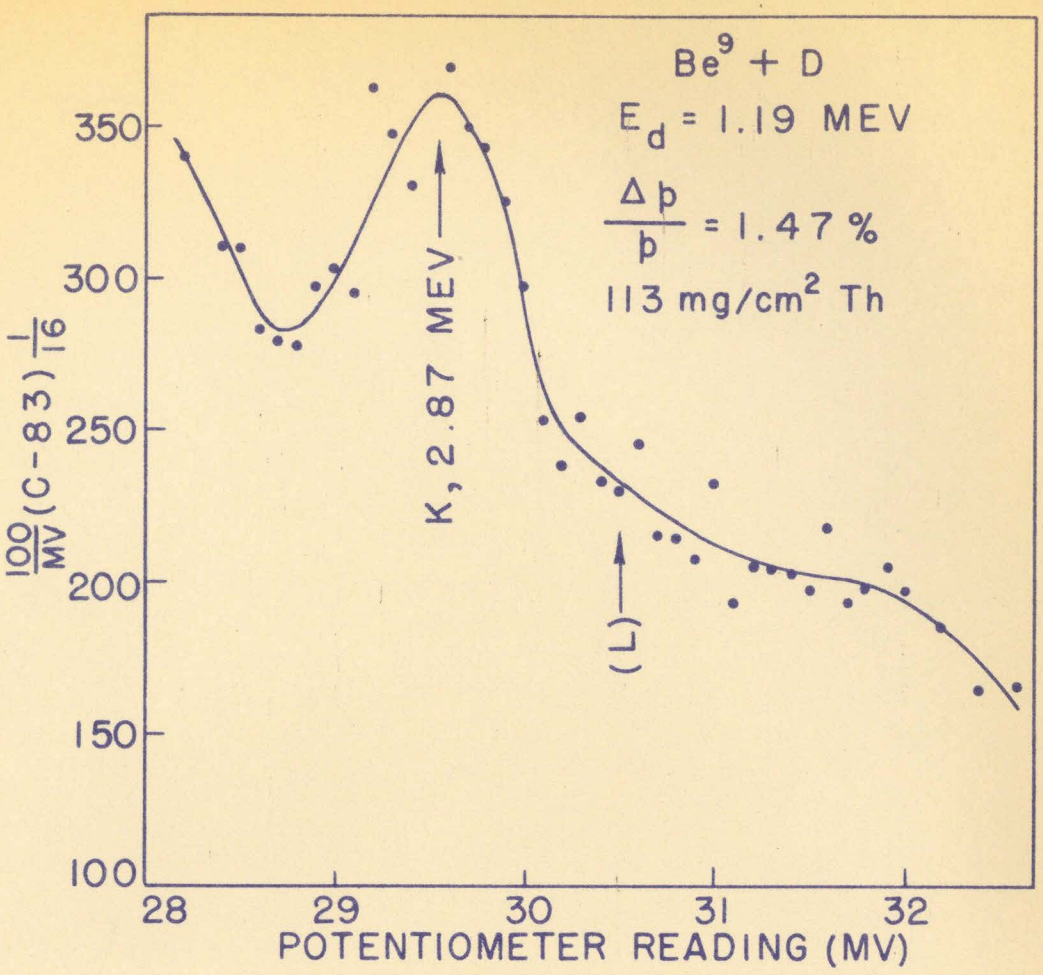

FIG. 28b

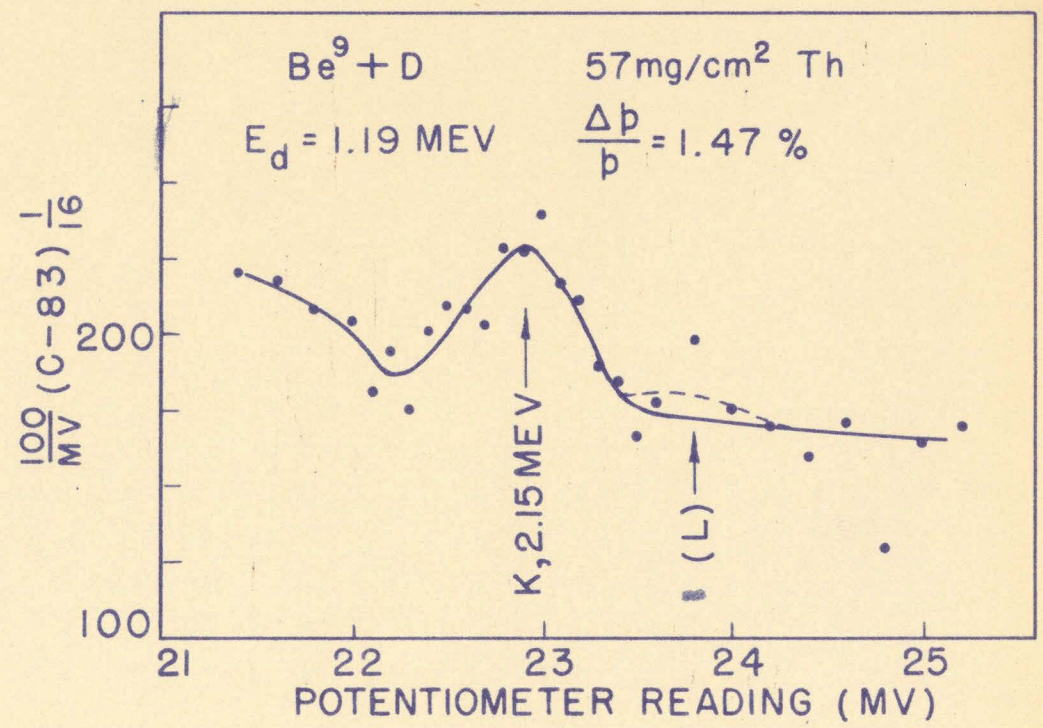

FIG. 28a

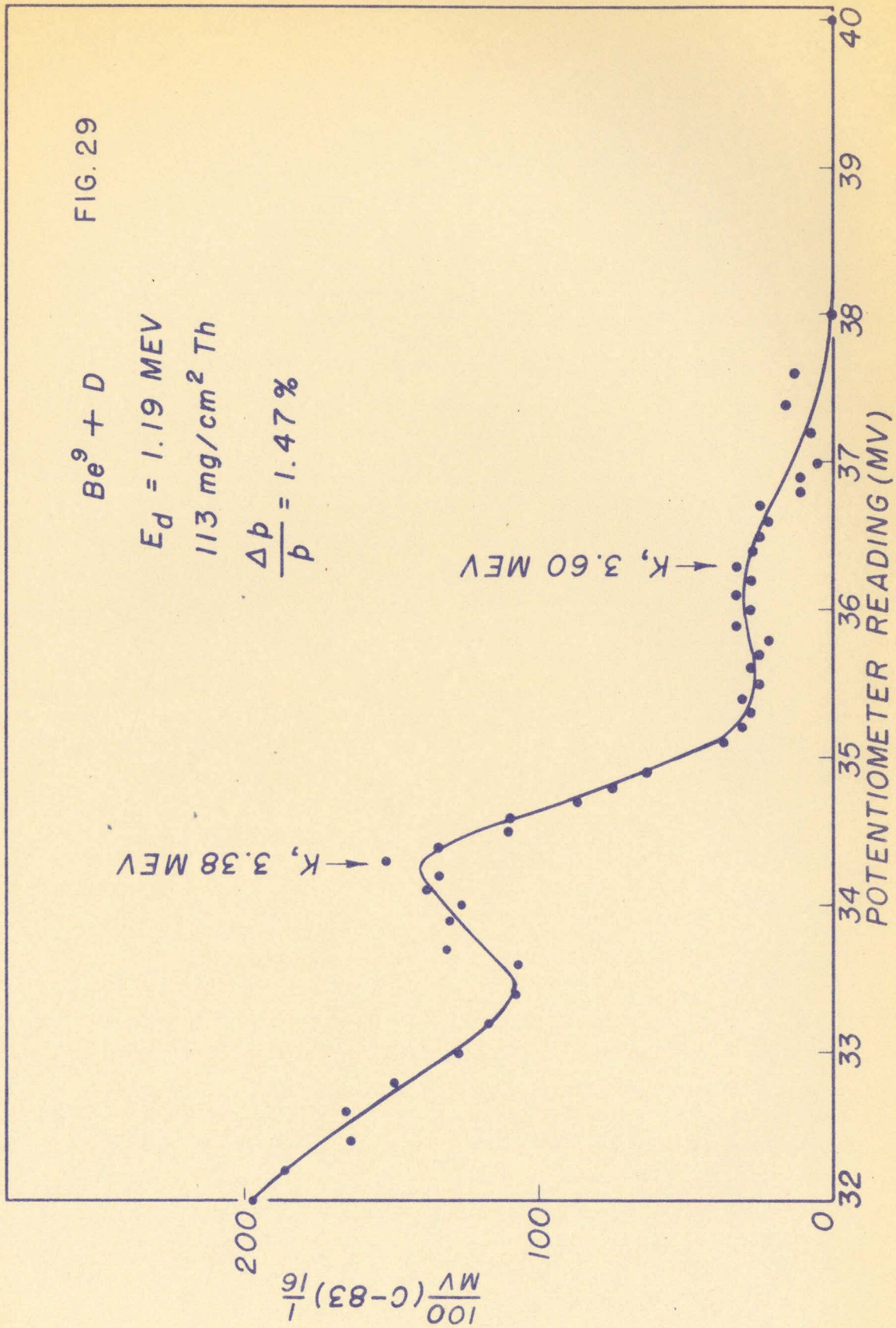
$Be^9 + D$
E_d = 1.19 MEV
113 mg/cm² Th
$\frac{\Delta p}{p}$ = 1.47 %
K, 3.60 MEV
K, 3.38 MEV
$\frac{100}{MV}(C-83)\frac{1}{16}$
200
100
0
32
33
34
35
36
37
38
39
40
POTENTIOMETER READING (MV)

FIG. 29

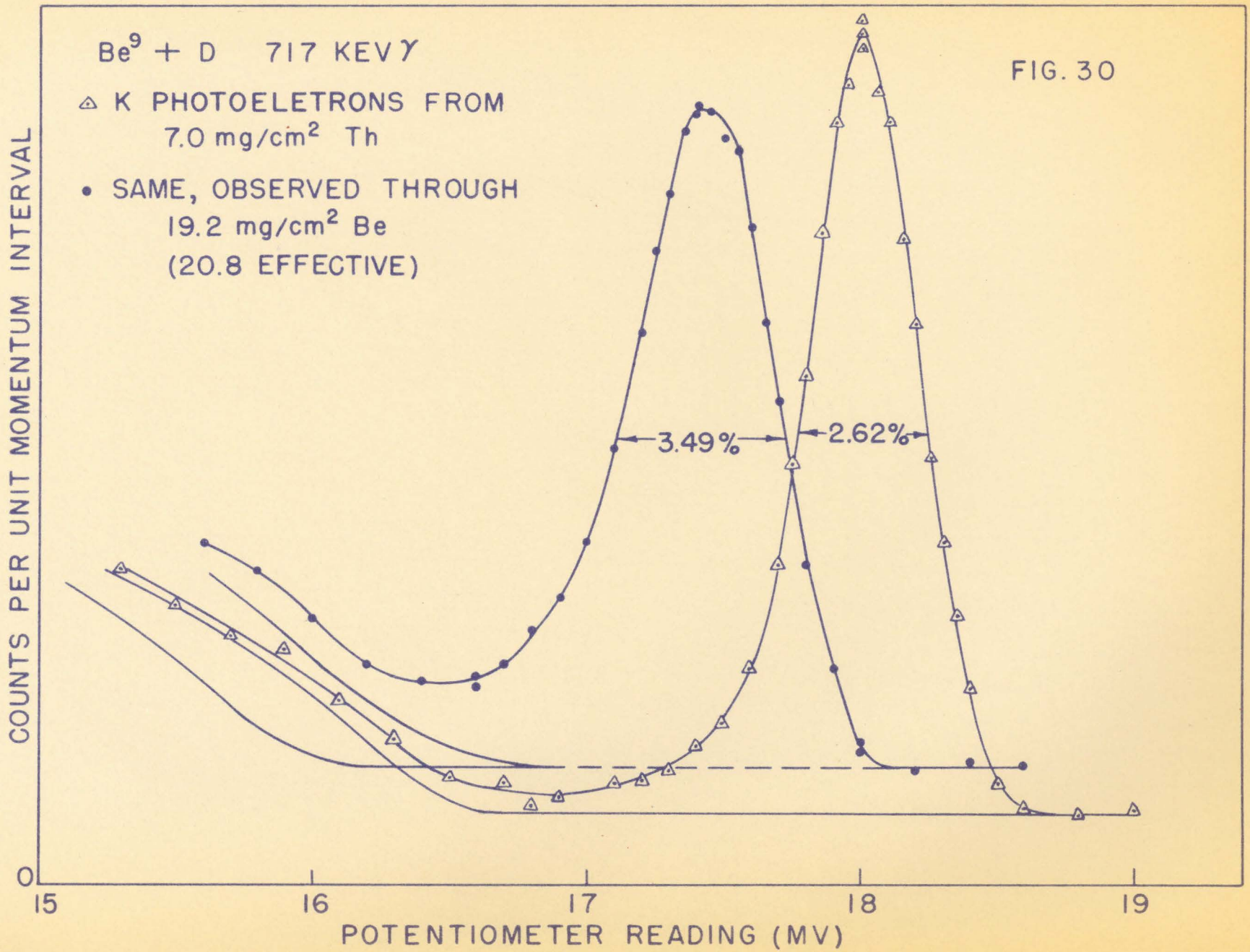
$Be^9 + D$ 717 KEV γ
△ K PHOTOELETRONS FROM 7.0 mg/cm² Th
• SAME, OBSERVED THROUGH 19.2 mg/cm² Be (20.8 EFFECTIVE)
FIG. 30
3.49%
2.62%
COUNTS PER UNIT MOMENTUM INTERVAL
0
15
16
17
18
19
POTENTIOMETER READING (MV)

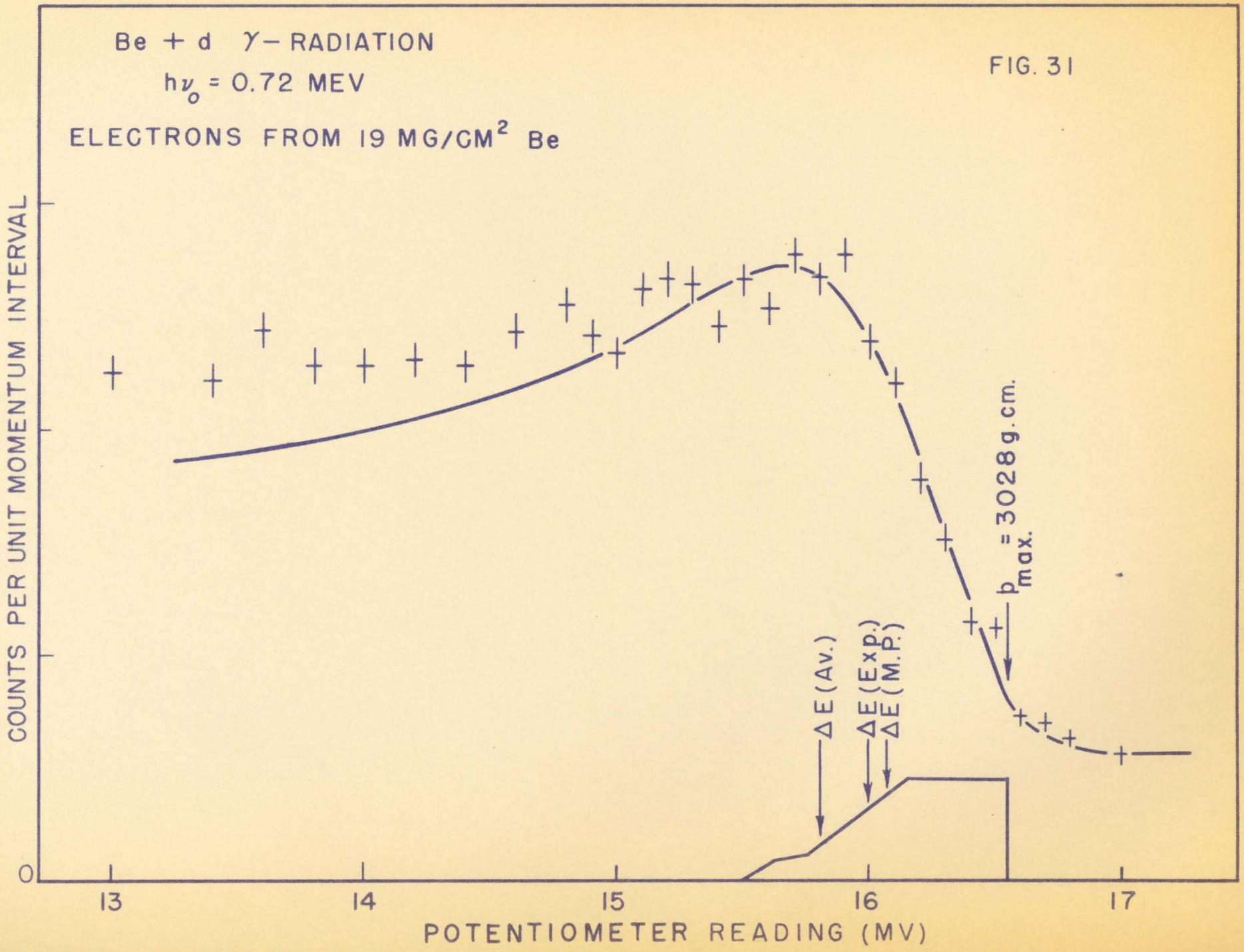
Be + d γ – RADIATION
$h\nu_o$ = 0.72 MEV
ELECTRONS FROM 19 MG/CM^2 Be
FIG. 31
COUNTS PER UNIT MOMENTUM INTERVAL
0
13
14
15
16
17
POTENTIOMETER READING (MV)
ΔE (Av.)
ΔE (Exp.)
ΔE (M.P.)
$p_{max.}$ = 3028 g.cm.

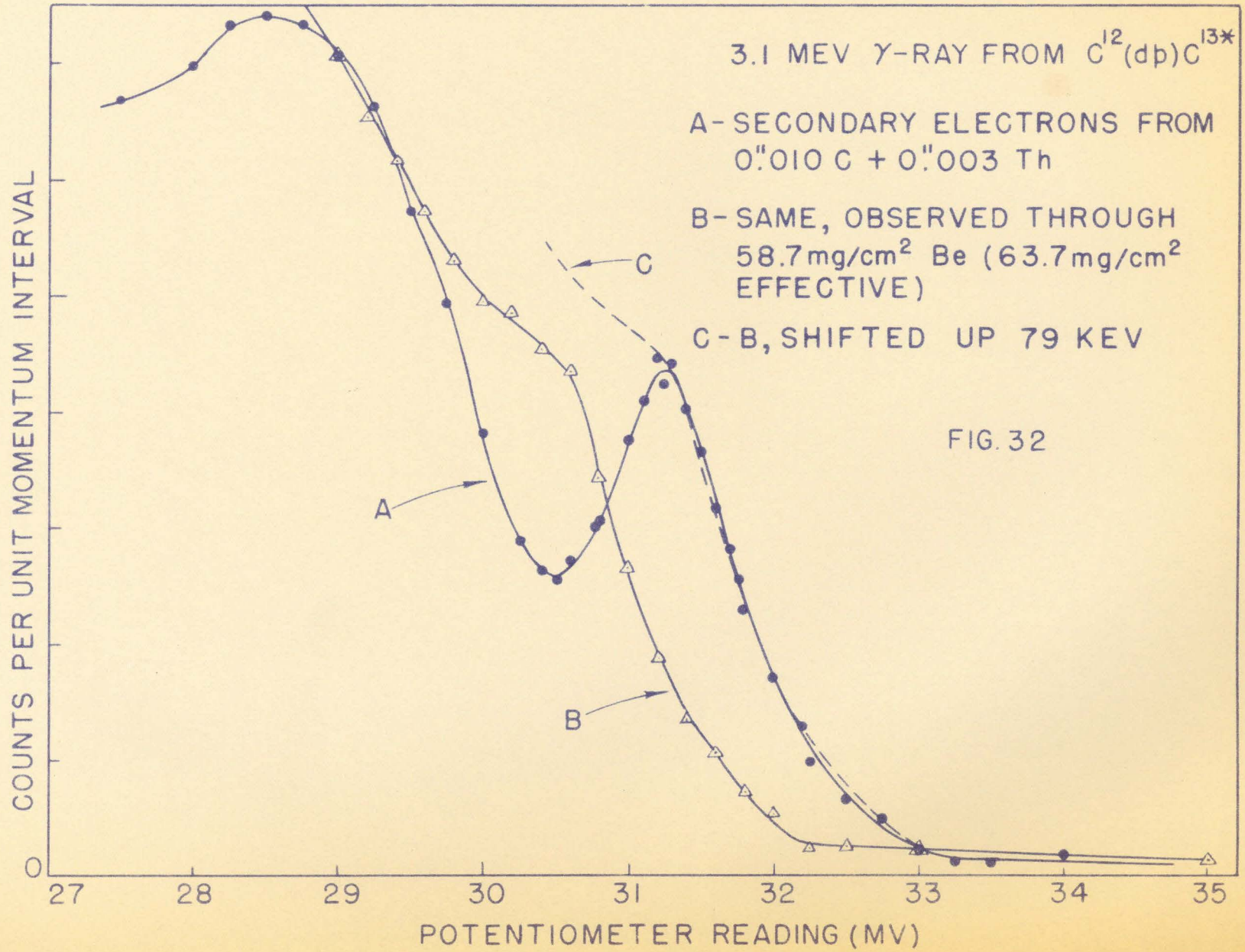
3.1 MEV γ-RAY FROM $C^{12}(dp)C^{13*}$
A - SECONDARY ELECTRONS FROM 0".010 C + 0".003 Th
B - SAME, OBSERVED THROUGH 58.7 mg/cm² Be (63.7 mg/cm² EFFECTIVE)
C - B, SHIFTED UP 79 KEV
A
B
C
COUNTS PER UNIT MOMENTUM INTERVAL
0
27
28
29
30
31
32
33
34
35
POTENTIOMETER READING (MV)

FIG. 32

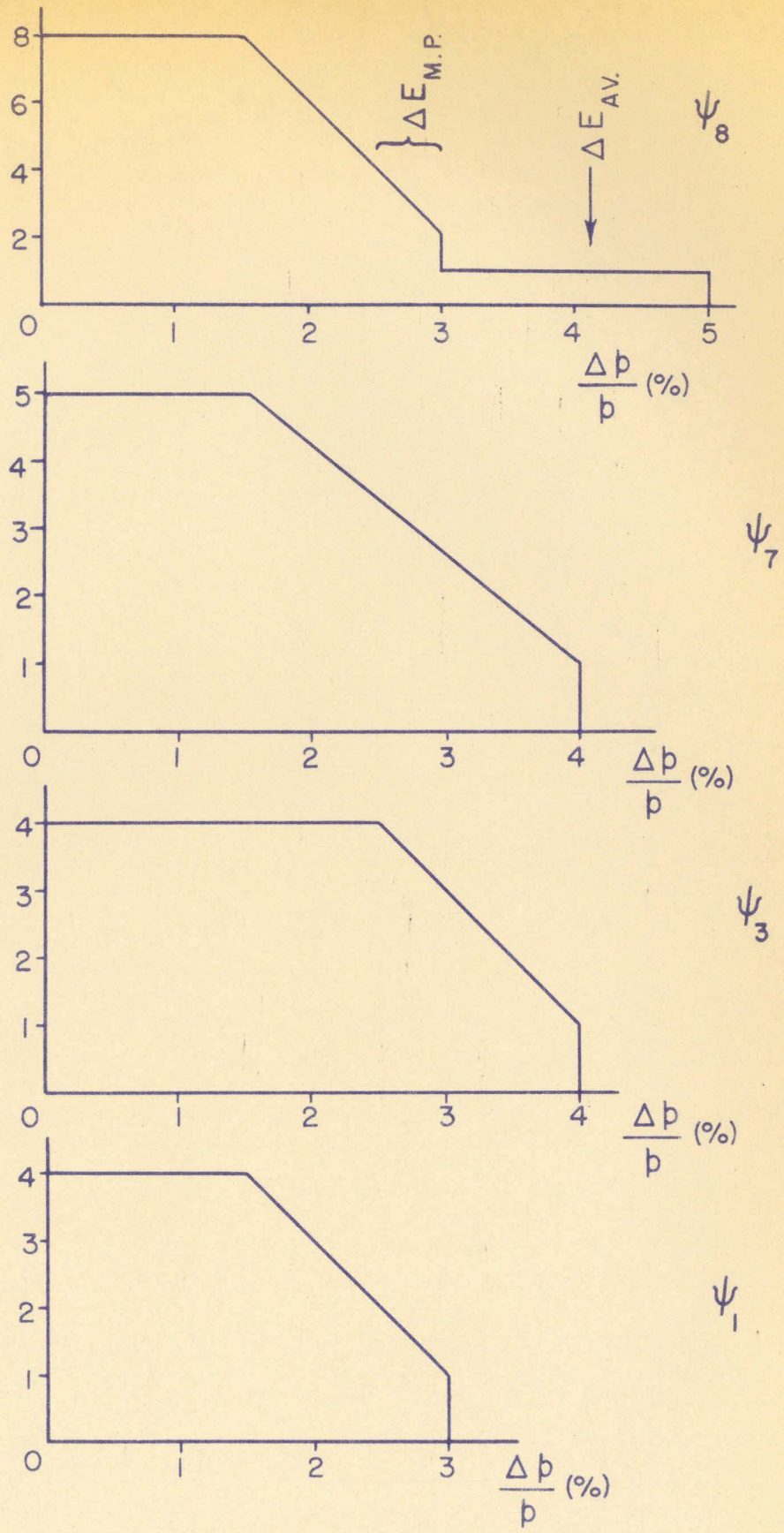

FIG.33 MOMEMTUM LOSS IN CONVERTER
USED IN CALCULATING COMPTON DISTRIBUTIONS NOTED

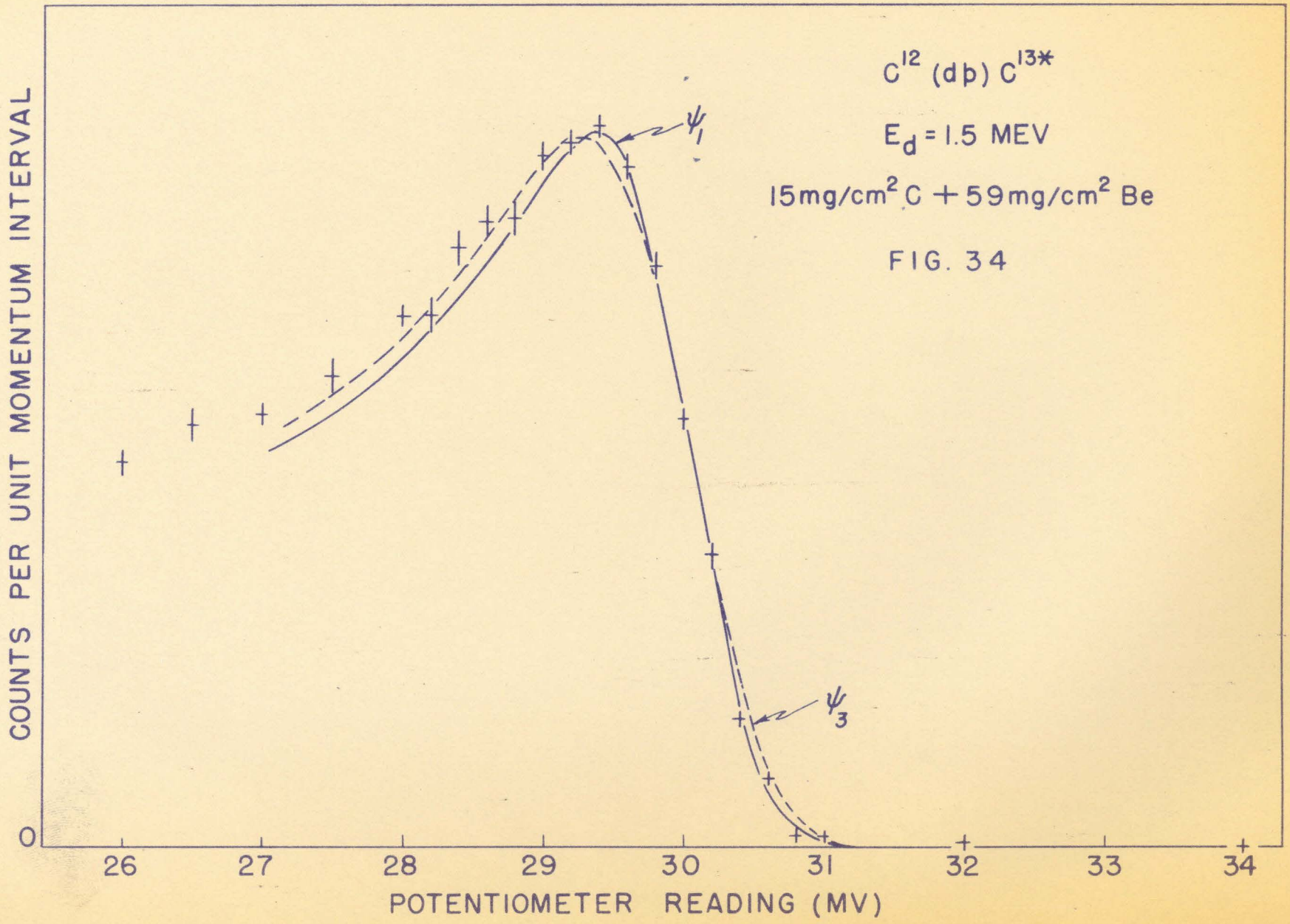
$C^{12}(dp)C^{13*}$
$E_d = 1.5$ MEV
15mg/cm² C + 59mg/cm² Be
FIG. 34
ψ_1
ψ_3
COUNTS PER UNIT MOMENTUM INTERVAL
0
26
27
28
29
30
31
32
33
34
POTENTIOMETER READING (MV)

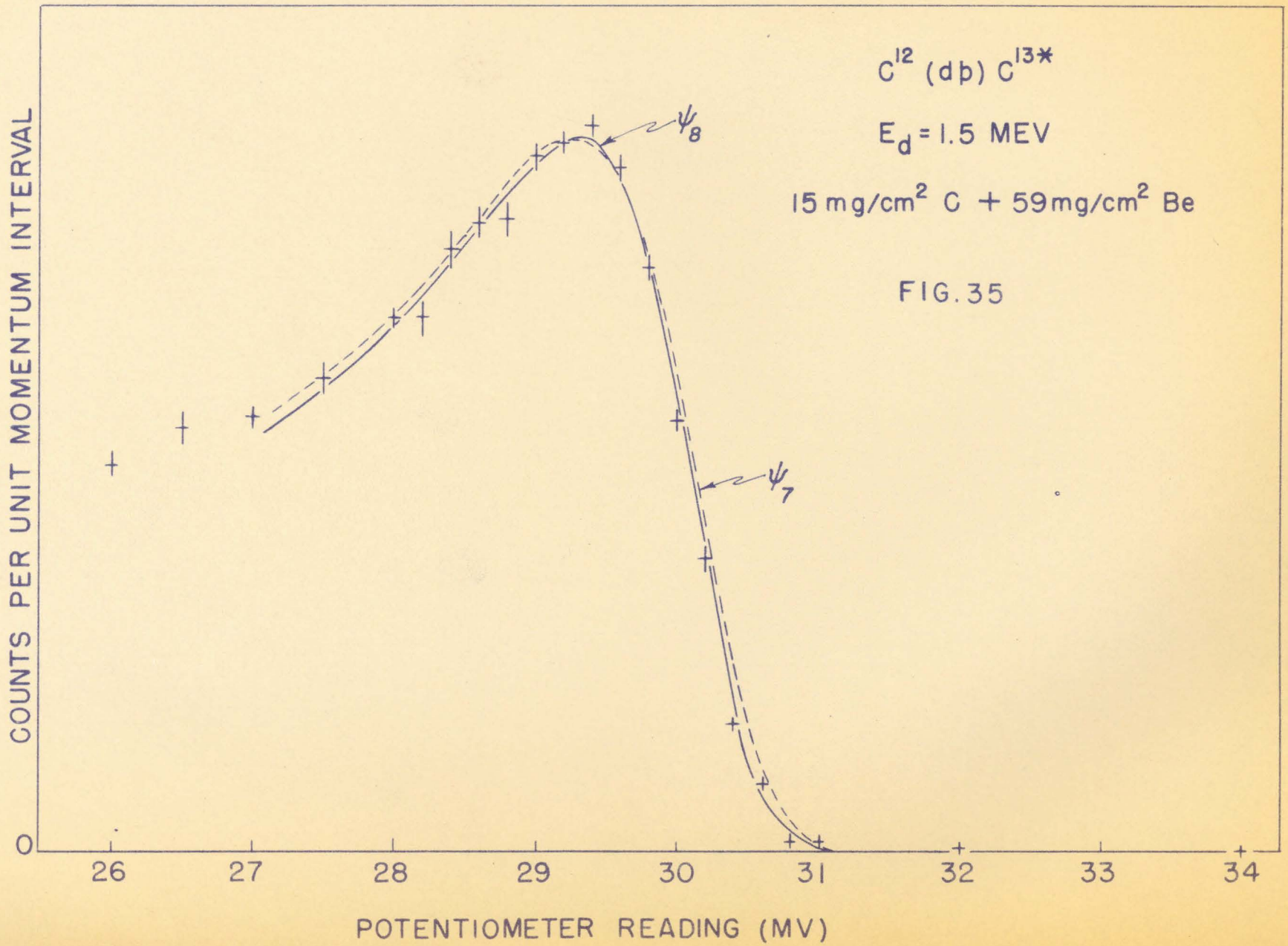
C^{12} (dp) C^{13*}
E_d = 1.5 MEV
15 mg/cm² C + 59 mg/cm² Be
FIG. 35
ψ_8
ψ_7
COUNTS PER UNIT MOMENTUM INTERVAL
0
26
27
28
29
30
31
32
33
34
POTENTIOMETER READING (MV)

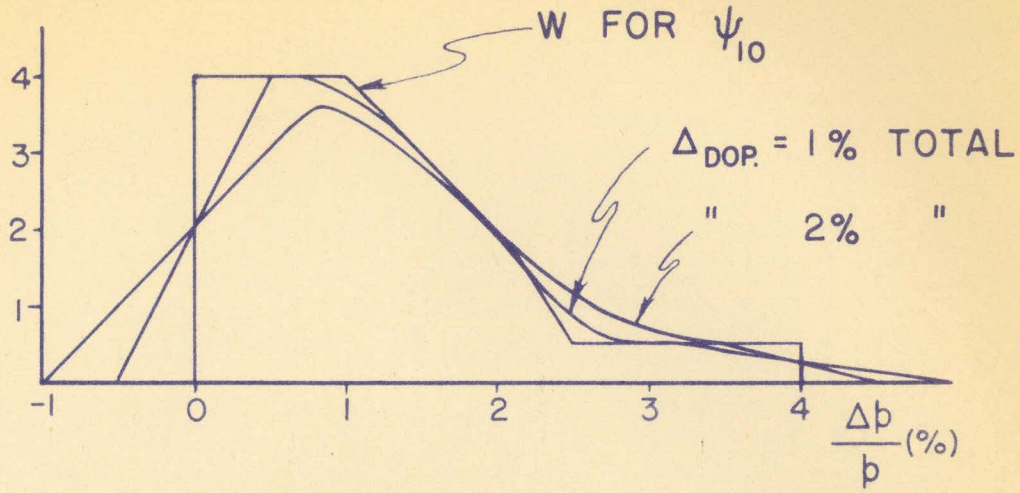

RECTANGULAR DOPPLER BROADING
FOLDED INTO DISTRIBUTION BELOW
FIG. 36b

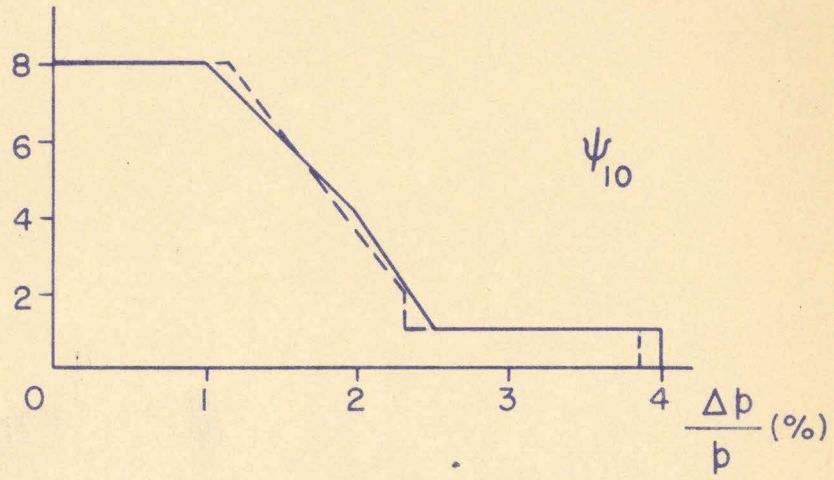

CONVERTER MOMENTUM DISTRIBUTION
USED TO CALCULATE COMPTON DISTRIBUTION ψ_{10}
DASHED LINE – DISTRIBUTION EXPECTED FROM ψ_8
FIG. 36a

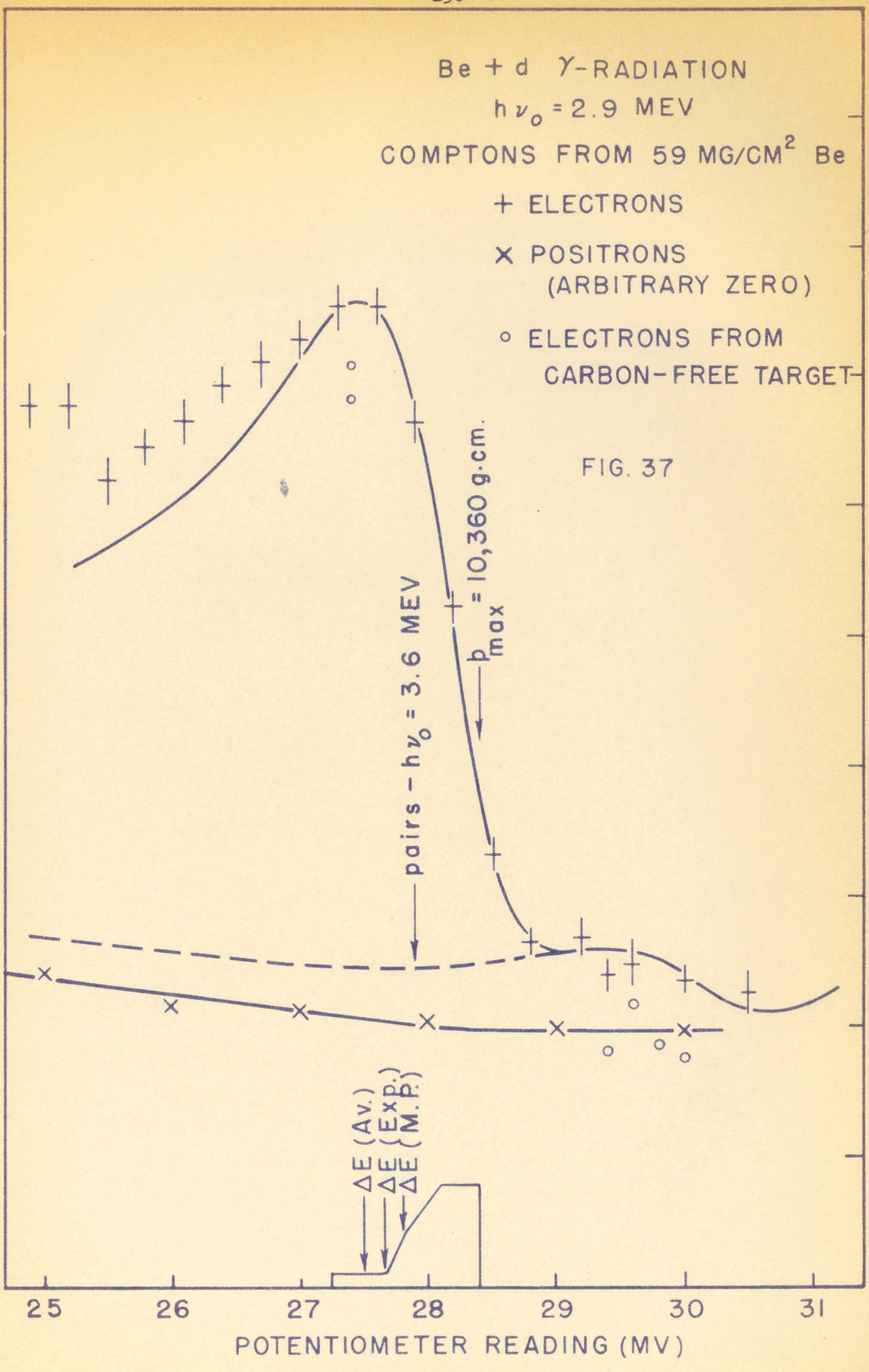
Be + d γ-RADIATION
hν₀ = 2.9 MEV
COMPTONS FROM 59 MG/CM² Be
+ ELECTRONS
× POSITRONS
(ARBITRARY ZERO)
○ ELECTRONS FROM
CARBON-FREE TARGET
pairs – hν₀ = 3.6 MEV
p_max = 10,360 g.cm.
ΔE (Av.)
ΔE (Exp.)
ΔE (M.P.)
25
26
27
28
29
30
31
POTENTIOMETER READING (MV)
(← SUPPRESSED ZERO — SAME SCALE AS FIG. 39) COUNTS PER UNIT MOMENTUM INTERVAL

FIG. 37

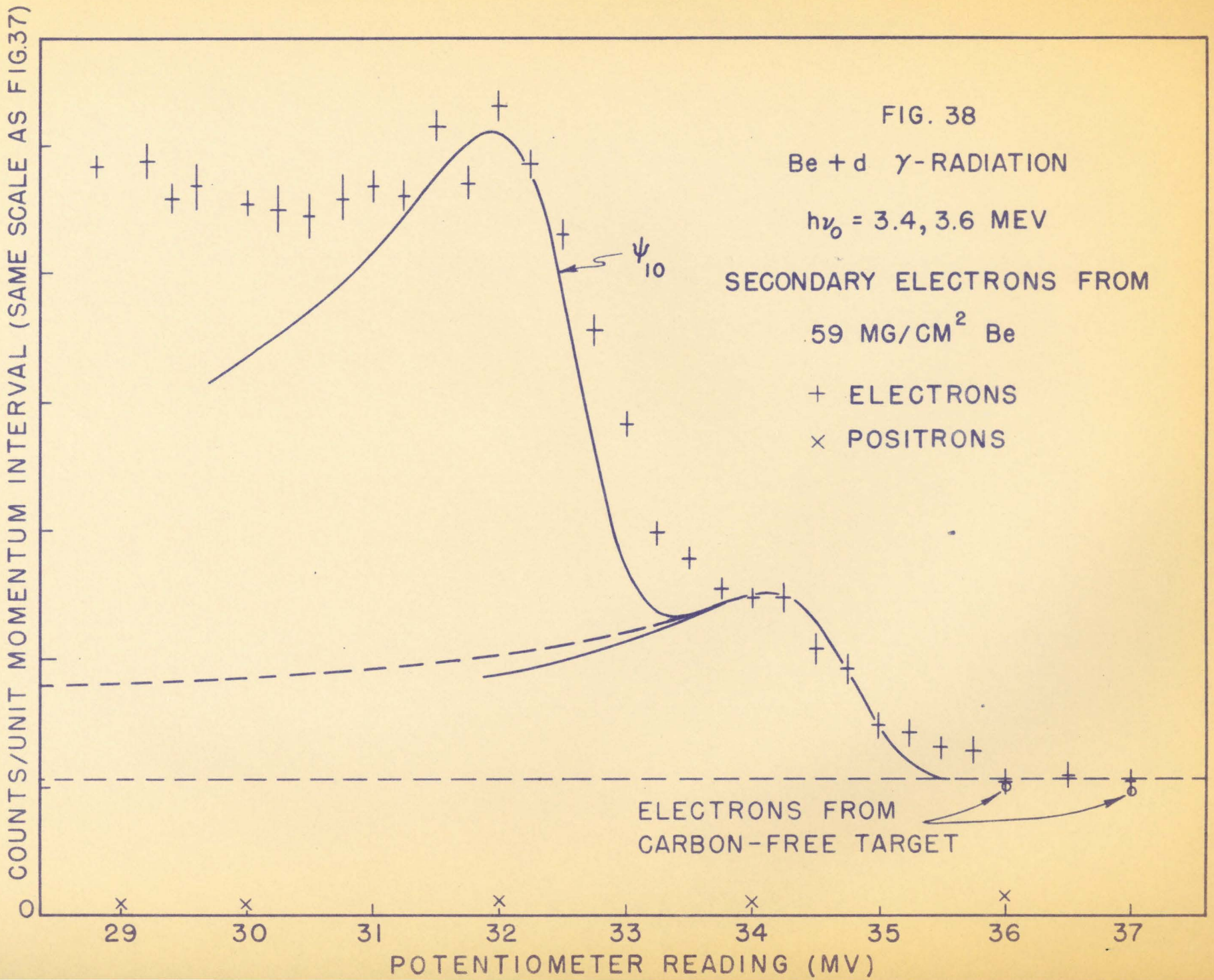

FIG. 38

Be + d γ-RADIATION

$h\nu_0$ = 3.4, 3.6 MEV

SECONDARY ELECTRONS FROM

59 MG/CM^2 Be

\+ ELECTRONS

× POSITRONS

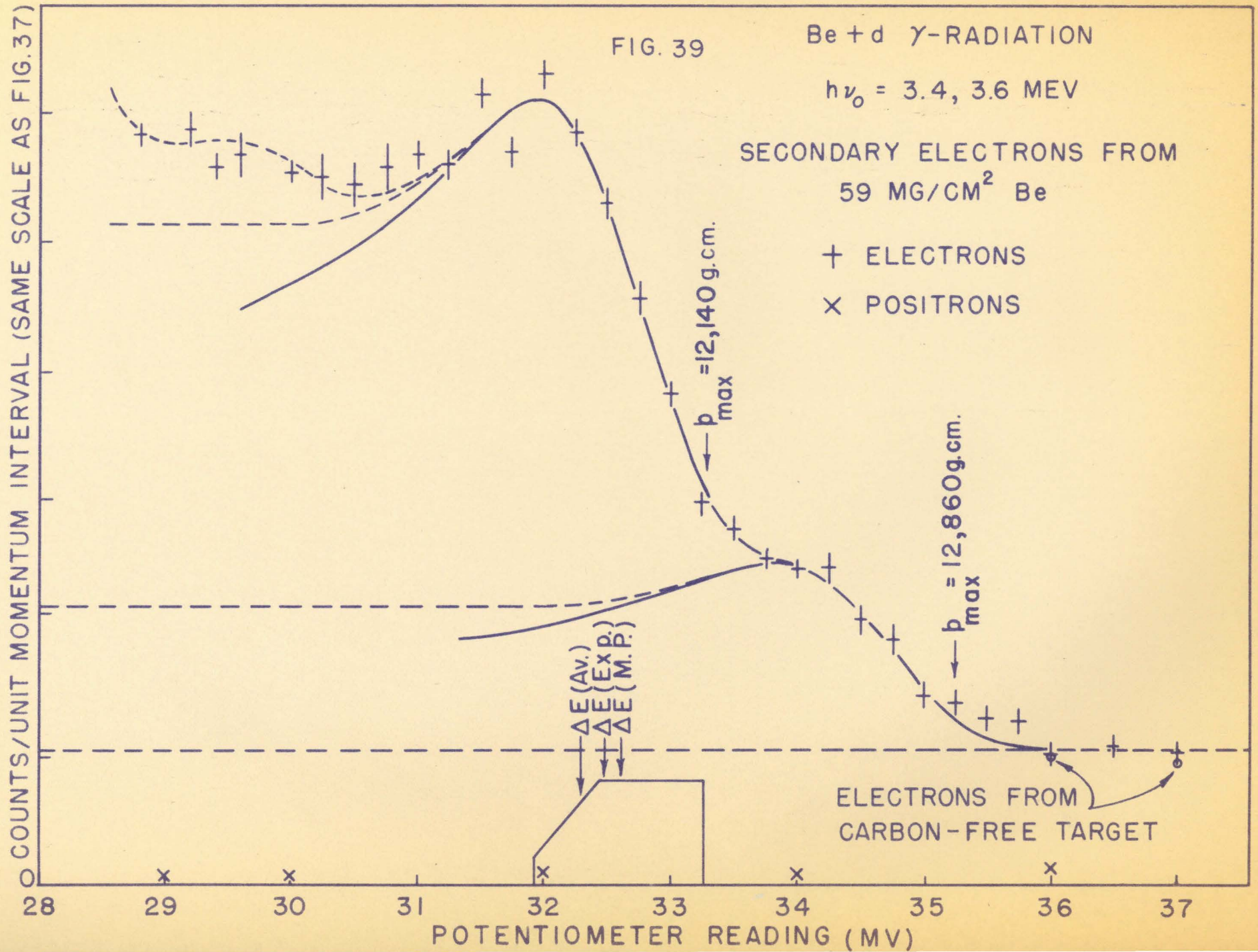
FIG. 39
Be + d γ-RADIATION
$h\nu_0$ = 3.4, 3.6 MEV
SECONDARY ELECTRONS FROM
59 MG/CM² Be
+ ELECTRONS
× POSITRONS
p_{max} = 12,140 g.cm.
p_{max} = 12,860 g.cm.
ΔE (Av.)
ΔE (Exp.)
ΔE (M.P.)
ELECTRONS FROM
CARBON-FREE TARGET
COUNTS/UNIT MOMENTUM INTERVAL (SAME SCALE AS FIG. 37)
0
28
29
30
31
32
33
34
35
36
37
POTENTIOMETER READING (MV)

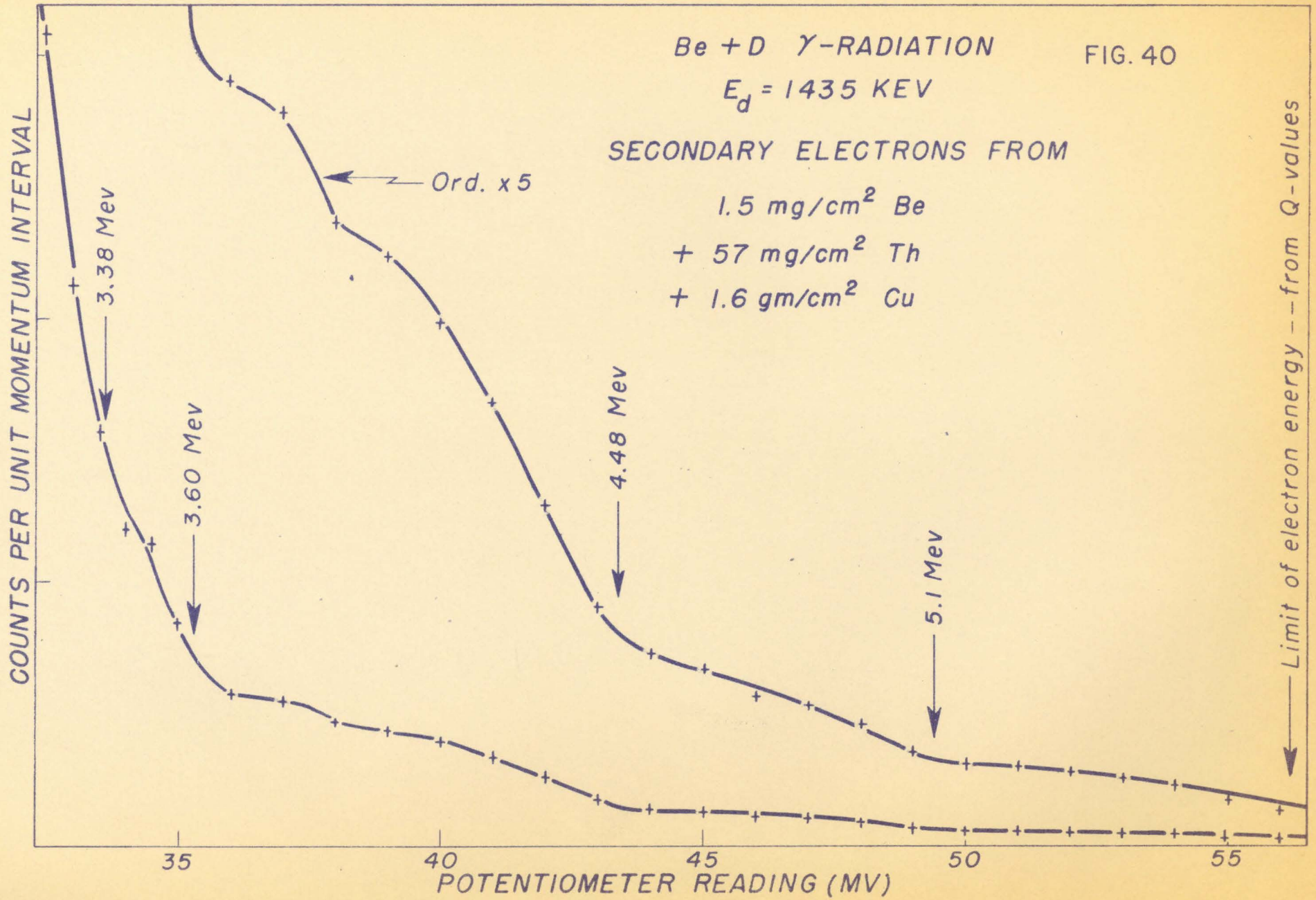
Be + D γ-RADIATION
FIG. 40
E_d = 1435 KEV
SECONDARY ELECTRONS FROM
1.5 mg/cm² Be
+ 57 mg/cm² Th
+ 1.6 gm/cm² Cu
Ord. x 5
3.38 Mev
3.60 Mev
4.48 Mev
5.1 Mev
Limit of electron energy -- from Q-values
COUNTS PER UNIT MOMENTUM INTERVAL
35
40
45
50
55
POTENTIOMETER READING (MV)

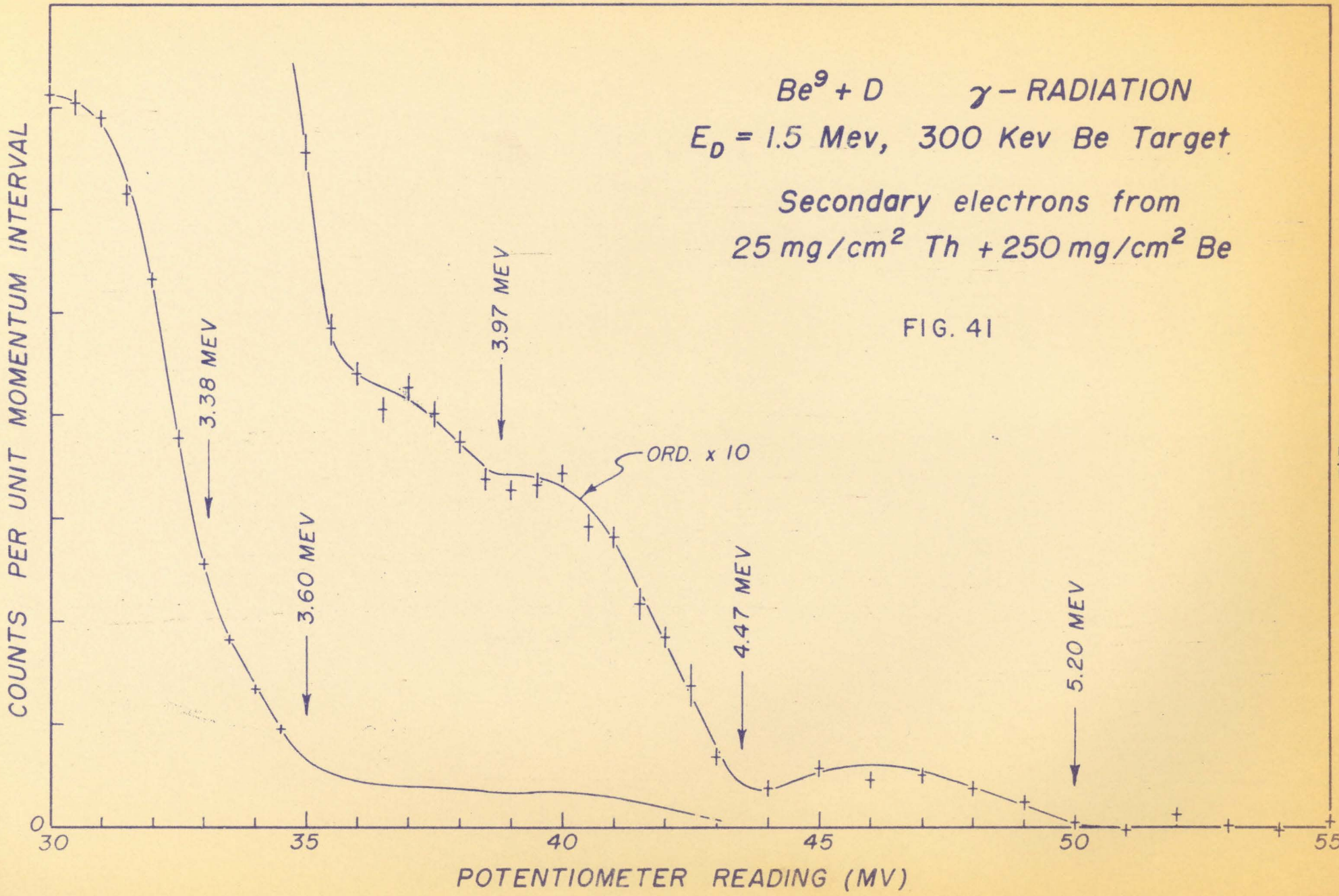
$Be^9 + D$ γ - RADIATION
E_D = 1.5 Mev, 300 Kev Be Target
Secondary electrons from
25 mg/cm² Th + 250 mg/cm² Be
FIG. 41
3.38 MEV
3.60 MEV
3.97 MEV
ORD. x 10
4.47 MEV
5.20 MEV
COUNTS PER UNIT MOMENTUM INTERVAL
0
30
35
40
45
50
55
POTENTIOMETER READING (MV)

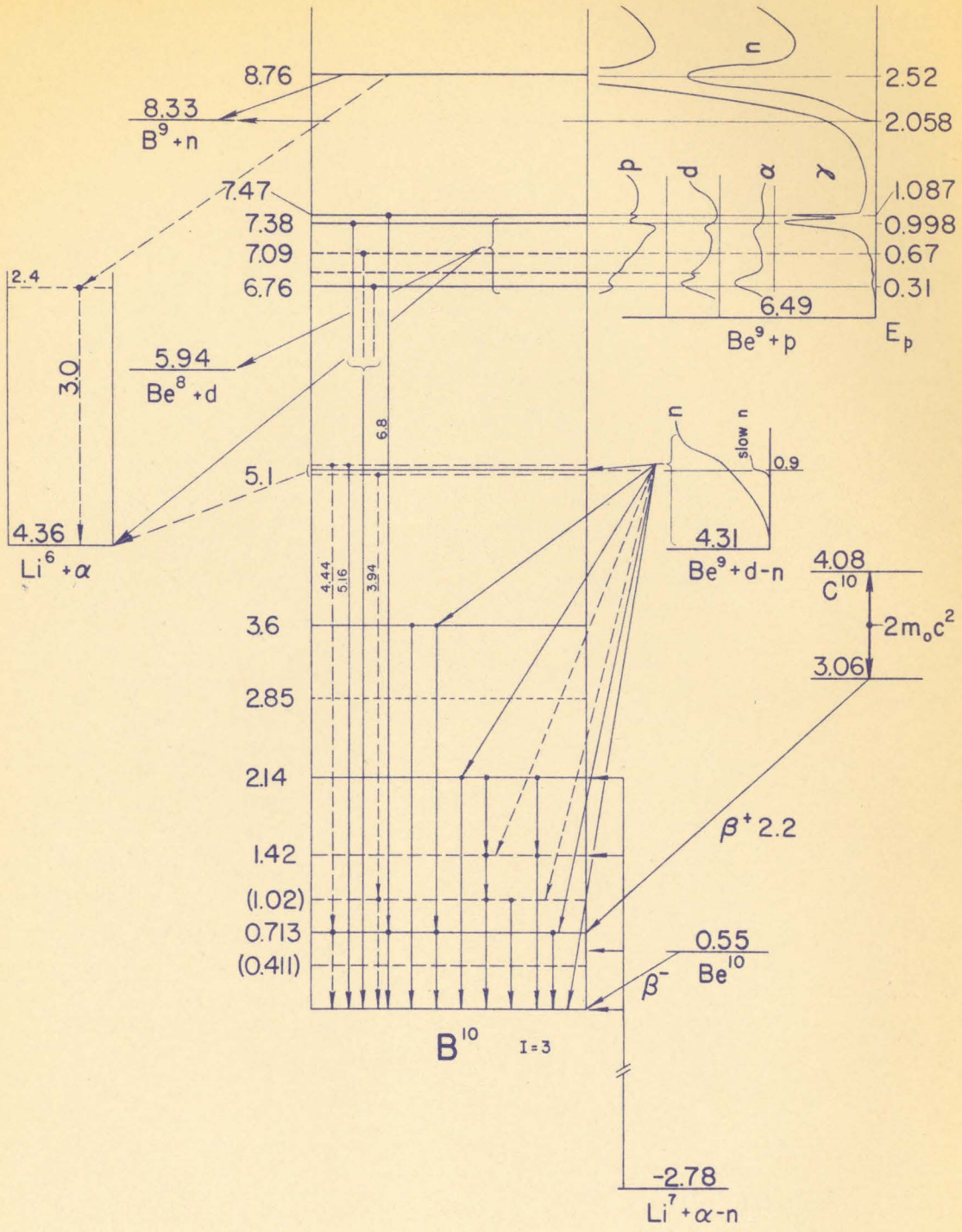
8.76
8.33
B9 + n
7.47
7.38
7.09
6.76
2.4
3.0
5.94
Be8 + d
4.36
Li6 + α
6.8
5.1
4.44
5.16
3.94
3.6
2.85
2.14
1.42
(1.02)
0.713
(0.411)
B10 I=3
n
2.52
2.058
p
d
α
γ
1.087
0.998
0.67
0.31
6.49
Be9 + p
Ep
n
slow
0.9
4.31
Be9 + d-n
4.08
C10
2mₒc²
3.06
β+ 2.2
0.55
Be10
β-
-2.78
Li7 + α-n

FIG. 42

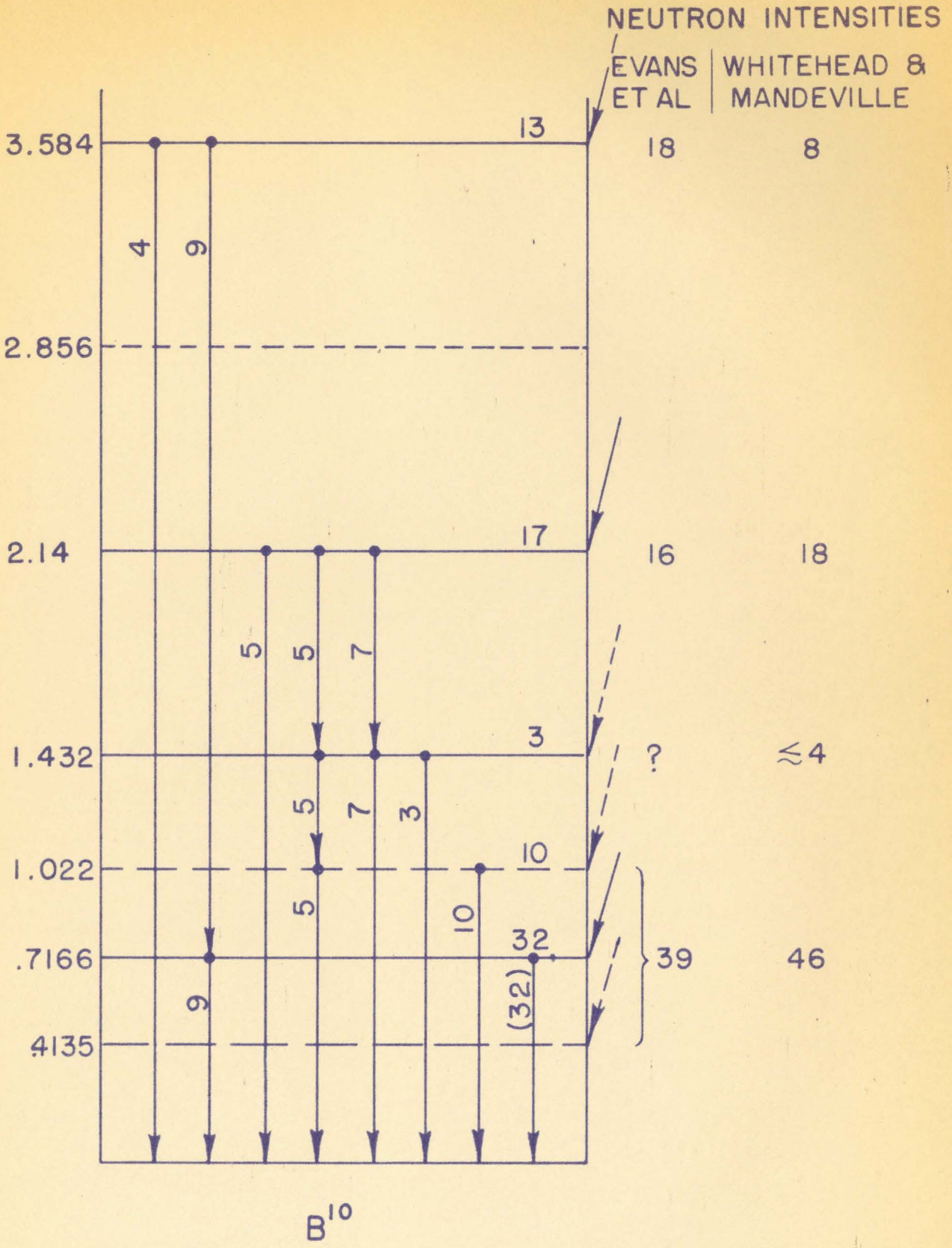
NEUTRON INTENSITIES
EVANS ET AL
WHITEHEAD & MANDEVILLE
3.584
2.856
2.14
1.432
1.022
.7166
.4135
13
18
8
17
16
18
3
?
≲4
10
32
39
46
(32)
4
9
5
5
7
5
7
3
5
10
9
B10

FIG. 43

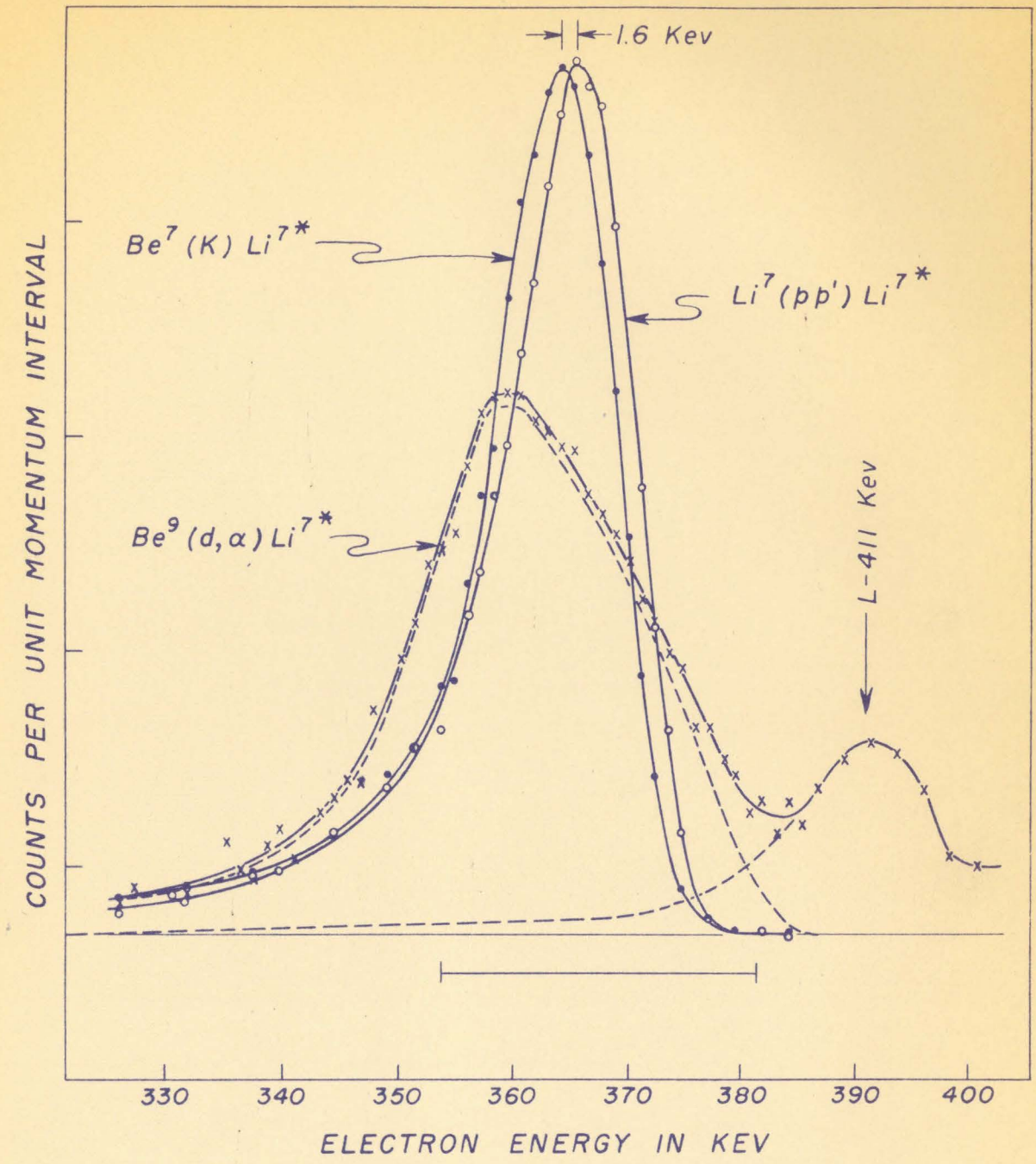
1.6 Kev
$Be^7(K)\,Li^{7*}$
$Li^7(pp')\,Li^{7*}$
$Be^9(d,\alpha)\,Li^{7*}$
L-411 Kev
COUNTS PER UNIT MOMENTUM INTERVAL
330
340
350
360
370
380
390
400
ELECTRON ENERGY IN KEV

FIG. 44

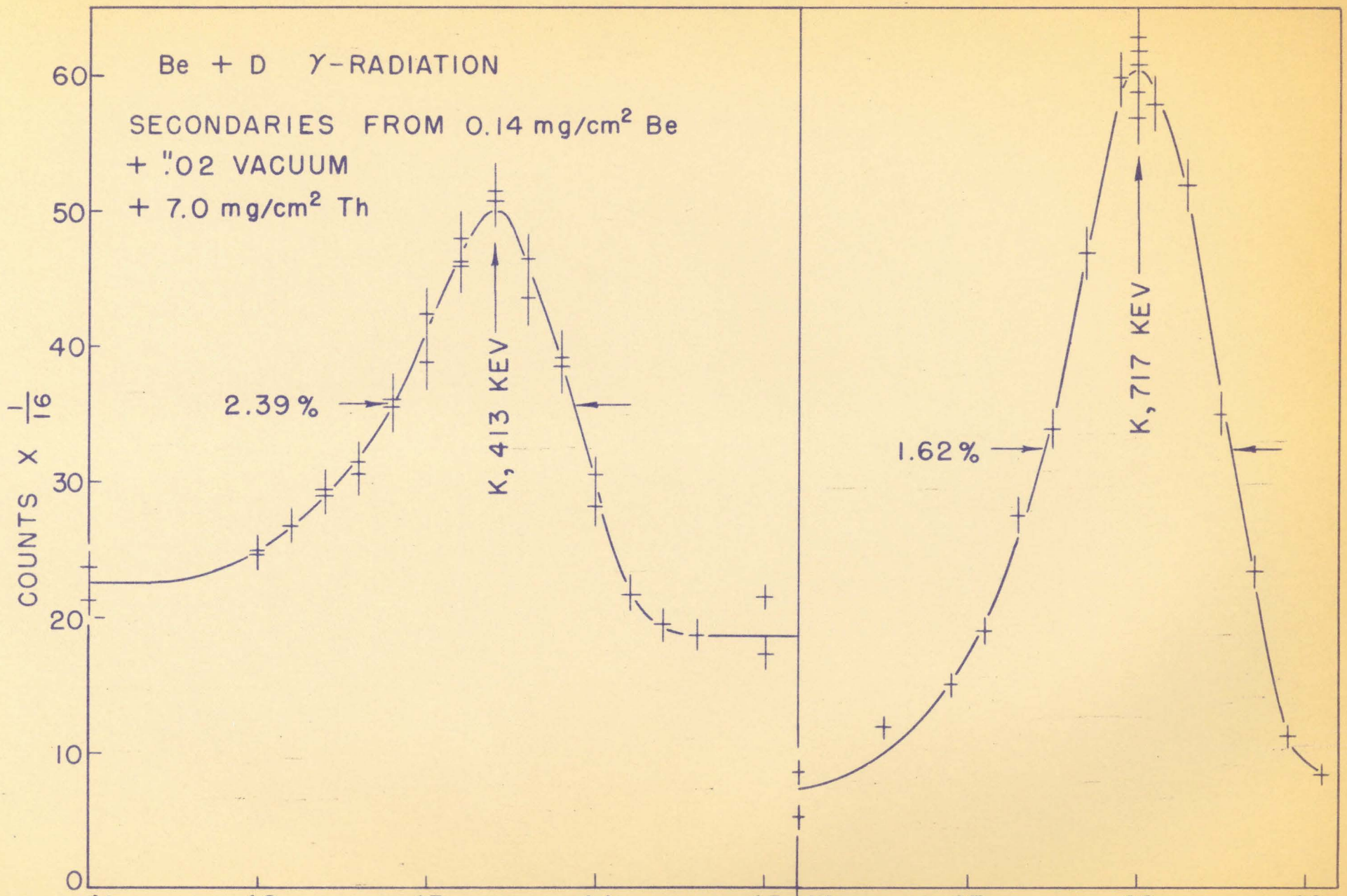
Be + D γ-RADIATION
SECONDARIES FROM 0.14 mg/cm² Be
+ .02 VACUUM
+ 7.0 mg/cm² Th
2.39 %
K, 413 KEV
1.62 %
K, 717 KEV
COUNTS X 1/16
POTENTIOMETER READING (MV)
0
10
20
30
40
50
60
41
42
43
44
45
66
67
68
69

FIG. 45

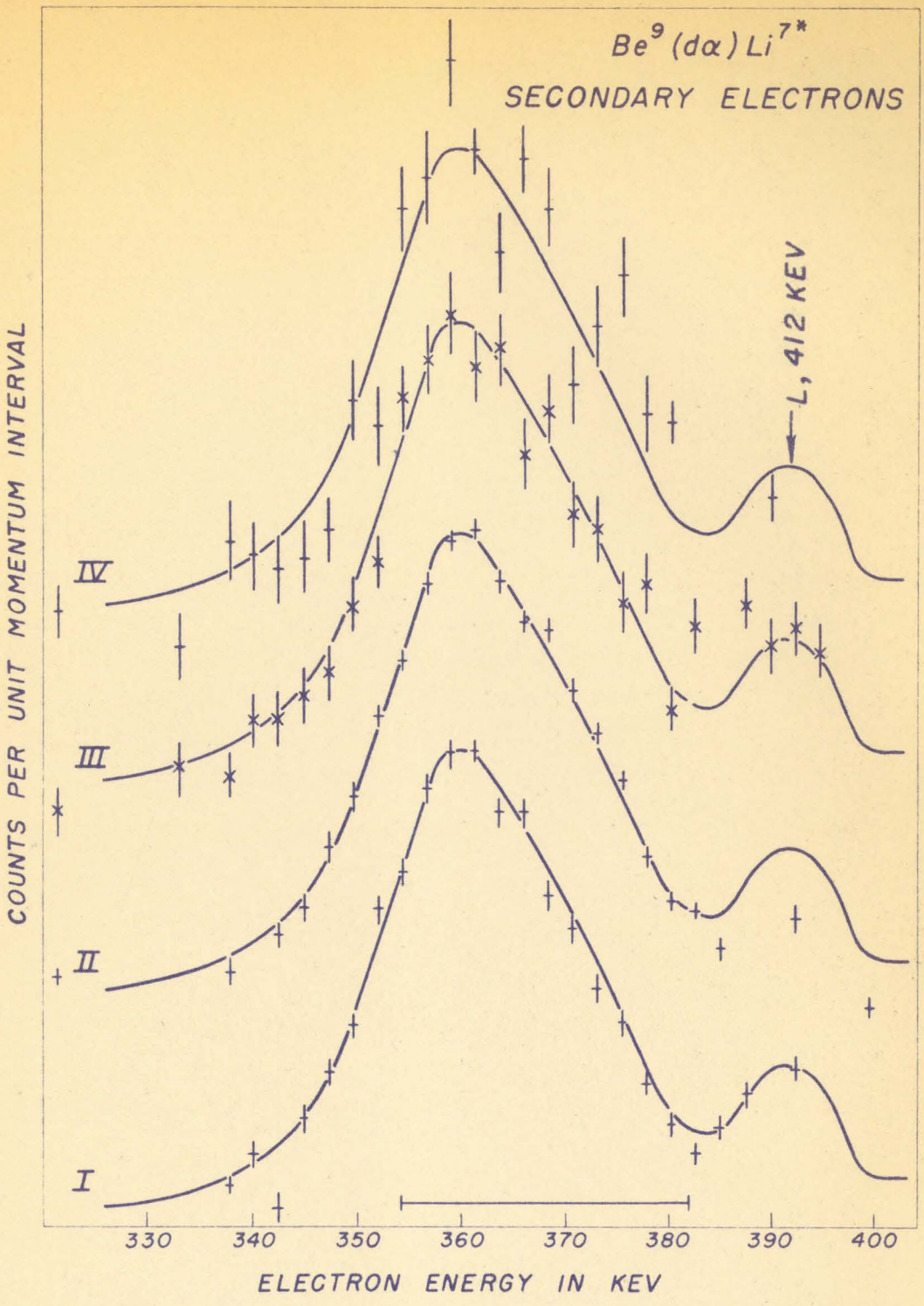

8.9 mg/cm² Be + 7.0 mg/cm² Th { I - 1210 Kev; II - 510 Kev }

0.14 mg/cm² Be + vacuum + 7.0 mg/cm² Th { III - 1180 Kev; IV - 1485 Kev }

FIG. 46

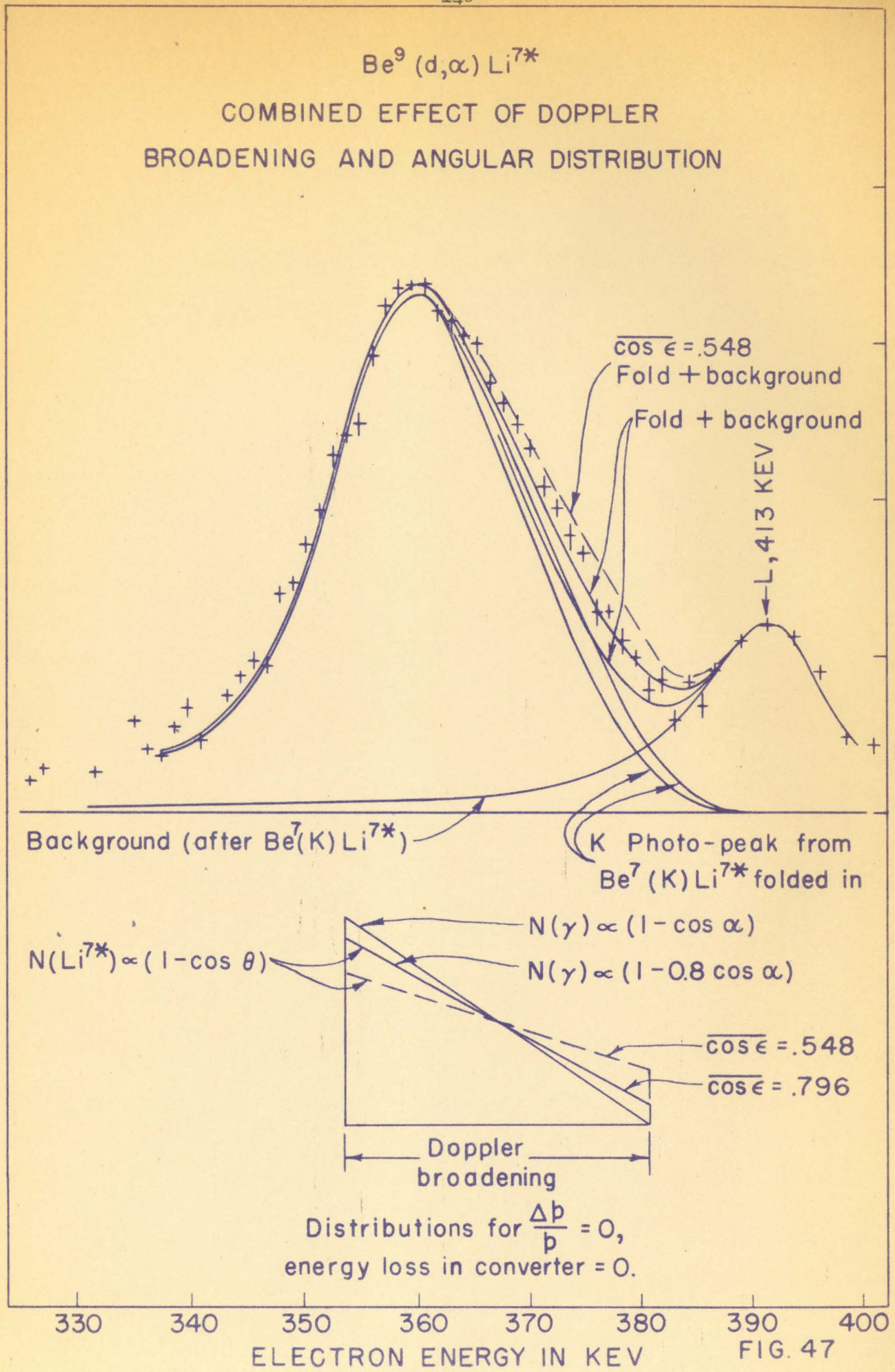
Be^9 (d,α) Li^{7*}
COMBINED EFFECT OF DOPPLER
BROADENING AND ANGULAR DISTRIBUTION
$\overline{\cos\epsilon}$ = .548
Fold + background
Fold + background
L, 413 KEV
COUNTS PER UNIT ENERGY INTERVAL
Background (after Be^7(K) Li^{7*})
K Photo-peak from
Be^7 (K) Li^{7*} folded in
$N(Li^{7*}) \propto (1-\cos\theta)$
$N(\gamma) \propto (1-\cos\alpha)$
$N(\gamma) \propto (1-0.8\cos\alpha)$
$\overline{\cos\epsilon}$ = .548
$\overline{\cos\epsilon}$ = .796
Doppler
broadening
Distributions for $\frac{\Delta p}{p} = 0$,
energy loss in converter = 0.
330
340
350
360
370
380
390
400
ELECTRON ENERGY IN KEV

FIG. 47

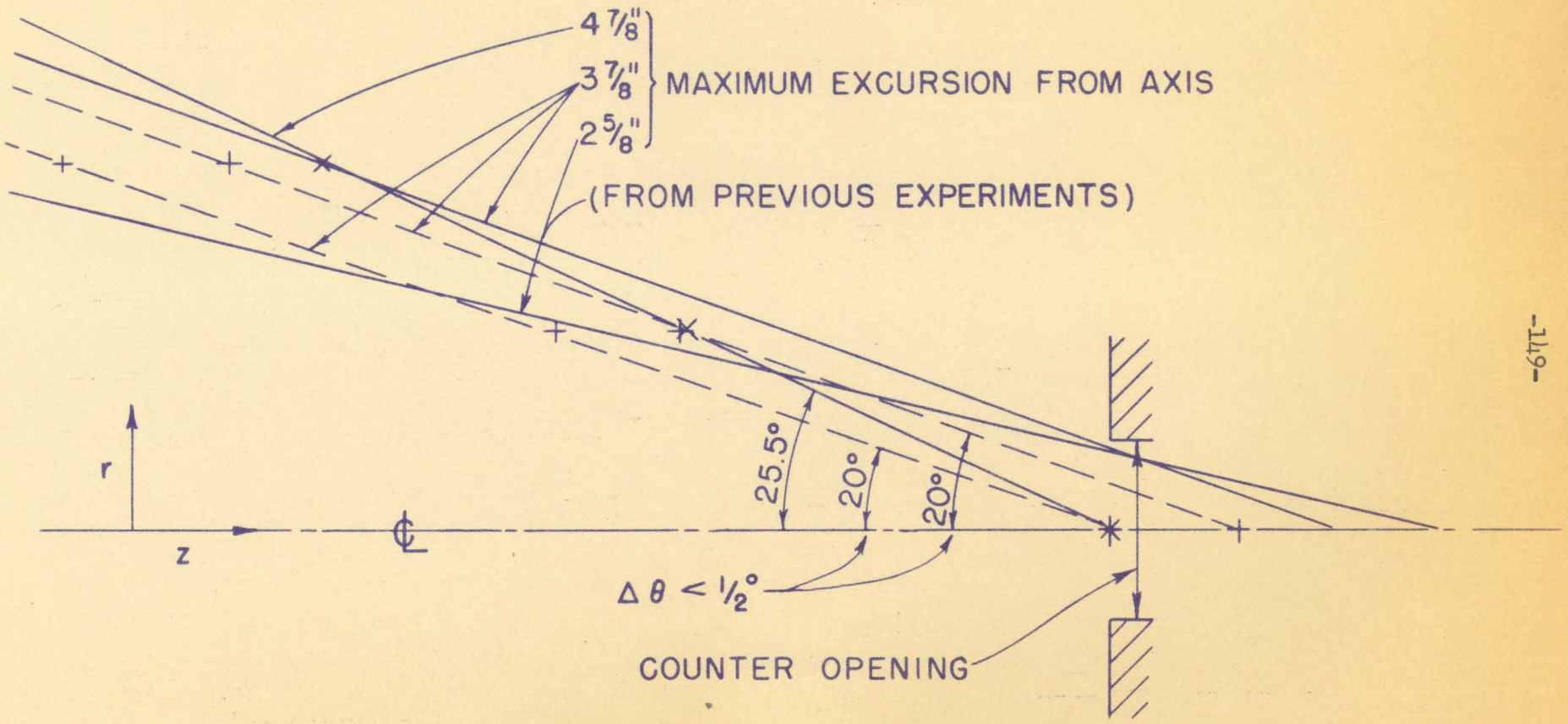

FIG. 48 RAY TRACING TO LOCATE RING FOCUS
(+, X — EXPERIMENTAL POINTS)